

**REAL-TIME ANALYSIS OF ATMOSPHERIC PARAMETERS
DURING THE PROCESSING OF VARIATIONS IN THE
ELECTRIC AND MAGNETIC FIELD OF SPACE PLASMA**

A

Thesis

Submitted towards the Requirement for the Award of Degree of

Doctor of Philosophy
In
Physics

Under the Faculty of Science

By

Bharat Singh Jayant
(Enrollment No.- 161595006205)

Under the Supervision of

Dr. S. Choudhary
Head, Department of Physics
Govt. Degree College, Karera, Dist. Shivpuri (M.P.)



Year-2023

P.K. University
NH-27, Village. Thanra (P.O. - DINARA),
Shivpri (M.P.)-473665

www.pkuniversity.edu.in

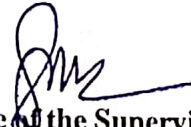


CERTIFICATE OF THE SUPERVISOR (PARA 26-C)

This is to certify that the work entitled "*Real-time analysis of atmospheric parameters During the processing of variations in the electric and magnetic field of space plasma*" is a piece of research Work done by **Shri Bharat Singh Jayant** under my Guidance and Supervision for the degree of Doctor of Philosophy of Physics in the P.K University (M.P) India, and that the candidate has put an attendance of more than 240 day with me.

To the best of my knowledge and belief the thesis:

- I – Embodies the work of the candidate himself/
- II – Has duly been completed.
- III – Fulfill the requirement of the ordinance relating to the Ph.D. degree of the University.
- IV – Is up to the standard both in respect of contents language for being referred to the examiner.



Signature of the Supervisor

Dr. S. Choudhary

DECLARATION BY THE CANDIDATE (PARA 26-B)

I declare that the thesis entitled “*Real-time analysis of atmospheric parameters during the processing of variations in the electric and magnetic field of space plasma*” is my own work conducted under the supervision of **Dr. S. Choudhary (Supervisor) at P.K. University, Shivpuri (M.P.)** approved by Research Degree Committee. I have put more than 240 days of attendance with Supervisor at the center. I further declare that to the best of my knowledge the thesis does not contain any part of any work which has been submitted for the award of any degree either in this University or in any other University without proper citation.

Besides this –

1. I have successfully completed the Course Work of one semester as per UGC Regulation 2009 norms.
2. I have also given a pre – Ph.D. presentation and successfully incorporated the changes suggested on the basis of feedback and comments received.
3. I have also published two research papers in an ISSN/ referred journal from the research work of the thesis and have produced an evidence of the same in the form of acceptance letter/ or the reprint.

Research Scholar



Bharat Singh Jayant

Enrollment No. 161595006205



P.K. UNIVERSITY

(University established under section 2f of UGC act 1956 vide mp government act no 17 of 2015)
Village- Thanra Tehsil, Karera NH 27 District Shivpuri M.P.}

FORWARDING LETTER OF HEAD OF INSTITUTION

The Ph.D. thesis entitled "*Real-time analysis of atmospheric parameters during the processing of variations in the electric and magnetic field of space plasma*"

Submitted by **Bharat Singh Jayant** is forwarded to the P. K. University in six copies. The candidate has paid the necessary fees and there are no dues outstanding against him

Name : Dr. Ashish Vishwakarma

Date : 31/7/23

Place: P.K. University, Shivpuri (M.P.)

Seal



Ashish

(Signature of Head of Institution Where the Candidate was registered for Ph.D Degree)

Signature of the Supervisor

Date : 31/7/23

Place: P.K. University, Shivpuri (M.P.)



“ACKNOWLEDGMENT”

In the name of the almighty, God the most gracious and merciful with his gracing blessing had led to success be upon this thesis. I would like to dedicate my research work to my parents **Mr. Ram Sahay Jayant and Mrs. Bhaghati devi Jayant.**

Its my pleasure to express my thanks to Honourable Chancellor **Shri J. P. Sharma** and **Prof. Dr. Ranjit Singh** Honourable Vice Chancellor, P.K. University, Shivpuri (M.P.) for his cooperation and also for giving me the opportunity to do the research work. I would also like to express my sincere thanks to **Mr. Jitendra Kumar Mishra** Director Admin, **Prof. G. Pavan Kumar** Dean Academic of P.K. University Shivpuri, (M.P.) and also thankful to **Dr. Deepesh Namdev**, Registrar P.K. University, Shivpuri (M.P.) my special thanks goes to **Dr. Bhaskar Nalla**, Dean Research, P.K. University (M.P.), **Dr. Aimna Fatima**, I/C of Research Cell and I am also thankful to **Mr. Praveen Kumar** Department of Physics also thankful to **Ms. Nisha Yadav**, Librarian and **Mr. Pankaj Singh** IT Cell for their Cooperation and **Mr. Ashish Gupta** Office Asst. Ph.D. Cell.

I would like to express my sincere thanks to my Supervisor **Dr. S. Choudhary** Department of Physics, Govt. Degree College Karera, Shivpuri (M.P.) and **Late Prof. Anand Kumar Tripathi** P.K. University Shivpuri (M.P.). I would like to thanks **Dr. N.K. Jain** Principal Govt. Girls College Shivpuri (M.P.) for given Permission to do research work from P. K. University Shivpuri (M.P.). I am thankful to my colleagues viz; **Dr. A. K. Moghey**, **Dr. M.S. Hindoliya**, **Prof. Manjula Sharma**, **Dr. Jyotsna Saxena**, **Prof. Mamta Rani**, **Dr. Renu Rai**, **Dr. Anita Kamore**, **Dr. G.K. Saxena**, **Prof. Mahendra Kumar**, **Dr. Vikas**, **Dr. L.S. Bansal**, **Dr. S.C. Koushik**, **Dr. A.S. Lahariya**, **Dr. S.K. Kirar**, **Dr. S.S. Nigam**, **Prof. Pramod Kumar Chidar**, **Prof. S.S. Mourya**, **Dr. R. K. Shakya**, **Dr. Ajay Singh**, **Shri Bhanu Raje**, Last but not the least, I am entremely thankful to my elder brother **Mr. S. S. Jayant**, **Mrs. Narayani Jayant**, **Mr. R.B.S. Jayant**, **Mrs. Asha Jayant** and My younger brother, **Mr. Sivraj Jayant**, **Mrs. Rekha Jayant**, **Mr. Rajveer Jayant**, **Mrs. Neelam Jayant**, my wife **Mrs. Laxmi Jayant**, My children **Himanshi Jayant**, **Yash Jayant**, My father and mother in law **Mr. Mansharam Nagar**, **Mrs. Jal Devi Nagar**, my nephew **Dharmesh**, **Lovkesh**, **Prashnat**, **Durgesh**, **Vansh**, **Bhumi**, **Misty**, for their moral support, patience and encouragement throughout the research work.

Research Scholar

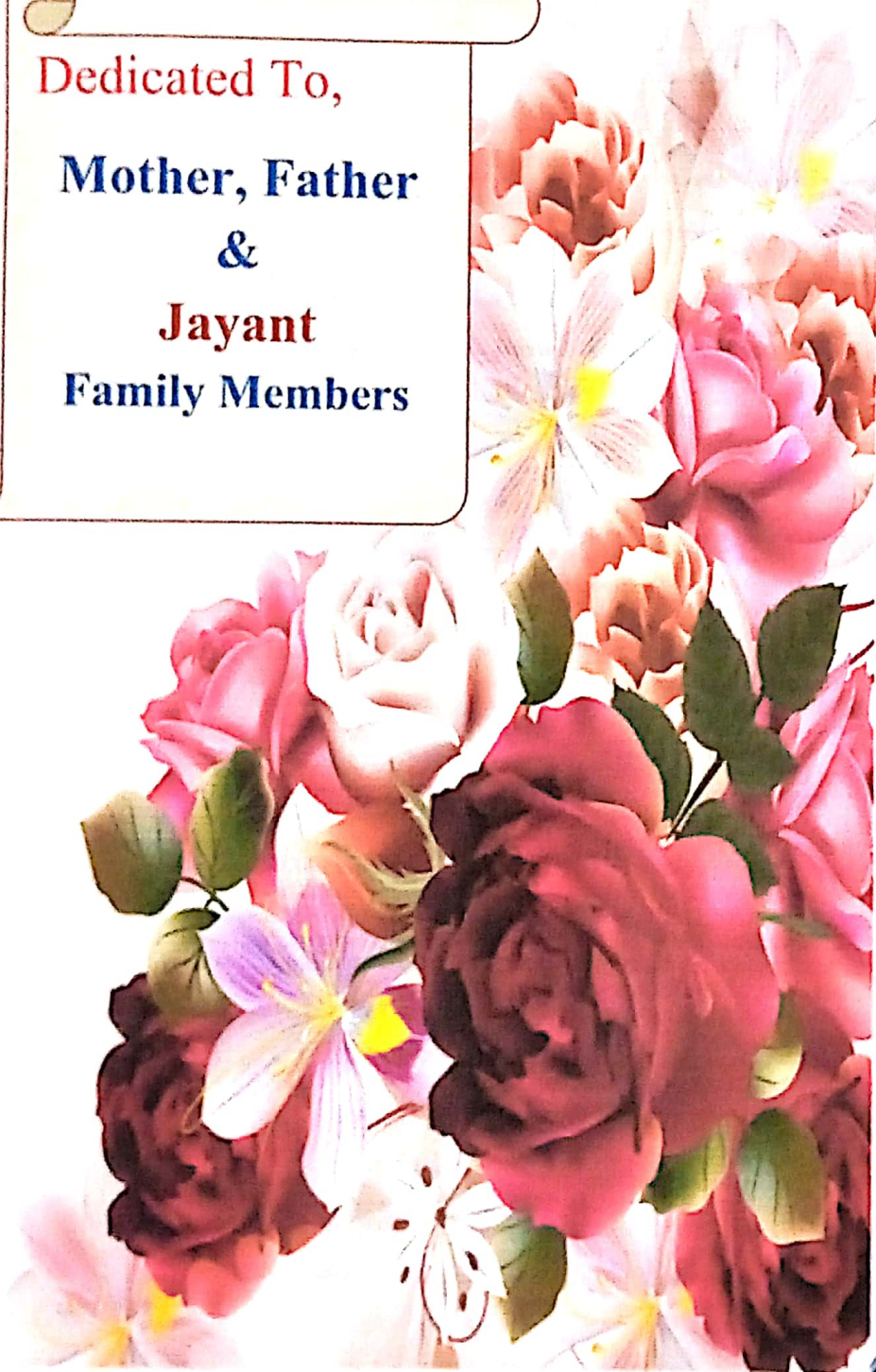
Bharat Singh Jayant

Enrollment No. 161595006205



Dedicated To,

**Mother, Father
&
Jayant
Family Members**



“List of Figures”

Fig 1.1	Theory of Atmospheric Electricity
Fig 1.2	Earth Atmospheric Gases
Fig 1.3	Earth Atmospheric Layer
Fig 1.4	The First Law of Thermodynamics
Fig 1.5	Effect on Earth Climate
Fig 1.6	Geomagnetism of Earth
Fig 1.7	Geomagnetic Storms
Fig 1.8	Factors Affecting Global Electric Circuit
Fig 3.1	Atmospheric Global Circulation
Fig 3.2	Electric Field Mill Installation at Kennedy Space Research
Fig 3.3	Mean diurnal variations between perturbed weather conditions (PW)– For each month from June 2015 to May 2016 the potential gradient (PG) was calculated. Months are aligned according to the season. Error bars are displayed on the graph
Fig 3.4	PG observations for the period from June 2015 to Sep 2015
Fig 3.5	PG observations for the period from Feb 2016 to May 2016
Fig 4.1	Earth Atmospheric Exchange Process
Fig 4.2	Atmospheric Electric Field Measurement Equipment
Fig 4.3	Sonnblick Observatory, Austria for Atmospheric electric field measurement
Fig 4.4	<i>Atmospheric Electric Field during perturbed day</i>
Fig 4.5	<i>Atmospheric Electric Potential during perturbed day</i>
Fig 4.6	<i>Electric Distribution Pattern during perturbed days</i>
Fig 4.7	<i>Lightening Intensity during observation period</i>
Fig 4.8	<i>Altitude-wise perturbations during perturb time</i>
Fig 5.1	Atmospheric Electric Field Mill at Maitri Station, Antarctica
Fig 5.2	Magnetic Field Intensity on 01/01/2019 - 02/01/2019
Fig 5.3	Variation of Atmospheric Electric Field (AEF) on January 1, 2019
Fig 5.4	Variation of Atmospheric Electric Field (AEF) on January 2, 2019
Fig 5.5	Magnetic Field Intensity on 19/01/2019 - 21/01/2019
Fig 5.6	Variation of Atmospheric Electric Field (AEF) on January 19, 2019
Fig 5.7	Variation of Atmospheric Electric Field (AEF) on January 20, 2019
Fig 5.8	Magnetic Field Intensity on 22/01/2019 - 25/01/2019
Fig 5.9	Variation of Atmospheric Electric Field (AEF) on January 24, 2019
Fig 5.10	Variation of Atmospheric Electric Field (AEF) on January 25, 2019



P.K. UNIVERSITY

SHIVPURI (M.P.)

Established Under UGC Act 2F, 1956

cf. No. PKU/2018/10/03/RO-STUD/03

Date. 07.07.18....

Course Work Certificate

To,

Bharat Singh Jayant,

Dear Student,

This is to certify that **Bharat Singh Jayant**, (Reg. No PH17SC1001PHY);

son / daughter of Mr. /Ms. Ram Sahay Jayant, student of Ph.D. (Physics)

under the Faculty of Science has successfully passed the course work

examination with 'A' grade from P.K.University, Karera, Shivpuri.

Registrar

ADDRESS : NH-25, Dinara, Shivpuri (M.P.) ● Mob. 7241115081





P.K. UNIVERSITY
SHIVPURI (M.P.)

University Established Under section 2F of UGC ACT 1956 Vide MP Government Act No 17 of 2015


CENTRAL LIBRARY

Ref. No. C.LIB/PKU/2023/Ph.D Scholar/102

Date: 05.07.2023

CERTIFICATE OF PLAGIARISM REPORT

1. Name of the Research Scholar : Bharat Singh Jayant
2. Course of Study : Doctor of Philosophy (Ph.D.)
3. Title of the Thesis : Real-Time Analysis of Atmospheric Parameters during the Processing of Variations in the Electric and Magnetic Field of Space Plasma
4. Name of the Supervisor : Dr. S.Choudhary
5. Department : Physics
6. Subject : Physics
7. Acceptable Maximum Limit : 10% (As per UGC Norms)
8. Percentage of Similarity of Contents Identified : 9%
9. Software Used : Ouriginal (Formerly URKUND)
10. Date of Verification : 06.09.2022


Signature of Ouriginal Coordinator
(Librarian, Central Library)
P.K. University Shivpuri (M.P.)
Shivpuri (M.P.)

ADD: VIL: THANRA, TEHSIL: KARERA, NH-27, DIST: SHIVPURI (M.P.) -473665
MOB: 7241115902, Email: library.pku@gmail.com



COPYRIGHT TRANSFER CERTIFICATE

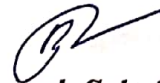
Title of the Thesis: *“Real-time analysis of atmospheric parameters during the processing of variations in the electric and magnetic field of space plasma”*

Candidates Name: *Bharat Singh Jayant*

COPYRIGHT TRANSFER

The undersigned hereby assigns to the P.K. University, Shivpuri all copyrights that exist in and for the above thesis submitted for the award of the Ph.D. degree.

Date:



Research Scholar

Bharat Singh Jayant

Enrollment No. 161595006205

Note: However, the author may reproduce/publish or authorize others to reproduce, material extracted verbatim from the thesis or derivative of the thesis for authors personal use provided that the source and the University copyright notice are indic

Abstract

Atmospheric electricity is a multi-parametric concept that refers to the infinite electricity in the air and clouds acts on the earth through induction mechanism. The electric potential increases until, it overcomes the resistance force of air. The atmospheric energy is calculated by potential differential measurements in between the point on the earth's surface and point some-where in the air. Atmospheric weather conditions are depend on reasonable local climate specifications or may be considered as perturbed weather conditions. The variation of the Earth's atmospheric electric field is close to the earth environment and enormously impact by extra-terrestrial or solar effects and these two components assume a significant part to frame earth atmospheric electric field potential. Finally, an overall correction coefficient is calculated the mean of 50% of regular determinations across the median, and it is used to correct the Potential Growth (PG) data. Due to the extreme statistical approach the PG values are considered relative to the standard value.

Lightning is a high-energy luminous electrical discharge occurs inside, or even between dark clouds, sudden pressure fluctuations rippling in the earth environment. Finally, it seems to have a tremendous impact on human life and their facilities. The worldwide atmospheric electric field is behaved like a current, atmospheric electric current penetrates into the ionosphere, and down to the surface of the Earth. The continuous measurements of atmospheric electrical parameters, like atmospheric electrical field, atmospheric conductivity is characterize the atmospheric Global Electrical Circuit (GEC).

These correlations of possibilities of atmospheric electric field or potential gradient as indicative factor for monitoring, investigating as well as controlling various weather related human problems. This study can be taken as model for further examining similar atmospheric electric field behavior in other parts of space. Furthermore a comparative analysis between two zones can also be a atmospheric potential and conclusion drawn under this study it is evident that atmospheric electric field is highly sensitive to the space weather as well as geomagnetic activities.

“Tables of Contents

Chapter	Topic	Page No
Chapter 1	Real-time Analysis of Atmosphere Electric Field	01-25
Chapter 2	Review of Literature	26-35
Chapter 3	Measurement of Atmosphere Potential Growth (PG) Variations at Local Climate Specification	36-61
Chapter 4	Analysis of Atmosphere Electric Field Characteristics during Lightening	62-76
Chapter 5	Measurement of Atmosphere Electric Field during Disturbed Interplanetary Magnetic Field	77-104
Chapter 6	Summary & Conclusions	105-115
	Bibliography	116-130
	Publications	

Chapter-1

Real-time Analysis of Atmosphere Electric Field

CHAPTER 1

Real-time Analysis of Atmosphere Electric Field

1.1 Introduction

The electrical system of the planet within the earth's atmosphere is referred to as atmospheric energy. The planetary global electrical circuit includes the ionosphere, mesosphere, troposphere, and atmosphere. Atmospheric electricity is a multi-parametric concept that refers to the infinite electricity in the air and also in the clouds that acts on the earth through the induction mechanism. An experiment showed that atmospheric electricity is typically negative but rarely positive, and that it is still available in the atmospheric network. The scientific study of atmospheric electricity started in the 18th century, with research into the electrical nature of thunderstorms, such as that notably conducted by Benjamin Franklin in 1750, when he produced a spark from his aerial device. The French botanist and scientist L.G. Le Monnier (Watson, 1746) discovered that the atmosphere was electrified except in good weather when he simulated Franklin's work with an aerial in 1752. (although he removed the grounding pole from the aerial and placed some dust particles near the apparatus to investigate electrostatic attraction. There is ample evidence that the electric and magnetic fields has become an important agent in the production of complex improvements in the space plasma as well as the earth atmosphere. The satellite technology competition has seen dramatic shifts in space plasma that have occurred increasingly as a result of many causes. However, this is observed to be an electromagnetic and magnetic phenomenon in space plasma. To comprehend the phenomenal changes in the space plasma, it is important to conduct a systematic analysis of the numerous atmospheric parameters that influence the space plasma and regulate the space weather conditions. One of the most

important parameters for understanding the dynamics of space plasma is the local atmospheric electric field (AEF). A variety of measured instruments can be used to investigate the atmospheric electric field. Furthermore, such research necessitates the existence of extensive data that has been accumulated over a long period of time in order to compare atmospheric events with improvements in space plasma. According to previous studies, the study of the ambient electric field is expected to make a substantial contribution to understanding the diurnal and annual fluctuations of the atmospheric envelope caused by climate change. As a result, the electric and magnetic fields of space plasma phenomena have become a broadly recognized area for researchers to study and discover the Earth's atmosphere. The ambient medium, with which we are surrounded, includes not only combined electricity, as does any other form of matter, but also a significant amount of a free and uncombined state; sometimes of one kind, sometimes of the other, but often of the opposite kind to that of the earth. Different layers or strata of the atmosphere are often observed to be in different electric states when positioned just a short distance away. There are three types of atmospheric electricity phenomenon. There are the electrical phenomenon of thunderstorms, the phenomena of continuous electrification of the air, and the polar Aurora, which is a third branch of the topic. Most experts believe, however, that whatever the source of free electricity in the environment, the electricity of immense voltages that disrupts the air and causes the phenomenon of lightning is caused by the condensation of the watery vapor forming the clouds; each minute vapor decrease as it passes through the air collecting a certain amount of free electricity on its surface. The electric potential increases until it overcomes the resistance force of the air as these drops of vapor coalesce into greater drops with a resulting decline in overall surface exposed. This remark becomes clearer as it is considered that the potential of a given charge of electricity increases when the electrical power

of the entity carrying the charge decreases, as occurs as minute vapor drops coalesce into larger drops. Atmospheric energy is plentiful in the environment; certain signs can be detected less than four miles above the earth's atmosphere, but it becomes more visible as one rises higher. The basic idea is that during fine weather, the air above the earth's surface is normally positively electrified, or at least positive with respect to the earth's surface, the earth's surface being comparatively negative. Furthermore, the existence of electrical activity in the atmosphere, induced by the accumulation of immense static charges of current produced presumably by agitation of the air upon itself, may explain the various lightning and thunderstorm phenomena. Other factors that contribute to the generation of energy in the environment include evaporation from the earth's surface, chemical modifications that occur on the earth's surface, and the extension, condensation, and alteration of temperature of the atmosphere and of the moisture contained in it. According to M. Peltier, the terrestrial globe is absolutely negative, and interplanetary space is positively charged; the atmosphere itself has no energy and is only in a passive state, so the effects detected are due to the relative power of these two great stores of electricity. Researchers are inclined to believe that the terrestrial globe has an abundance of negative electricity, at least on its solid portion, and that the same holds true for bodies situated on its surface; nevertheless, it seems to them that the atmosphere itself is positively electrified, based on the different observations made. This positive electricity is simply derived from the same source as the negative electricity of the globe. It is most likely that it exists in the aqueous vapors that the atmosphere is still more or less packed with, rather than in the particles in the air itself; however, it does occur in the atmosphere. Potential differential measurements between that location on the earth's surface as well as a point anywhere within the atmosphere above it can be understood as such atmospheric calculations. The atmosphere in various areas is often found to

have varying local potentials that vary from the earth's potential, often by as much as 3000 Volts. According to investigations, the electrostatic field and the difference in potential of the earth field is around 60 to 100 volts in summer and 300 to 500 volts in winter per meter of difference in height, a simple calculation gives the result that when such a collector is arranged, for example, on the ground, and a second one is mounted vertically over it at a distance of 2000 meters and both are coaxial The air in the upper atmosphere is extremely amorphous and conducts closely to the rarefied gases in Geissler's tubes. When dry, the lower air is a non-conductor. The higher stratum is thought to be positively charged, while the earth's surface is negatively charged, with the stratum of denser air between behaving like the glass of a Leyden jar in holding the opposing charges apart. The theory of atmospheric electricity discusses many phenomena, including free electricity, which is manifested during thunderstorms and is the cause of the former, and electricity of lower tension, which is manifested during an aurora borealis show and is the cause of the latter. The most common cause that deters or inhibits electrical signals is the electric environment. Through floods, some equipment operates irregularly, interrupting the passing of heavy currents instantaneously, which

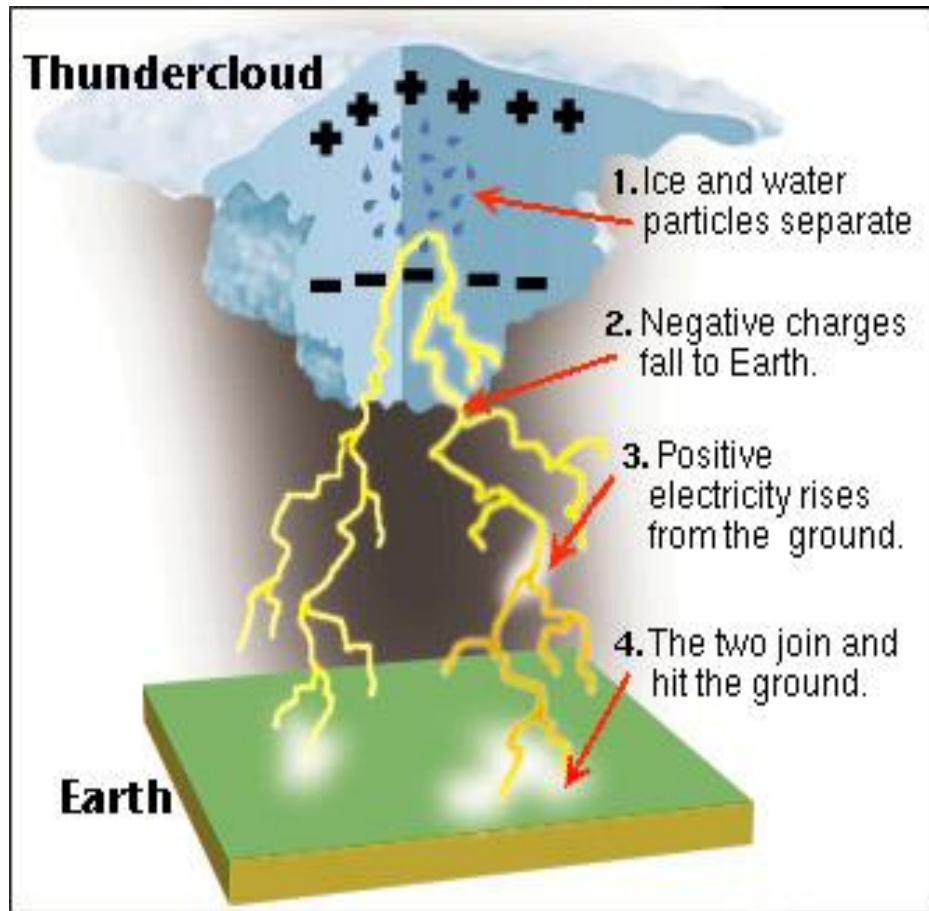


Fig 1.1: Theory of Atmospheric ELeCtricity (<http://www.ces.fau.edu/nasa/>)

often creates dazzling sparks on the apparatus in the workplaces, between metallic points; in telegraphic networks, the armatures of the electro-magnets are drawn up with great intensity, and the wires and other metallic substances around the instruments fused. It is often found, though less often, that current exist for a longer or shorter period of time interfere with the activity of communication networks. There have been some speculative theories about the cause of these semi-diurnal meteorological cycles, but they have all been secondary in nature. The several complex mechanisms caused by the thermodynamics of radiation simply have a primary source. It is hoped that with adequate practice, the formulas deduced and outlined here would yield additional useful data about the atomic and subatomic operations involved in the modifications

of the fundamental terms and their various derivatives. Diurnal differences discovered by frequent signs (during fine weather) indicated two maxima occurring in summer at roughly twelve hours apart and two minima occurring in summer at roughly nine hours apart. The maxima roughly correspond to hours of varying temperature, while the minima correspond to hours of stable temperature. In general, atmospheric electricity hits its highest in January, then steadily declines until the month of June, where it reaches its lowest intensity; it then gradually rises until the end of the year. The disparity between the high and low is much more palpable in sunny weather than in cloudy climates. Over the various months, the electricity of the air is more strong when the atmosphere is clear than when it is gloomy, except in June and July, when the electricity reaches a peak, the intensity of which is approximately the same regardless of the state of the sky. The average electric strength observed during fogs is almost identical to that observed during snows. This is a very high value that corresponds to the mean maxima observed for the first and last months of the year. A curious finding shown by recent observations is that moisture behaves in a very different way in the cold and hot months; it increases energy in the winter and decreases it in the summer. The basic truth is that humidity behaves in two ways, the results of which appear to contradict each other. On the one hand, it facilitates the escape of electricity stored in the upper regions of the atmosphere to the stratum where the discovery is made; on either side, it promotes the escape of electricity possessed by this layer into the earth. This study proposes to analyze various weather phenomena using measurements made in the sense of the atmospheric electric field. The electric field mill is an extremely sensitive instrument that senses even small shifts in the electric field and conducts accurate measurements. Since this instrument has a minor effect on the surrounding environment, it is important to consider the mounting settings before installing the Atmospheric Electric Field Mill. The proposed research work

observed the relation between atmospheric conditions and the variation of the electric and magnetic fields of space plasma in this analysis. The observation of the atmospheric electric field is a very promising and fruitful area of scientific research. Such research will greatly add to the body of knowledge about different climatic factors and ongoing natural and meteorological phenomena. A rigorous examination of the effect of various local meteorological factors on the nature of the atmospheric electric field has the potential to provide a systematic method of examining the behavior of the gaseous envelop surrounding us, which controls the various weather conditions ranging from fair to extremely turbulent. This research is also inspired by the aim of establishing a long-term method for assessing the severity of impending natural disasters and predicting them well in advance, thus assisting in the development of timely preventive steps. Such a thesis would undoubtedly be extremely profitable, both scientifically and commercially.

1.2 Earth Atmospheric Compositions

The abundant supply of sustainable energy found in the dense cover of air covering the Planet, known as the atmosphere, has made the Earth sustainable. This envelope of air is important for the survival of human existence because its absence may allow thermal changes induced by solar terrestrial phenomena to have a negative effect on the Earth's surface. This can result in extremely hot days and extremely cold nights, all of which are totally unsuitable for natural habitation. The Earth's atmosphere is mainly composed of nitrogen and oxygen, all of which are visible to incoming solar radiation. They are often invisible to incoming thermal radiation, but they do not absorb or emit solar or infrared radiation. Ozone (O_3) is relatively minor greenhouse gas, but it is found in relatively low concentrations in the troposphere.

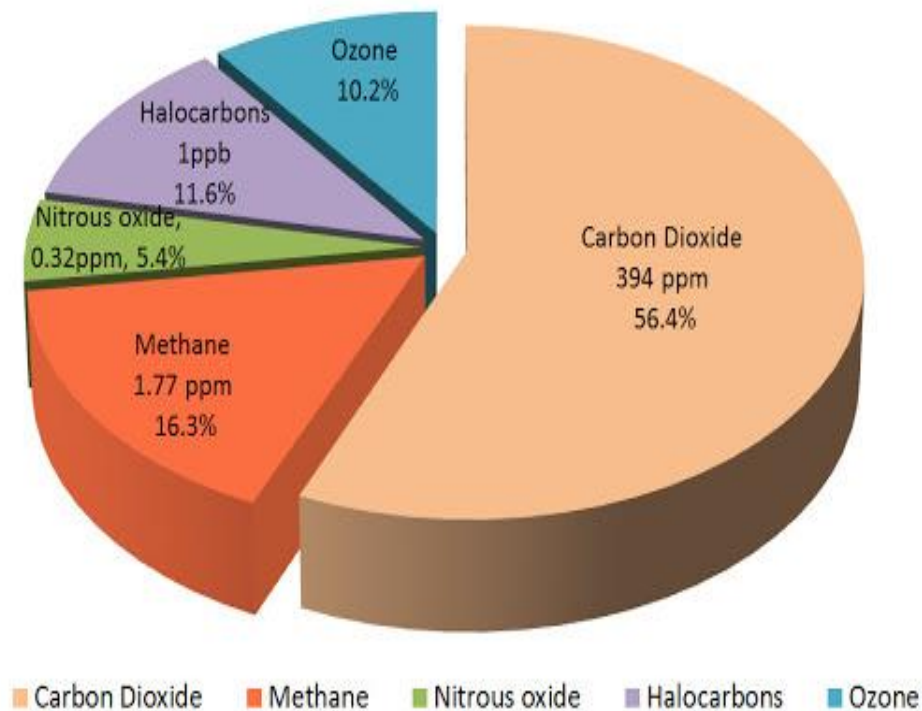


Fig 1.2: Earth Atmospheric Gases (<http://www.ces.fau.edu/nasa/>)

The air in the Earth's atmosphere is mainly composed of 78 percent nitrogen, 21 percent oxygen, and 0.037 percent carbon dioxide, with small concentrations of other gases such as H, He, Ar, Ne, Kr, Xe, O₃, and water vapour. Increasing a height in the atmosphere, the density of such gases reduces. This envelop is thickest in the lower atmosphere (around 15 km above the Earth's surface). The thickness and purity of the gases in the atmosphere have a significant impact on the climatic conditions. The Earth's atmosphere is the principal source in monitoring the favorable existence factors on the planet during the days and nights. This layer of gasses plays an important part in regulating the general climatic environment on Earth and is the cause of events such as global warming, which is caused by ozone depletion which is a cause of the green house effect. Furthermore, such phenomena are caused by an increase in the percentage of carbon dioxide in the atmosphere, which absorbs heat radiations and prevents them from escaping the atmosphere.

This is the primary cause of the constantly rising atmospheric imbalance, which results in repeated occurrences of natural calamities of various types. Humans' risky practices and uncontrolled exploitation of natural resources have often disrupted the equilibrium of the environment by contaminating the composition of the air, resulting in the depletion of the critical ozone layer and acid rains. The observable wavelengths of radiation from the sun quickly travel into the atmosphere and enter Earth. About 51% of this sunlight is absorbed by the soil, water, and plants on Earth's surface. Any of this energy is reflected back to the Earth's surface as infrared radiation. The longer wavelengths of outgoing infrared radiation from the Earth's crust are absorbed by water vapor, carbon dioxide, nitrogen, and other trace gases in the atmosphere. The infrared light is then released by these molecules in both directions, both outward toward space and downward toward Earth. This mechanism generates a second stream of energy to warm the soil – visible radiation from the sun and ultraviolet radiation from the atmosphere – causing Earth to be colder than it would be otherwise. This is known as the natural greenhouse effect, and it holds the Earth's surface global temperature at around 15°C (59°F). When greenhouse gas concentrations rise, more infrared radiation is captured and released back onto the Earth's atmosphere, resulting in an intensified or amplified greenhouse effect.

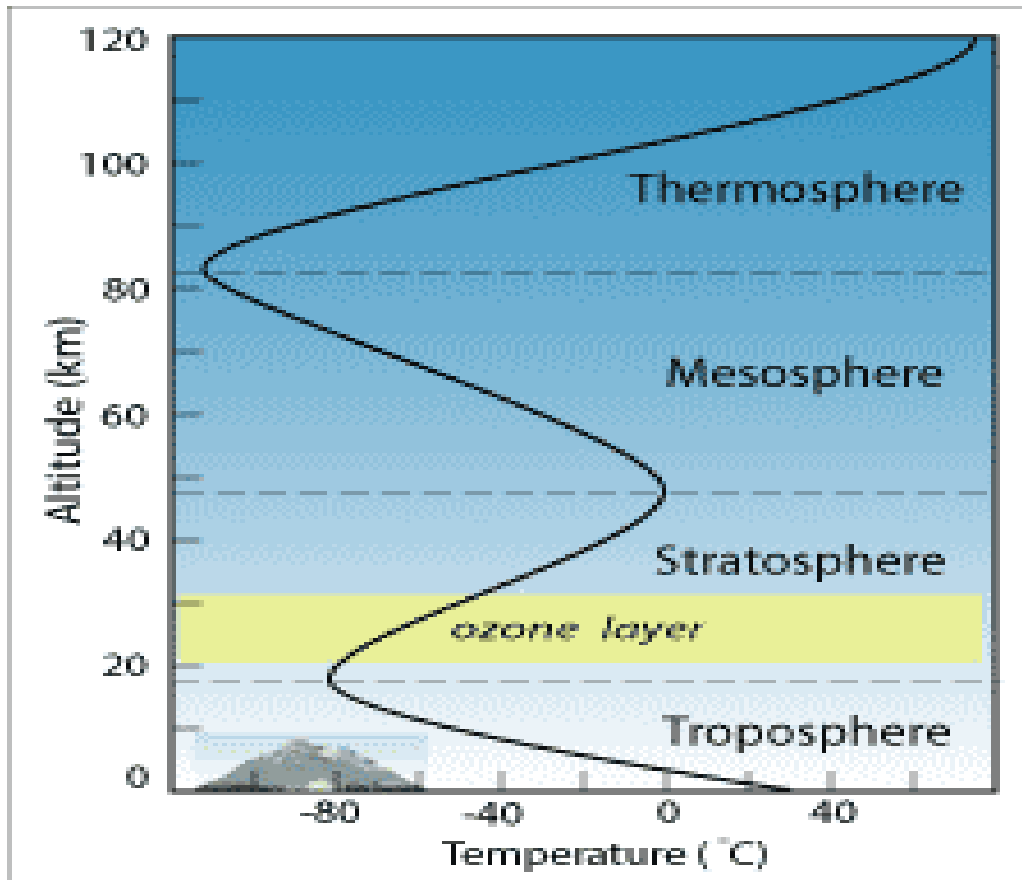


Fig 1.3: Earth Atmospheric Layer (<http://www.ces.fau.edu/nasa/>)

1.3 Climate and Atmosphere

Climate refers to the short-term state of the atmosphere at a given time and place. Atmospheric pressure, temperature, solar radiations, relative humidity, precipitation, wind direction, and cloud cover are all important variables in determining this transient state of weather. Climate, on the other hand, is characterized as a combination of those transient weather conditions that have prevailed at a location over a long period of time (on an average 30 years). Aside from the factors listed above, geological characteristics such as height, ocean, lakes, and so on influence a region's weather and climate. Weather is a natural occurrence that exists in the lowest strata of the atmosphere, known as the troposphere, and extends up to 8km above the Earth's surface. The

troposphere is the area where clouds form and precipitation occurs. Local climate and atmosphere have always been the most influential influences in determining human settlement, agriculture, and lifestyle patterns. Climate instability and reoccurring unforeseen natural disasters have culminated in constant human concern. There have been several studies on designing technologies that can predict such phenomena and provide humans with enough time to brace for calamities such as cyclones, anti-cyclones, earthquakes, Earth quakes, hail storms, thunderstorms, ground slides, and several others. However, no mechanism has yet been established that can fulfill this function precisely. This dissertation is an attempt along the same lines. The science of changing weather and environment can have a significant impact on people and such research can aid in providing an in-depth overview of the causes of climate change and can suggest mitigation steps for the future. Our atmosphere is essentially powered by the equilibrium between incoming solar energy and outgoing Earth energy. The first law of thermodynamics, also known as the law of conservation of electricity, controls this energy balance. According to this rule, energy can be moved from one device to another in a variety of ways, but it cannot be produced or lost. As a result, any energy "loss" during one phase will be offset by the same amount of energy "gained" during another. The sun's incoming energy and Earth's released energy are nearly equal, maintaining the average global temperature within the small range that protects and sustains life as we know it. The unique atmosphere of Earth and its position in moderating our environment, as well as the equilibrium of incoming solar energy and outgoing Earth energy.

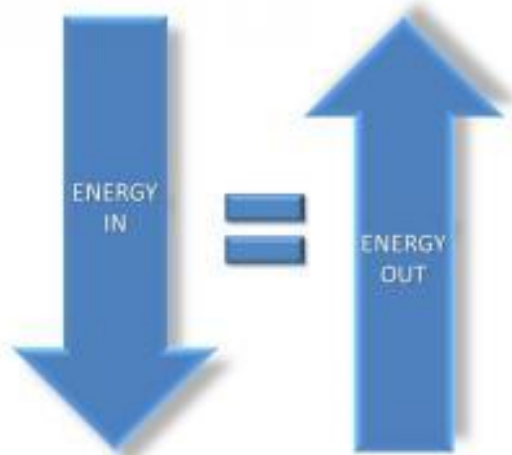


Fig 1.4: The First Law of Thermodynamics (<http://www.ces.fau.edu/nasa/>)

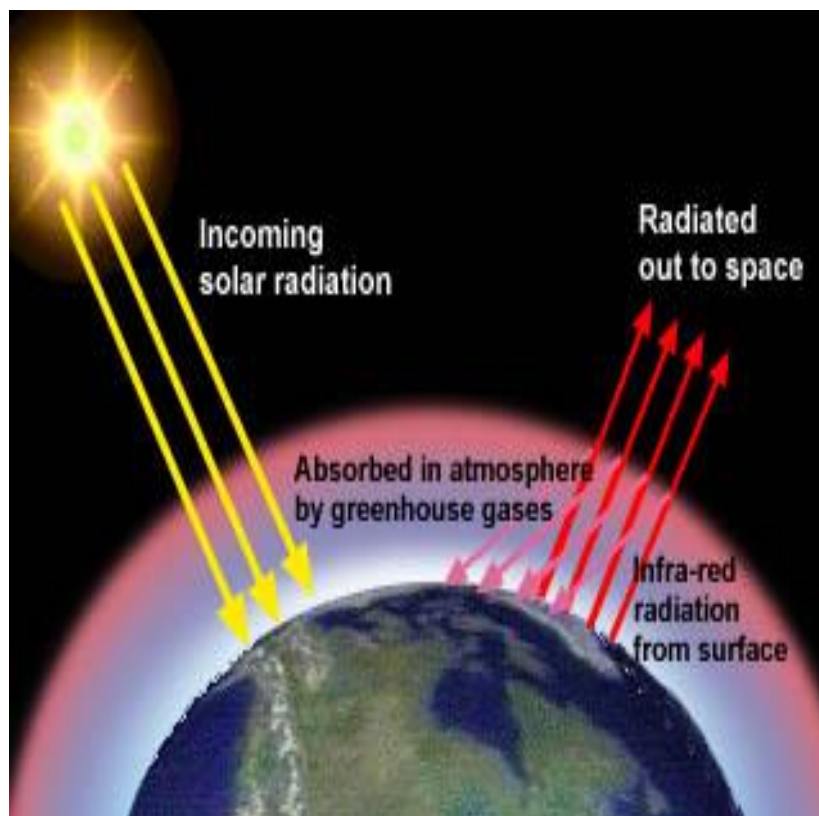


Fig 1.5: Effect on Earth Climate (<http://www.ces.fau.edu/nasa/>)

1.4 Geomagnetism on Earth

Geomagnetism refers to the magnetic properties of the Earth. The magnetism of the Earth is caused by the dynamo operating in the Earth's centre. The collision of this magnetic field with the plasma of the ionosphere produces a cavity around the Earth known as the magnetosphere. The magnetosphere is the area of space around the Earth that is dominated by the Earth's magnetic field which reaches several thousand kilometers into space. Geomagnetic events are the result of changes produced in this area as a result of solar activity intrusion. Subsequent research has proved that solar events such as Coronal Mass Ejection (CME) and Solar Wind have a significant effect on the geomagnetic environment, creating a number of geomagnetic activities. Previous experiments and tests have demonstrated that geomagnetic behavior is closely linked to solar activity. The magnetosphere acts as a defensive cover for the Earth, shielding it from the Sun's dangerous radiations. As a result, it is often regarded as the primary element that makes the Earth habitable. Time-dependent magnetic-field fluctuations caused by ionosphere and magnetosphere currents produce electric currents in the crust, seas, and mantle. Internal magnetic fields are produced as a result of these currents. The skin depth at which induced currents diffusively penetrate is determined by the subsurface electrical conductivity of the Earth and the strength of the overhead magnetic-field variations. Magnetic fluctuations of intervals ranging from a second to tens of minutes, for example, penetrate approximately 20–100 km into the crust. Of note, an observatory tests the overall magnetic field, which is a superposition of the external inducing field and the internal induced field. Mathematical isolation between the two necessitates a huge number of simultaneous observations, densely spread around the Earth's surface; this challenge is not well matched to the comparatively sparse distribution of magnetic observatories. As a result, extensive geographic analyses of Earth's conductivity structure often include the deployment of temporary sensor arrays to test both the magnetic field at the Earth's

surface and the generated electric field in the crust. Direct inspection of observatory data will provide qualitative insight into geomagnetic induction. Figure 4 depicts magnetograms collected from four European observatories during a large magnetic storm. Each observatory displays magnetic field H has a similar difference. The most of it is the magnetic signature of a large-scale, overhead ionospheric and magnetospheric current system that was maintained during the storm.

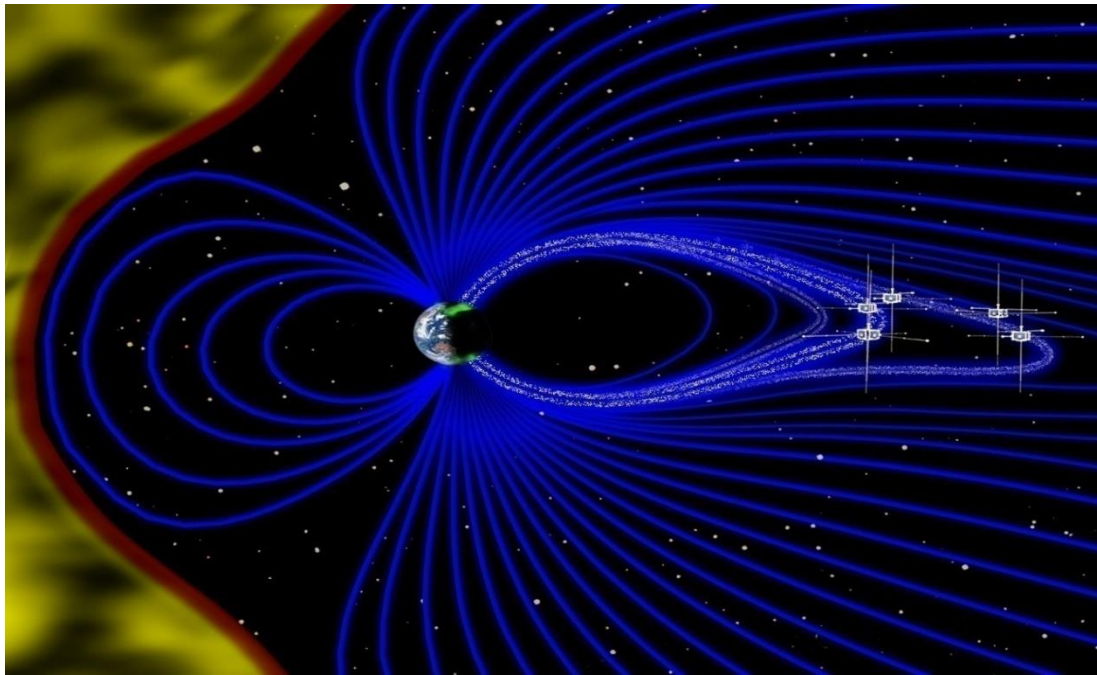


Fig 1.6: Geomagnetism of Earth (<http://www.ces.fau.edu/nasa/>)

1.5 Geomagnetic Storms:

Disturbances in the magnetic field are created as a result of high strokes of solar wind and solar flares to the bubble of magnetic field around the Planet, which can be the source of geomagnetic storms depending on the strength of the disturbances. Solar activity is largely responsible for these storms. Another element that influences geomagnetic storms is the Coronal Mass Ejection (CME). CMEs are solar phenomena that occur when a large volume of plasma from the Sun

enters the magnetosphere, an intense phenomenon causes geomagnetic storms. Solar activity and the interplanetary magnetic field (IMF) have been proven to be the key sources of geomagnetic storms. It's because of the effective transfer of energy from solar winds to the magnetosphere. This massive amount of energy causes dramatic changes in the current and plasma in the magnetosphere, resulting in hurricanes. Extremely strong solar winds are only successful when their period is very long on a time scale. The geomagnetic storm phenomena was developed by Chapman and Ferraros (1931). They illustrated that the emission of plasma clouds is often correlated with the Sun's solar flare. This released plasma begins to move through the Earth at a certain velocity and penetrates the Earth in 113 days. This plasma cloud collides with the magnetosphere, compressing the Earth's magnetic field and thereby increasing the magnetic field's effect. This disruption in the Earth's geomagnetic field will induce an abnormality in the Earth's atmosphere. As the study shows, it is crucial to comprehend the dynamics of the solar-terrestrial system, which are caused globally by fluctuations in the Earth's magnetic field. Furthermore, such changes in space conditions can result in life-threatening problems and disruptions to Earth's communication systems.

1.6 Geomagnetic Index

Geomagnetic indices have investigated to study and understand fluctuations in the Earth's magnetic field caused by irregular events such as the coupling of solar wind and the magnetosphere, internal shifts in the magnetosphere, and the coupling of the ionosphere with the magnetosphere. K-index is used to analyze the horizontal portion of the Earth's magnetic field. The Kp and Ap indexes can be used to measure and calculate the Earth's daily average magnetic activity. The Kp index and the celestial K-index are also very good metrics for determining the severity of geomagnetic storms. Since this index is a very significant indicator of any turbulences

happening in the Earth's magnetic field, it is used to issue geomagnetic storm alarms and notifications. K_p is the average normalized K index from 13 geomagnetic observatories located between 44° north and 60° south latitude. The letter 'K' is derived from the German word 'Kennziffer,' which means 'characteristics digit.' In 1938, Julius Bartels invented the word "K-index." The A_p index measures the overall amount of geomagnetic activity over the globe for a given time span. This index is determined based on changes in the geomagnetic field induced by currents swirling in the Earth's ionosphere and magnetosphere. The A_p index is a daily average degree of geomagnetic activity indicator.

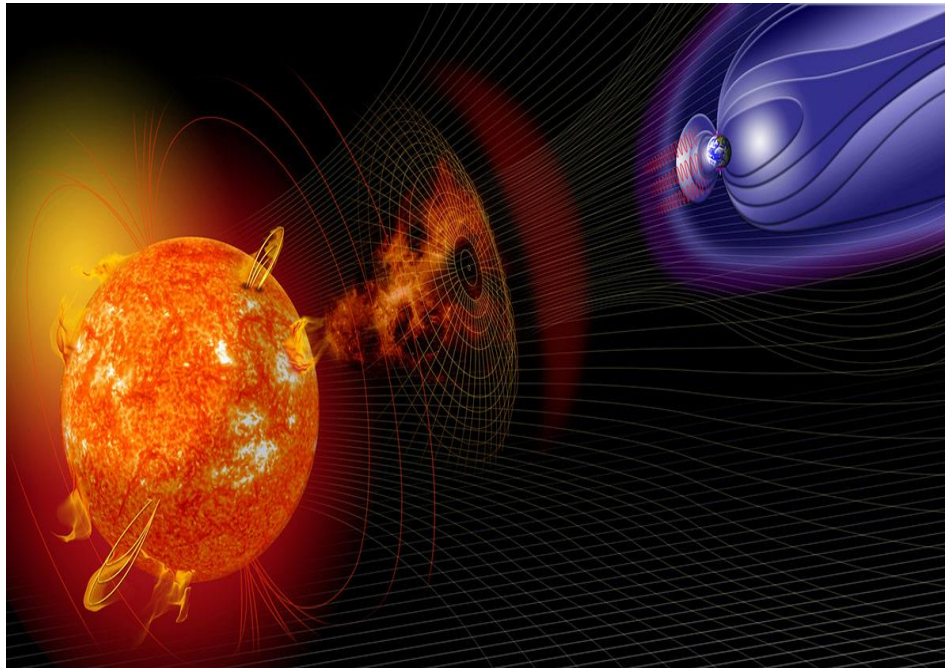


Fig 1.7: Geomagnetic Storms (<http://www.ces.fau.edu/nasa/>)

1.7 Electric Field of Atmosphere

D'Alibart, a French physicist, revealed the presence of an electric field in the earth's atmosphere in 1752. Later, in the month of June 1752, it was studied by the well-known personality in this area, Benjamin Franklin of the United States, who deduced the same effects of atmospheric

electric phenomena. Many observations have been conducted since then to interpret and conclude the electrical nature of the Earth's atmosphere. In 1753, a physicist from the United Kingdom, John Canton, conducted an experiment and concluded that the air is positively charged with respect to the earth's atmosphere under natural weather patterns, and that improvements have been observed in various meteorological phenomena and weather conditions. Another French physicist, L. G. Lemonier, studied the relationship of various patterns of atmospheric electric field in different weather conditions and confirmed that atmospheric electric field has some pattern relating to different weather conditions and came to the conclusion that electric field is a permanent feature of the earth's atmosphere. Later, C. A. Coulomb studied the atmospheric electric field as part of an attempt to better explain the conductive quality of air. When he opened a well-insulated conductor to sunlight, he discovered that the conductor quickly lost its charge. He came to the realization that air is conductive enough in nature to take the charge along with it. In terms of the charging process of the earth's atmosphere, Alessandro Volta suggested a theory that the transportation of charge from the earth's surface to the atmosphere occurred by the evaporation of water found on the earth's surface. As the water vapors pass upward, the positive charges are taken up to the Planet's atmosphere, while the negative charges linger on the Earth. As a result of the separation of positive and negative charges, an upper earth atmospheric potential is created. Unfortunately, this study was deemed inapplicable, and A. Peltier proposed a new model of this study in which the planet is a large source of negative charge, and these charges move upward to the earth's atmosphere with water vapor. The concentration of negative charges in the atmosphere is smaller than on the earth's surface. And the smaller the concentration of negative charge in the environment with respect to the earth's crust, the more positively charged the atmosphere is with respect to the earth's surface.

Lord Kelvin conducted a critical study of the “water dropper” electric field sensor in the mid-nineteenth century. He discovered a connection between the atmospheric electric field and various weather conditions through his experiment. He claimed that observing the electrical indication of the earth's atmosphere will easily forecast the weather. With the observation of diurnal fluctuations in the electric field, temporal variations have also emerged. Wilson proposed in 1906 that diurnal changes in electric field are governed by a global cause or phenomena, such as a global thunderstorm. The transparency of the variations, however, was determined by the local earth's atmospheric activities. The most critical parameter that can be calculated to gain a better understanding of the atmospheric electric field is air earth current. This arrangement of positive charge in the atmosphere and negative charge on the ground generates an electric field, which retains electrical energy. The global electric circuit involves the ambient electric field. Alternative models for the global electric circuit exist, some of which assume that the Earth is highly negatively charged.

The electrification of the environment is caused by a variety of causes. However, the presence of ions in the atmosphere is the primary cause of atmospheric electricity. J. Elster and H. Geitel (1899) suggested a definition of positive and negative ions as charge carriers in the atmosphere to describe atmospheric earth conductivity. Tiny ions are the most critical in transferring charge in the atmosphere. The presence of gamma rays and naturally occurring radioactivity is largely responsible for the ionization of the lower Earth atmosphere (60 km above the earth's surface). The Sun is a vast and persistent source of cosmic rays composed of positive and negative electrons. Any of the negative charge penetrates the upper Earth atmosphere and is captured by water droplets and dust particles on the earth's surface, while the positive charge is kept out by the air. In fine or natural environmental conditions, the air above the Earth's atmosphere is

typically positively charged with respect to the Earth's surface. Cosmic rays are the primary cause of ionization in the Earth's atmosphere.

1.8 Challenges Relate for Atmospheric Electrification

The sun's high-energy beams often ionize the bonds of nitrogen and oxygen in the upper atmosphere. This results in the formation of free electrons and strong positively charged ions. Because of their lighter mass, free electrons can be kept back by the environment, while strong positively charged ions can only live in the lower Earth's atmosphere. Previously, the effect of ionization on atmospheric electricity was explored. For each source, the ionization rate induced by GCR, EEP, SPE, and Rn222 varies according to altitude and latitude. The energetic electron-driven ionization increases with height to a limit in the mesosphere/thermosphere, while the maximum for GCR is about 18 km and then decreases with height. The Rn222 induced ionization is greatest in the boundary layer regardless of latitude, but with a geographical trend related to radon emission. The most important force affecting the Earth's atmospheric electricity is naturally occurring everyday radioactivity on the Earth's surface. This causes daily ionization across the ground area and has the ability to penetrate the lower Earth's atmosphere up to one kilometer above the Earth's surface. Nuclear radiations emitted from radioactive elements found in soil and rocks ionize the air above the Earth's surface. Radioactive gases produced by radioactive element decay are transmitted horizontally and vertically and contribute to ionization at a wide scale. Nuclear experiments conducted in the atmosphere are also seen as a major cause of ionization. Water plays an important role in ionization only on the surface because it serves as an opaque medium for radioactive radiations. The nuclear activities have had little effect on the atmosphere above the bodies of water. Ionization of the Earth's atmosphere is often governed by solar events, which are not very common. Solar storms, which intensify towards the Earth's

surface during coronal mass ejection, are also a source of atmospheric electricity. Long-term solar interactions induce variations in the atmospheric electric field, which occur as a result of modulation of the force of the solar magnetic field, which determines the amount of cosmic rays penetrating the Earth's atmosphere. At high latitudes, variations are caused by the interaction of the solar wind with the geomagnetic field, resulting in a differing electric field ranging from 30 to 100KV per meter, based on the magnetosphere and solar wind. Cosmic rays from deep space are continually bombarding Earth. Cosmic rays have a direct effect on the electrification of the Earth's atmospheric electric field, which reacts with the atoms in air and induces ionization, resulting in an avalanche of secondary ions or secondary cosmic rays, and creates a runway for ions from the lower Earth's atmosphere to the ionosphere. This action has a significant impact on the thunderstorm discharge. Thunderstorms act as a broad steady reservoir of electric potential in the atmosphere. If the situation is very advanced, cloud electrification occurs very quickly during a thunderstorm. Thunderstorms contain a potential difference of more than 100MV, any method of separating positive and negative charges Positive charges are transported to the storm cloud's peak, while negative charges are transported to the Earth's lower atmosphere. As a result, negative charges penetrate the Earth's crust, which becomes negatively charged in comparison to the atmosphere. This charge divergence produces a vast amount of electric potential (electric field), and the difference of electric field creates a steep curve. Lightning is a natural phenomenon of electrostatic discharge and sound. Good charges are carried upwards in the cloud during lightning strikes, while negative charges are transported downwards. The cause of this positive and negative charge drift is still being studied. The potential disparity depends according to the size of the cloud. If it occurs within the same cloud, it is referred to as intra cloud

discharge; if it occurs within two or more clouds, it is referred to as inter-cloud lighting. When lightning hits the Earth's atmosphere, this is referred to as cloud to ground discharge.

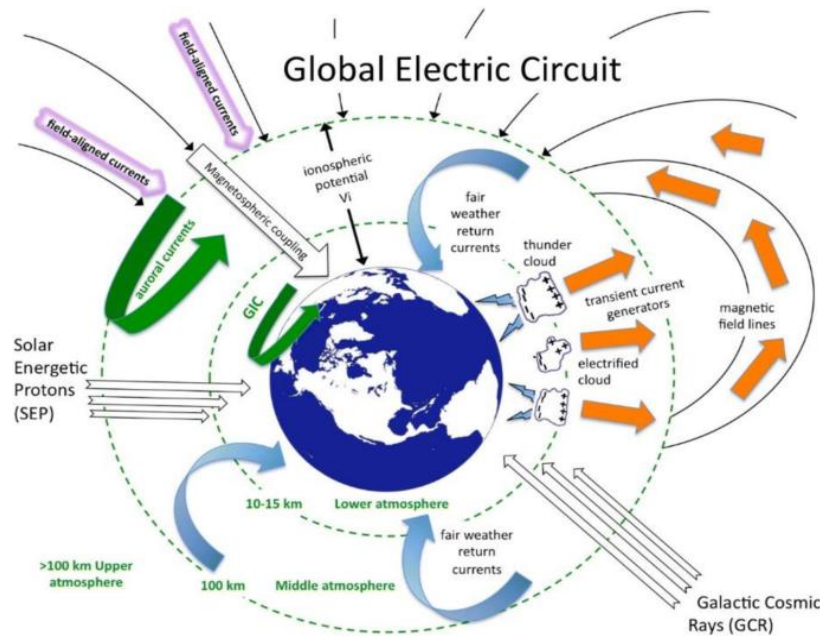


Fig 1.8: Factors Affecting Global Electric Circuit (<http://www.ces.fau.edu/nasa/>)

The theory of Wilson's global atmospheric electrical circuit concept is still regarded as the best explanation for the global variation of PG and JC, due to the increasing weight of observations in agreement with the main principles of the theory, the details of which will be discussed in this section. Columnar Resistance During fair weather (away from any local sources of charge separation), the conduction current density JC is related only to the ionospheric potential. Since JC is the most fundamental parameter of the global circuit measurable from the surface due to it being largely unaffected by local surface conditions (e.g. Dolezalek, 1978), it offers the best method of global circuit monitoring. For this, the variation of RC must either be known or assumed to be negligible for the diurnal variation of JC to represent the strength of the global circuit via ionospheric charging by global thunderstorm activity. It is therefore of significant importance to investigate changes in RC at all timescales and under different conditions. One of

the principal components to the Wilson theory of a global electric circuit as that of the large but finite electrical resistance between the ionosphere and surface. This resistance termed the columnar resistance, RC , by Gish (1944) can be determined experimentally by measuring the vertical profile of total air conductivity (Chapter 1). This was first done using the stratospheric balloon flight of Explorer II in 1935 (Gish, 1944), obtaining a columnar resistance of the order $100\text{P}\Omega\text{m}^{-2}$ (Sagalyn and Faucher, 1954). The relative contribution of the atmosphere to this columnar resistance was strongly height dependent, with Sagalyn and Faucher (1954) reporting columnar resistances of between $90\text{-}250\text{P}\Omega\text{m}^{-2}$, of which 40-73% originated from the surface boundary layer. These observations have been used to explain the large air-earth current densities found at the summit of mountains (e.g. Kasemir, 1951 reported a JC of up to ten times higher than at sea level) where the mass of atmosphere above is less (and generally cleaner). The first investigation of the diurnal variation of RC was made by Sagalyn and Faucher (1956) using equipment carried by balloons to measure the total conductivity profile from the surface to 4.57km (Figure 2.3). The shape of the profile was demonstrated to be a function of the height of the boundary layer, with the upward transport of aerosols by turbulent mixing around midday increasing the total aerosol number concentration in the column and hence RC . The slope of the curve and the 40% daily fluctuation are roughly in alignment with current estimates of the diurnal cycle and variation of boundary layer turbulence (Hoppel et al., 1986). Tropospheric balloon flights measuring negative conductivity between 1957-1962 were used to calculate the seasonal variation in RC near Tokyo, Japan (Uchikawa, 1972). It was found that a distinct seasonal variation existed, being proportionally greater in the winter (December) than the summer (June). However, no seasonal variation was found over the Hachijojima, an island in the Pacific Ocean, 200km south of Tokyo, making the clean-air site more suitable for assessing

seasonal variation of VI using measurements of JC as any seasonal be attributed to the greater influence of air pollution near Tokyo than at Hachijojima, as aerosol removes small ions in the column by attachment, increasing RC. The seasonal variation in RC over Tokyo varied in the opposite sense to the air-earth current density calculated in the stratosphere by the balloon soundings, but only half the relative amplitude. This difference in variations of RC and current density was approximately equal to the variation in VI observed in Weissenau, Germany, thereby suggesting an Ohmic relationship (Uchikawa, 1972). The Ohmic assumption between JC and VI was used more recently by Harrison (2005b) to calculate RC using coincident JC data from the Wilson apparatus at Kew, London and VI soundings from Weissenau. The RC over Kew varied between ~ 50 to 400 Pm^{-2} . The reason for this variability was not straightforward, with cosmic ray-induced aerosol formation being a suggested factor. A method of remotely detecting the total number of cluster ions in the atmospheric column using infrared absorption was investigated by Aplin and McPheat (2005). Remote sensing of total number of ions in the atmospheric column.

1.9 Source of the global circuit

More work was done on the source term of the global circuit by Krumm (1962) who reinvestigated the relationship between global thunderstorm area and the Carnegie curve using more modern and extensive data (from the 1956 World Meteorological Organisation thunder days dataset) than available during the first investigation by Whipple (1929). Although the variation found by Krumm (Figure 2.5) appears to have a similar minima time as the Carnegie curve (Figure 2.1), the maximum number of global of thunderstorms appears to be at a sooner time than that found by Whipple (Figure 2.6) and the Carnegie curve, although an offset between thunderstorm area and the Carnegie was also acknowledged by Whipple. Reasons for this discrepancy between the Whipple (1929) and Krumm (1962) analyses seem to be due to the

inclusion of oceanic data with a maximum of around 13UT (unlike Whipple who included no maximum time for oceanic storms) and the similar maximum amount of Asian/American storms used by Krumm (Figure 2.5), with Whipple using a lower occurrence of Asian storms relative to American, although conversely, the annual global thunder days used by Krumm (Figure 2.4) still appear to imply a greater occurrence of American storms. The differences between Whipple and Krumm's thunderstorm estimations are likely to be a result of improved spatial representatively of global thunderstorm occurrence due to a longer recording history of more frequent and reliable meteorological stations in 1959 than those available to Whipple in 1929. It is therefore of interest that the departure of estimated global thunderstorm area produced by Krumm (1962) from the Carnegie curve is greater than that of Whipple (1929).

CHAPTER 2

Review of Literature

Review of literature

Since the environment is also a critical factor in scientific research and study. A variety of significant works have been proposed in this regard using different analytical methods and technologies. Some of the latest notable study, as well as a summary of previous work, is outlined below:

A. Kh. Adzhiev. 2015, The variation of the near-surface atmosphere's electric field has been studied. Investigations project that global fluctuations in the electric field strength of the near surface atmospheric layers can be recorded at mountainous stations. The findings suggest that the morning low, as well as the daily and evening maximums, constitute the diurnal direction of the electric field. Over the spring-winter season, the minimum value rises

Akinyemi M L. 2014, This dissertation contains a short discussion of the lightning phenomena and atmospheric electricity. How does the lightning phenomena impact the telecommunications grid, and what precautions can be taken to protect it? The research also included a few protective equipment. Some examples include: 1. Static charge dissipating device 2. Strike-stopping mechanism

Gwal A.K. 2012, A research has been submitted to link changes in the NmF2 (maximum electron density of the F2 layer) parameter to seismic activity. Data from two Ionosondes are obtained from two separate sites. One is from the Earth quack preparing zone, and the other is from beyond. Anomalies in NmF2 parameters before the Earth quack was discovered using

correlation techniques. Perturbations in the F-layer have a close correlation with the seismic electric field generated by Earth quacking. Anomalies in the F-layer may be caused by an inflow of radiation from the Earth into the ionosphere.

Valentino Straser 2011, The number of radio wave disturbances detected on the ground has been analyzed from continuous observation by the satellite system in Italy both before and after the Earth quack. During the Earth quack, there was a sudden drop followed by an unexpected rise. Just a few minutes after the main shock, the gravimeter detected a significant decrease in the gravitational field, which has been interpreted as a transient swelling of the Earth's crust caused by the seismic shock's force.

Zhang 2012, DEMETER satellite registered approximately 69 powerful Earth quacks between 2004 and 2010. Since extensive research, it has been determined that the perturbations in the ionosphere are spread over a wider region prior to the Earth's quack. However, as the observation time reached the Planet quack event, the anomalous region shrank and perturbations still occurred in the nearest orbit apart from the epicenters.

Wei He 2011, On the basis of atmospheric electric field data and lightning position data, an analysis of the lightning alert and forecasting phase was performed. According to the study, the interval between the lightning site and the atmospheric electric field instruments is a significant factor in alert and forecasting. The combined system of electric threshold warning and differential electric threshold warning is more efficient in lightning warning and forecasting, resulting in less damage

Guha 2010, In Tripura, Northeast India, a comparative analysis was carried out to measure the fair weather atmospheric electricity parameter. The diurnal variance of E (Electric field intensity) and Jx (Electrical conductivity) has been studied and found two different peaks between

14:00:00 UTC and 20:00:00 UTC, as well as a minimum near 03:00:00 UTC. The average vertical potential gradient is 108 V/m, and the air Earth current density is 1.85 PA/m². At ground level, the average bipolar ambient electrical conductivity is 19.6 FS/m. With a correlation coefficient of 0.96, E and J_x have an impressive positive correlation.

Based on graphical analysis, it has been proposed that the vertical distribution of Convective Available Potential Energy (CAPE) can also play a role in the absence of severe weather at ground level despite the presence of large lightning flash rates. All electric field changes after a lightning discharge indicated the presence of strong lower positive charge centers (LPCC) in the active and dissipation zones. 2010 (Pawar et al.)

(R Giles Harrison. 2010). According to reports, the solar wind influences the flux of interstellar cosmic rays. The main cause of electrical conductivity over the ocean and high above the continents is cosmic ray ionization. Differential solar modulations of the cosmic ray energy spectrum affect cosmic ray ionization at different latitudes, allowing the overall atmospheric columnar conductance to change. This redistributes current flow in the global atmospheric electrical circuit, as well as the local vertical current density and the associated surface potential gradient. At cosmic ray limit, all lower troposphere atmospheric electric concentrations are greatly increased, with a relative improvement greater than cosmic radiations

A link between the monitored area and the preparatory stage of a powerful intermediate Earth quake is formed in the Vrancea region by deploying a complex geophysical monitoring and recording system at the Plastina observatory in Romania. Moldovan and colleagues (2010)

The development of a natural laboratory is being researched in order to study the lightning effect on electric overhead lines in an operational distribution network as well as ambient energy in a

high stormy environment. And the key goal of this lab is to perform an experimental analysis of distribution lines exposed to practical conditions of non-ideal conducting and flat terrain, as well as the region's actual lighting parameters. (2009) (Jimnez et al.)

Using the atmospheric electric field monitoring network (REMCEA) in the Curitriba PR area, behavioral shifts in the local electric field were studied in relation to other meteorological parameters such as relative humidity and wind speed. The study's results clearly indicate that atmospheric pollution has an effect, as Ohm's law notes that an electric field increases as conductivity decreases. There is also a correlation between wind speed and electric field. Both parameters are inversely proportional, which means that the electric field intensity reduces as ion mobility increases. (Jusevicius and colleagues, 2009)

Researchers are investigating the surface fair weather possible gradient and its various trends. Data from 13 months (July 2005 – July 2006) at a resolution of 10s was collected and analyzed over the tiny tropical island station Suva. Following research, it was discovered that the average PG on fair weather days was about 139 V/m. Local meteorological parameters had a negligible impact on PG. PG was still higher in the dry season than in the rainy season. In contrast, it has been recorded that during the wet season, lightning activity peaked around 2000LT and increased, indicating that regional thunderstorm activity has no clear relationship with the local fair weather and PG. (Vickal V Kumar et al. 2009)

Data was collected and processed around the clock using an electrostatic field mill (JCI 131) positioned on a 2m column. Following study, it was expected that the atmospheric electric field would exhibit varying trends in turbulent, apart from the same meteorological conditions The

potential gradient varies from little steady-state augmentation in fog to major steady-state enhancement of fog and significant variations in thunderstorms. (Bennett and colleagues, 2008)

Data from the DEMETER satellite are used to study ionospheric perturbations. Prior to the Earth quack, DEMETER reported some odd findings over a seismically active area. Any peculiar characteristics of waves, plasma, and energetic particle fluxes were observed at the epicenters of future Earth quakes. These results emphasize geoseismic behavior and expect a true association between ionospheric perturbations and geoseismic activity. (2006) (Parrot et al.)

Preliminary findings of atmospheric electric field observations at Maxico are described here in order to record the various phenomena of atmospheric electricity (S Pulinets. 2006).

At Kolkata, the ambient electric field and VLF sferics were measured, and the data was analyzed by correlating the results. The diurnal variation of vertical electric field has been found to establish strong communication with the diurnal variation of VLF sferics behavior. The deviations agree with the agreed unitary diurnal shifts in vertical electric field and thunderstorm incidence frequency curve, with a mean around 1900 hrs UT and a low around 0400 hrs UT (S S De. 2006).

A field mill built in Ziracco is used to provide a description and analysis of the Earth's electric field over the Friuli plain (UD). A common sequence of atmospheric electric fields revealed during stormy weather, including lightning strikes. During an ambient electrical discharge, the magnitude of the Earth's electric field quickly changes, and a spontaneous inversion is often observed. The importance of interpreting Earth electric field measurements at the ground is highlighted in this report. Bressan and colleagues (2004)

The atmospheric electric field fluctuations were compared using data from the Vostok station and the lightning flash strength for ten fine weather days in April 1998. There is no association between the 5 minute averaged values of electric field and electric flashes, according to the findings. The mean diurnal fluctuations of the electric field over a 10-day period are inconsistent with the mean diurnal variations of the corresponding electric currents over the same period (O A Troshichev. 2004).

To describe the fair weather situation, a relationship between Maxwell current and atmospheric electric field is also developed. The hourly averaged diurnal variance curves of Maxwell current and electric fields have two peaks during the chosen fair weather conditions. The first peak is caused by the local "sunrise effect," while the second peak is caused around 1900 UT, when global thunderstorm activity is at its peak. The correlation coefficient is strong for all fair-weather days, indicating that it must be a carbon emissions fair-weather day (Panneerselvam et al. 2003)

Long-term variations in the atmospheric electric field have been observed at Hungary's Nagyecenk geophysical observatory. The theoretical gradient estimated at the Eskdalemeir observatory in Scotland has seen a long-term decrease. This drop in PG implies a global change in atmospheric electricity caused by a decrease in cosmic rays. It is demonstrated at Nagyecenk, local effects are unlikely to have dominated a shift (F. Marcz. 2003).

The diurnal and seasonal variation of fair weather days is also observed and analyzed in order to examine variables such as emissions and space charge creation induced by large diurnal variation. The findings demonstrate that the electric field has a high persistent importance during the monsoon. Winter evenings have the highest value due to high atmospheric stability

conditions, while summer afternoons have the lowest value due to high atmospheric stability conditions (R. Latha, 2003)

At Maitri, Antarctica, the atmospheric electric field and conductivity of both polarities were measured. Since analyzing 21 fair weather days, it was found that the highest value of the atmospheric electric field was at 1300 GMT and the minimum was at 0100GMT. The second maximum can also be found at 1900GMT. The disparity between the diurnal variation curve at Maitri and also the uniform variation curve at the tides. The electric conductivity may not improve much during the day at Maitri or in the north atlantic. Electric conductivity has been found to decrease in cloud cover regions (C G Deshpande. 2000).

Using satellite data, researchers investigated the global atmospheric electric circuit and different parameters of control. It is expected that changes in Changes in conductivity produced by the time-varying presence of energetic charged particles are associated with changes in the global circuit and that solar wind can affect the global electric circuit by its effect on cloud microphysics, temperature, and dynamics in the troposphere. Here, a good picture of the variation in the global atmospheric electric circuit caused by aerosols is achieved (M J Rycroft. 2000).

Five field mill sensors curve is mounted on the AC160 Transall aircraft to measure ambient electrostatic fields in the vicinity and within connective clouds. In 1984, tests were made as part of the LANDES – FRONT trial. In the case of reasonably electrified cells, the calculation conducted with the redundant five simultaneous measurements indicates a very strong coherence with the uniform field model (P. Laroche. 1986)

A reciprocal relationship has been formed between solar activities in terms of Wolf numbers and the vertical gradient of electro atmosphere potential measured in the geophysical observatory of Macerata, the geomagnetic field measured in the nearby town of Aquila, and thunderstorm activity over the entire Italian region. These parameters behave in an anti-parallel manner. Despite their anti-parallel behavior, the maxima and minima of these two parameters do not always coincide in time, but are replaced by the variable duration. Murri and colleagues (1973)

The electric field was continuously recorded in this analysis using automated instrumentation. The data was collected from five remote stations that are geographically isolated and situated under different environmental environments. It has been discovered that using several locations allows for the detection of local anomalies. The conclusion has been reached that all variations discovered to be universal to all locations may be the result of a large-scale phenomenon with global implications (R. V. Anderson and Eva Mae Trent. 1969)

During the summer of 1958, atmospheric electric measurements were obtained from the top of Mt. Washburn in Yellowstone Park, Wyoming. The electric field, positive and negative electrical conductivities, charge on individual droplets, scale and charge of multiple cloud droplets, as well as the applied voltage current from the Earth's surface correlated with strong electric fields underlying thunderstorms were all measured. The electric field was calculated to be greater than 600V/m (W.E. Cobb. 1967).

In this article, the author discussed his thesis on different field measurement methods, as well as a comparison of those methods. It has been discovered that an independent cylindrical field mill is an ideal instrument for measuring the electric field in the atmosphere (Harold Kirkham)

This thesis looked at a recent phenomenon that happens three hours before and three hours after the related powerful Earthquake's hypocentral period. A field mill data set is used to study this phenomenon. In this case, the electric field displays a declining pattern over a two-hour cycle. This pattern abruptly changes about eleven minutes before the hypocentral moment, and the AEF level has been nearly constant for about 15 minutes. The study of the reported data indicates a relationship between the number of recorded cases of this occurrence and the frequency of Earthquakes examined (Glavatovic Branislav).

Since 1950, the network of Roshydromet stations has continuously tracked the atmospheric electric field and air polar electric conductivity. Data analysis indicates that variations in atmospheric electric parameters are exacerbated by both human combustion of aerosol gases and radioactive substances emitted during nuclear tests. As a result, it has been expected that further changes in temperature would result in changes in atmospheric electric parameters near the Earth's surface (Popov I B).

CHAPTER 3

Measurement of Atmosphere Potential Growth (PG) Variations at Local Climate Specification

3.1 Introduction

Atmospheric weather conditions are depend on reasonable local climate specifications or may be considered as perturbed weather conditions, Nearby variation of the Earth's atmospheric electric field is close to the outside of the Earth environment. It is enormously impact by extra-terrestrial or solar effects and these two components assume a significant part to frame earth atmospheric electric field potential. As aggravated atmospheric conditions, extraordinary climate conditions or extreme meteorological unsettling influences may be considered. Higher wind intensity, moisture, temperature, precipitation, or more are all rainstorm exercises that create aggressive climatic conditions in the near-earth atmosphere. Atmospheric electric field is unequivocally affected by wind speed, dampness and precipitation. Transient varieties in the barometrical electric field likewise happen in the fair weather conditions. Environmental electric field sensitivity changes in intensity or strength somewhat like controls during maelstrom. Precipitation, moisture, blast and wind intensity are the normal pointers of the annoyed atmosphere. These elements have such a great influence on the analysis of the electric field of the Earth's atmosphere. This part describes the observed atmosphere electric field influenced by certain forces that disrupt the climate. The atmospheric Global Electric Circuit (GEC) relationship with various metrological parameters can be detected through various climate change factors and it is criticality examine with multi tasking knowledge or by other effects. In any circumstance, there is indeed a significant scarcity of uncertain and constant measurements

of atmospheric electric field strength properties that have probably contributed to a lack of information of GEC as well as its interaction local atmosphere. At the surface, the ionospheric potential, vertical air-earth conduction flow, and ambient electric field are monitored. Last but not least, the predicted atmospheric parameters are known as Potential Growth (PG). PG is defined as the percentage of adjacent potential at height z to that height, $PG = dV(z)/dz$. During fair climatic times, PG is defined as optimistic and $E_z = -PG$ is associated with the vertical component of the environmental electric field. When estimated at contamination-free locations, for example, seas, mountain pinnacles, and Glaciers and under FW conditions, PG has the potential to represent variations in GEC. In comparison, for wide distances, PG is most likely the most naturally estimated ambient electrical limits. The resulting surplus of recorded and contemporary data for different areas helps to enhance atmospheric GEC understanding. In continental locations, which are not considered suitable for GEC monitoring for the most part, Experiences in PG surroundings are more plentiful than ones in moderately clean environments. PG is sensitive to the effects of neighboring continental sources, such as air pollution, space charge and signature radioactivity, which may alter or obscure the day-to-day and periodic GEC signal. In any event, these impacts do not preclude, PG estimated under perturbed weather conditions from seeing GEC highlights on some occasions or by averaging, thereby making mainland locations similarly beneficial in the understanding of GEC. In addition of taking into account the fact that PG is responsible for the impacts of airborne pollution, space charges and common radioactivity at mainland locations, as recently alluded. Bits of information in a number of various wonders, periods, or times, such as explosions, air pollution, perceivability, limit layer observation, natural radioactivity measurement, and seismic tremors, can also be provided through its analysis at such destinations. In comparison, in the discovery of significant

meteorological phenomena, the ease of PG estimations, Parts of atmospheric electric field data in a number of various phenomena, processes, or occurrences, such as storms, air pollution, deceivability, maximum surface observation, typical radiation measurement, and seismic tremors, can also be provided through its analysis at such destinations. In comparison, in the discovery of significant meteorological phenomena, the utility of PG estimations, Carnegie twist is an ordinary technique for separating times where PG corresponds to worldwide GEC along with varieties including local variables on hourly, occasional, and annual time scales.

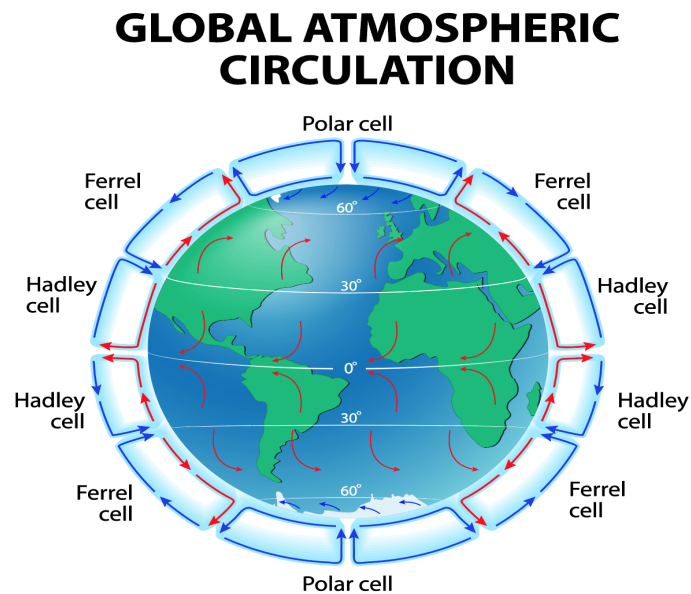


Fig 3.1 Atmospheric Global Circulation (<https://www.internetgeography.net>)

In this study, PG data is recorded from from June 2015 to May 2016 at station situated in the southern Balkans close to Xanthi, Greece. The nearest stations are Nagycenk, Hungary, a ways off 970 km and in Mitzpe Ramon, Israel, away from 1500 km. In addition to the integration of local PG climatology, the validity of the location in measuring GEC is investigated in this study. Furthermore, the possibility of deploying barometer estimates in assessing the step by step variation in PG is examined, and extraordinary concept is generated for the events when the

enhanced description corresponds with the expected occurrences of the GEC signal. Since this is a novel angle in the investigations of PG identified with atmospheric electric field, we intend to address this theme covers completely in future work. In contrast to the realistic atmosphere curves, the electric field diagrams recorded under disturbed atmospheric conditions provide an unusual contrast. Such curves could be considered almost as a context to correlate the normal atmosphere day with typical disturbances. The purpose of this chapter is just to develop up the ability to have these chronicles to forecast certain probable global electrical disaster.

3.2 Methodology and Dataset

In the present work datasets contains electric field strength measurements for each sensor on the Advanced Ground Dependent Field Mill network (AGBFM). The AGBFM network consists of 34 field mills, only 31 of which are operational as of 05/29/97. Such data were used in real time by the Launch Pad Lightning Warning System (LPLWS). Each field mill detects the electrostatic field strength overhead of the system using stainless steel plates (stators) that are respectively shielded and exposed to the current atmospheric electric field by a grounded device. The data is recorded at a rate of 50 Hz with a sensitivity of 4V/m. Fields of up to $\pm 32\text{kV/m}$ can be recorded with higher readings leading to a severe thunderstorm overhead.



Fig 3.2 Electric Field Mill Installation at Kennedy Space Research (Florida)

The symbol convention applies to the atmospheric probability curve where the fair weather region is favorable. The data is then converted into 50 Hz raw field mill data, which is divided into hourly files and 1 Hz data that is sampled from 50 Hz. The data is contained in separate day-to-day directories and includes data plots in postscript files at 1 Hz, 50 Hz, and 1 Hz. For all of the active field mills, each postscript file displays a time series of electric field intensity during the day.

An electric field metre (EFM Campbell Scientific Co., Utah, USA) has been installed since February 2011. An EFM sits in reverse on a 2-m tripod, surrounded by natural and man-made barriers such as trees, walls, poles, and cargo containers. However, since these obstacles are at least 30 m away and do not protrude higher than 18° above the horizon as seen from the ground at the EFM location, they really had no effect on the measurements (Campbell Scientific Inc. 2011). The PG values are symbolic if the distance between the measuring sensor and a field-

distorting disturbance is five times the height of the disturbance or three times the height for thin obstacles such as pillars. These criteria are met by our platform; other stations have similar site characteristics. Because the CS110 is a factory-calibrated field mill, no further tweaking is required for use (Campbell Scientific Inc. 2011). The calculation of a site-dependent correction coefficient, on the other hand as compared to an upward-facing flush-mounted installation, the elevated and reversed orientation of the EFM affects the effective gain. The coefficient was derived statistically based on the assumption that FW circumstances approximate to a theoretical PG value of 100 V m^{-1} . Select a set of reference FW days and divide the mean daily PG of each of these days by the usual FW–PG of 100 V m^{-1} to get a number of daily determinations. Finally, an overall correction coefficient was calculated as the mean of the 50% of regular determinations across the median, and it was used to correct the PG data. Because of the severe statistical technique utilised to define the PG values, they are seen in relation to the conventional FW–PG relationship (100 V m^{-1}). The comparison FW days are chosen from datasets that include features from the FW standard definition, such as cloud cover less than 3/10 based on the MOD08 D3.051 cloud dataset with a resolution of $1^\circ \times 1^\circ$, wind speed (WS) less than 3 on the Beaufort scale (4 ms^{-1}), no precipitation events.

Atmospheric Potential Gradient

The Atmospheric Potential Gradient (PG) is the vertical electric field present in the atmosphere, with positive values indicating a downward pointing field. The atmospheric potential gradient leads to an ion flow from the positively charged atmosphere to the negatively charged earth surface.

Measurements of atmospheric electric field were made in conjunction with PG using an instrument fitted with a Gascard II Edinburgh Sensor (Schumann Analytics, Germany) from June 2011 to May 2012, spanning 150 days through the seasons. A reference analyzer was used to calibrate the CO₂ analyzer. Using a 0.52 l s⁻¹ pump, ambient air was continually sampled from the same 2 m height position where the PG was calculated. Since June 2011, commercially available sensors put at the same site as the EFM have provided standard meteorological characteristics such as WS/direction, temperature, relative humidity, pressure, and precipitation. Wind speed and direction were measured using a Wind Sentry Kit, which comprised a three-cup anemometer and a wind vane with 0.5 m s⁻¹ and 5° accuracy, respectively. Temperature and relative humidity were determined using a 1.5 percent and 0.3-K precision thermometer/hygrometer, respectively (Model HygroClip S3; Rotronic Co., Switzerland). A 0.3-hPa precision barometer pressure sensor was used to measure the pressure (Model PTB110; Vaisala Co., Finland). The precipitation was measured using a tipping bucket rain gauge (Model 52202; Young Co., Michigan, USA). From February to May 2012, two additional temperature (T) sensors (HOBO Pro v2 T/RH U23-001; Onset, Massachusetts, USA) with sun shields at 2% accuracy and 0.2% precision were placed at 2.5 and 1.5 m heights to give the vertical temperature gradient (DT). Except for the additional T sensors, which ran at $f = 1/60$ Hz, all sensors ran at 1 Hz, and data were recorded as 1-min means. After that, one-minute PG data were utilised to measure 10-minute data, which was subsequently used to generate hourly means. At regular intervals, the data collecting PC communicated with the National Institute of Standards and Technology (NIST) time server. Wherever the phrase "local time" (LT) appears in the book, it refers to Coordinated Universal Time (UTC) + 2; hence, no Daylight Saving Time was observed throughout the summer. The data provided in the range from February 2011 to

December 2017. In the present studies data from June 2015 to May 2016 were examined in greater depth. It is the first complete year of constant PG calculations and statistics for any of the other variables so far.

3.3 Results

The analysis of the data collected on the mention days, and mean diurnal variations between perturbed weather conditions (PW)–potential gradient (PG) for each month of the period June 2015 to May 2016 at local climatic conditions.

- a) The magnitude of the atmospheric electric field is highly sensitive to the smallest perturbations in the local climate variations. The data substantiates this premise as wave behavior shows extreme disturbance under the effect of the perturbed PG values.
- b) Under the influence of extra terrestrial effect and perturbed weather conditions, atmospheric electric field undergo very sharp fluctuations with definitive sharp peaks and dips. A perfect correlation can be seen between the highest values of the PG and Atmospheric Electric field.
- c) The extra terrestrial disturbances also affect the range in the magnitude of atmospheric electric field drastically. These waves oscillate with very sudden and sharp crest and troughs in extreme positive and extreme negative directions.
- d) The most peculiar observation made in the behaviour of atmospheric electric field under the local climatic variation is the phenomena of wave inversion, which means the values of the magnitude of the atmospheric electric field falling in the negative direction, away from the earth with very high intensity which is never observed during the fair weather days. Such values fall as low as -20.70 kV/m.

- e) The range of the magnitude of the atmospheric electric field during perturbed conditions is much broader as compared to those on fair weather days. The values of the atmospheric electric field tabulated in this chapter show a range of +20.897 to +0.25 kV/m (+20.647 kV/m) which is a much broader range as compared to the values obtained in fair weather days which fall in the range +1.11 to +0.24 kV/m (+0.87 kV/m).
- f) The comparative plotting of the values of the perturbed weather conditions (PW)–potential gradient (PG) with the magnitude of the atmospheric electric field depicts a very high correlation value as much as 0.605 which is a considerably high value.

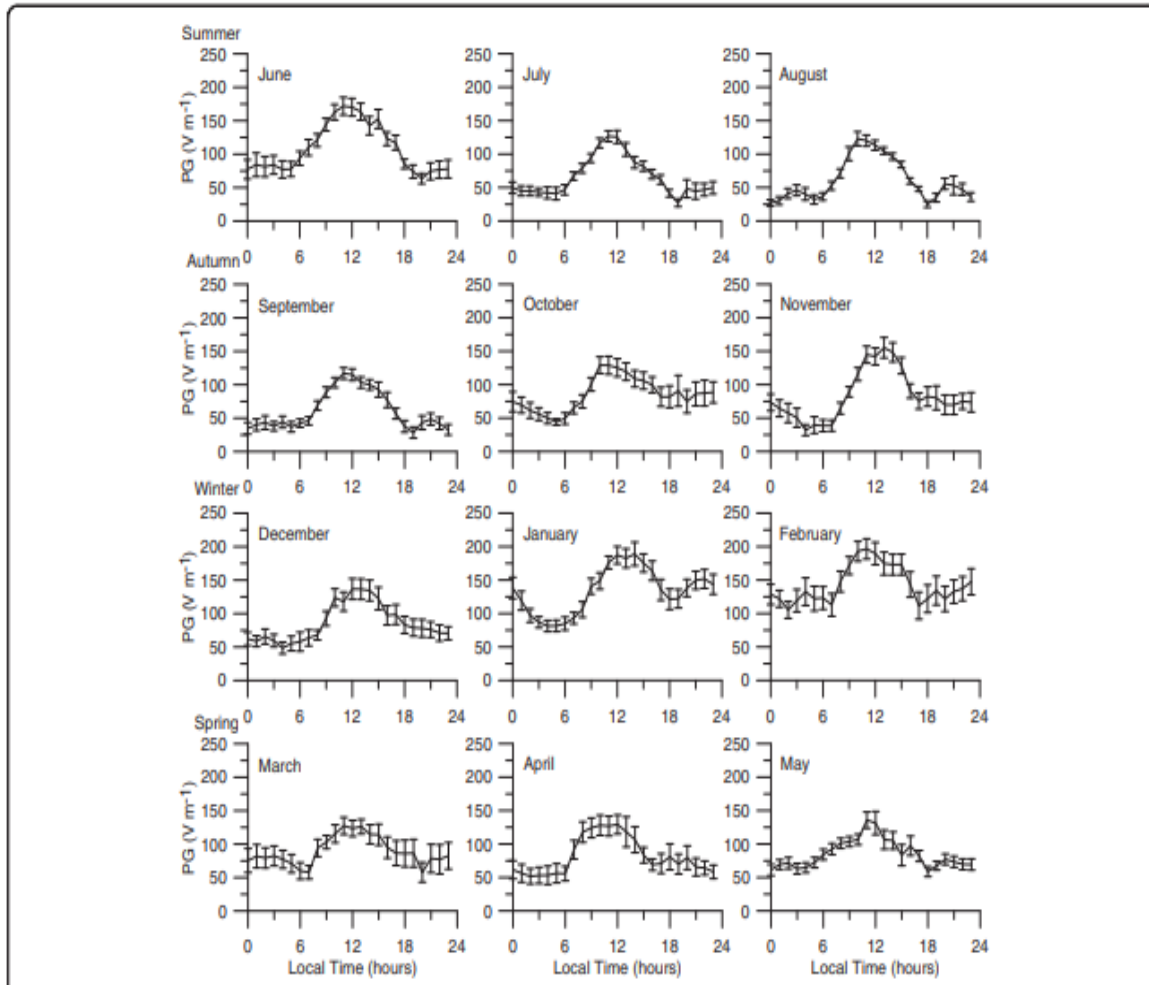


Fig 3.3 : Mean diurnal variations between perturbed weather conditions (PW)– For each month from June 2015 to May 2016 the potential gradient (PG) was calculated. Months are aligned according to the season. Error bars are displayed on the graph

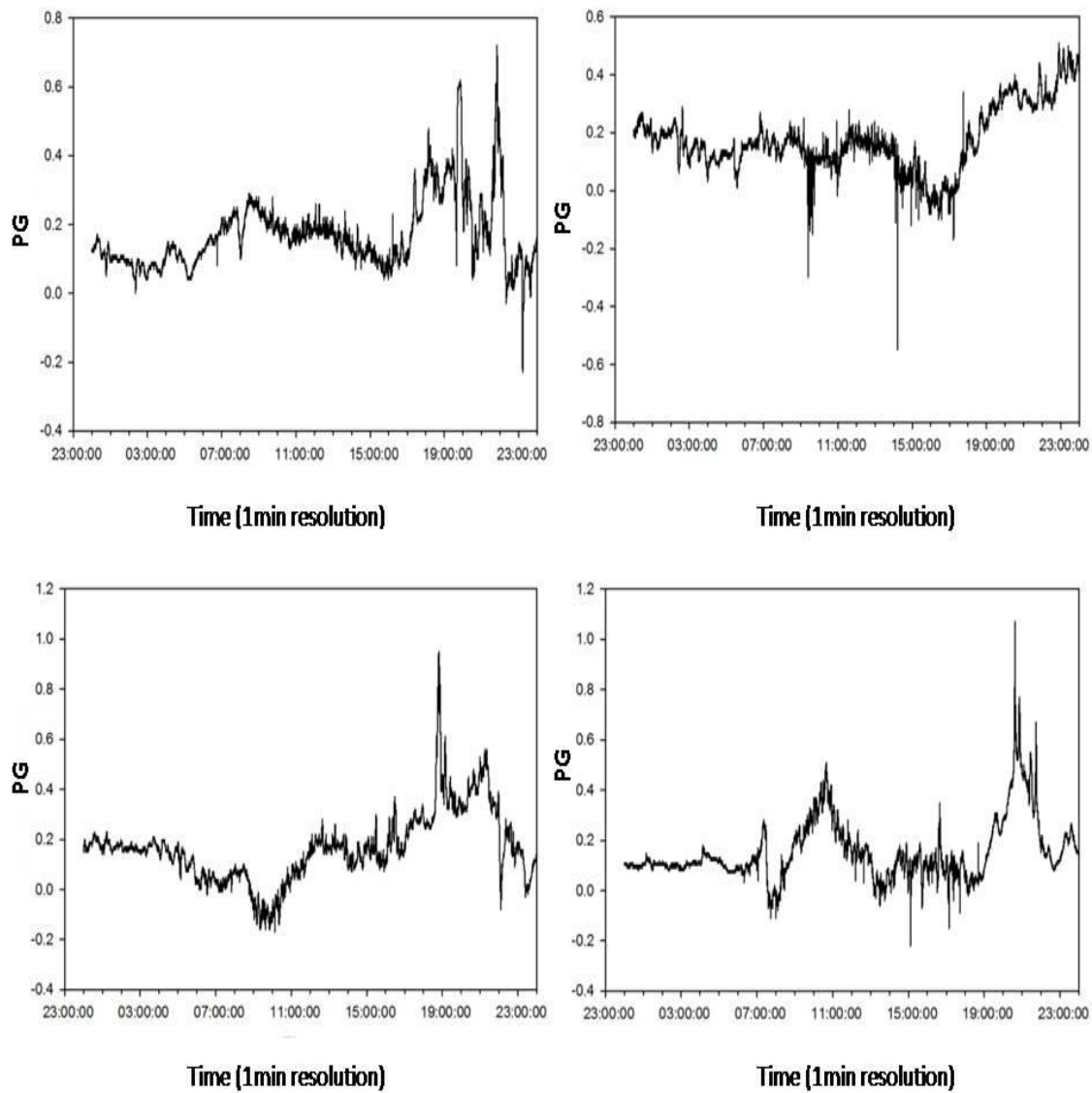


Fig 3.4 PG observations for the period from June 2015 to Sep 2015

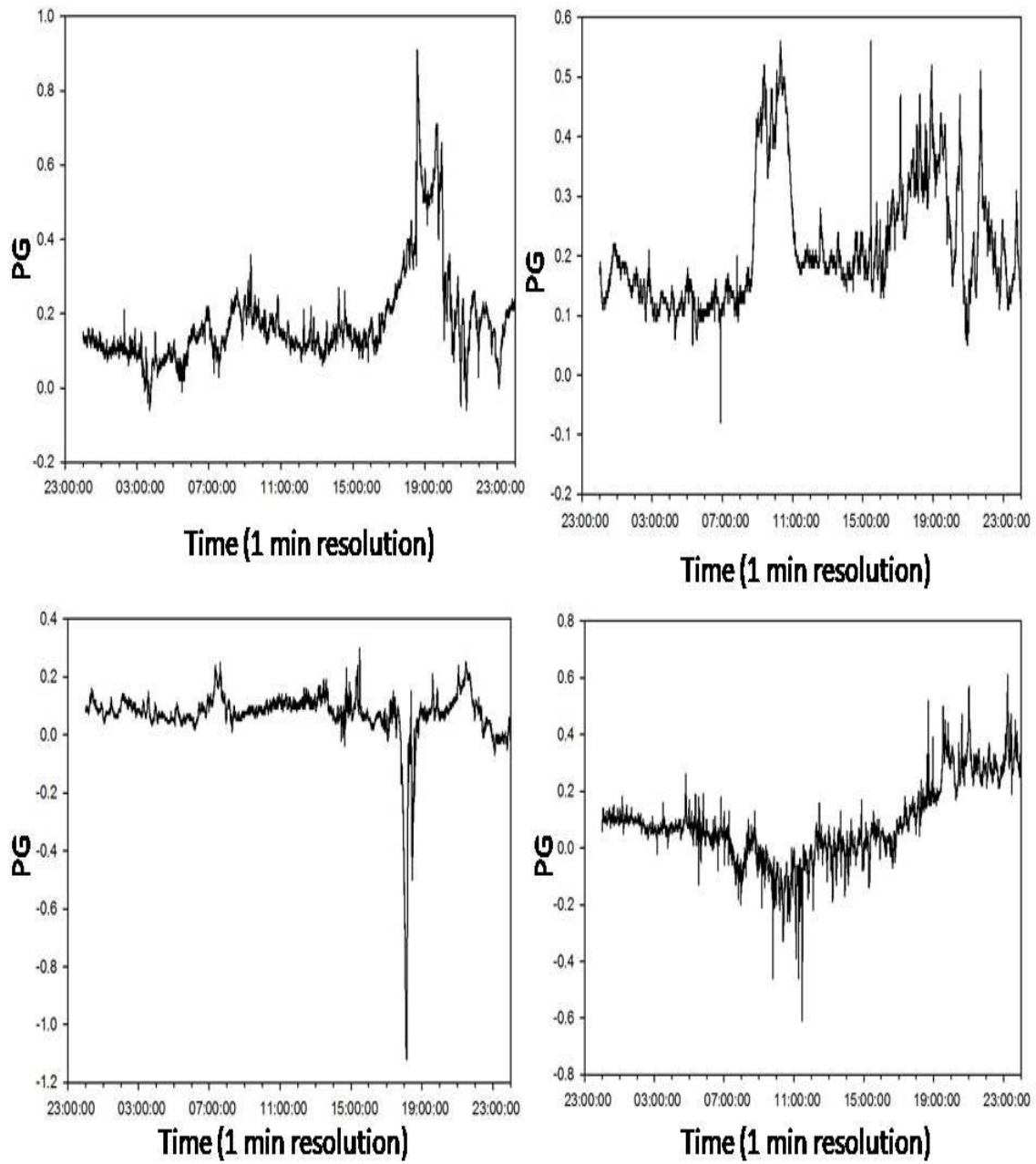


Fig 3.5 PG observations for the period from Feb 2016 to May 2016

Hourly PG observations means the data resolution is 10 V m^{-1} for the period from June 2015 to May 2016 under local climatic condition. The vast majority of the values (93.6 %) was concentrated in the range of -200 to 350 V m^{-1} with all bins presenting a $>0.1 \%$ frequency of occurrence. The mean value and standard deviation (STD) were 66.24 and 649.90 V m^{-1} , respectively. In Xanthi, the mean diurnal variation of FW–PG followed the normal continental trend of the double peak. The main maximum occurred between 11:00 and 12:00 LT, while the secondary maximum occurred at 21:00 LT; the previous minima occurred at 5:00 and 18:00 LT, respectively. The rising tendency of FW–PG throughout the early hours, followed by a main maximum around noon, is ascribed to local variables, including the “sunrise effect” and aerosols. This STD is unusually high due to the presence of disturbed circumstances, which can result in PG values of up to 15 kV m^{-1} or more, and the location has some of the highest levels documented in the southern Balkan Peninsula. We can see that the peak level is defined as the average number of days per year when thunder can be heard in a specific region and represents the probability of a thunderstorm occurring. DW circumstances do not only include thunderstorms, but also incidents of charged clouds passing over the EFM and rain showers. Because of their strong electrostatic nature, these variables are thought to generate PG values that exceed the range of 200 V m^{-1} PG 350 V m^{-1} , accounting for the remaining 6.4 percent of the entire distribution. The quantity of hourly values falling into the range $200 \text{ PG } 0 \text{ V m}^{-1}$ is a substantial component of the distribution, accounting for 16.9 percent of the sample, in contrast to other locations where negative values are significantly less common. Because DW circumstances frequently produce PG reversal to negative values, these hours can be ascribed to them. The bulk of these values occur at night, independent of weather conditions; this suggests the presence of a local generator (local source of space charge production) powerful enough to

produce enough negative space charge to cause PG reversal. Natural radioactivity is the most likely source of the event due to its timing and repetition. Radioactive chemicals such as radon and its daughter products are confined near to the ground during nocturnal inversion, creating the reversed electrode effect and increasing negative space charge density, which decreases PG values. The notion that natural radioactivity is a local generator that produces PG reversal is reinforced further by the station's position, which overlies granitic deposits and uranium ores with some of the greatest radon fluxes. Recent observations have verified this effect, which may also be responsible for enhanced conductivity around the research region. This component, together with the typically low aerosol concentrations exhibited by typical heavy pollution sources such as industry and big cities such as Athens, was responsible for a decreased PG mean value of 66.24 V m^{-1} . Despite the apparent sub-hourly stability, the PG exhibits minor variations within each hour, primarily between 4 and 20 V m^{-1} , indicating the impacts of changing local variables such as space charge and aerosols. So far, it is clear that the prevailing climatic circumstances during that hour (i.e., the presence of thunderstorms, the passing of charge clouds) and the presence of local generators have a substantial impact on both hourly PG values and their associated STDs (e.g., radon). These effects are of local origin and have the potential to totally conceal the PG response to GEC diurnal fluctuation. An FW–PG dataset was constructed to allow analysis of the diurnal and seasonal fluctuation of PG without the influence of DW situations and those with strong ionisation. Two basic criteria were utilised to choose the data for the FW set: $0 \text{ PG} \leq 350 \text{ V m}^{-1}$ and $\text{PG-STD} \leq 100 \text{ V m}^{-1}$. Negative PG readings were eliminated since they are related to either local sources (natural radioactivity) or DW circumstances. Furthermore, those with values greater than 350 V m^{-1} , accounting for 2.7 percent of the distribution, were eliminated since they are associated with DW conditions or high aerosol

concentration occurrences. The additional filter of PG-STD > 100 V m1 was used to exclude any hourly values that subsequently fell within the range of 0–350 V m1 during the averaging process, despite being recorded under DW circumstances. The FW set had 78 percent of the total number of hourly means during the studied period. This large percentage of FW hours is advantageous for the station as compared to stations further north in Europe.

The approach of using PG statistics to determine the conditions under which it was collected and, ultimately, define an FW–PG set is beneficial, especially when cloud cover and local generator activity data are not available in high resolution and therefore the conventional FW definition may be used. In case for the Xanthi site the method are found for Marsta Observatory, Nagycenk Geophysical Observatory, are customized for diurnal and seasonal PG variation data. The diurnal variation of FW–PG exhibits two characteristic patterns, those of single and double peaks. The single peak (Carnegie curve) is followed at environments in which local effects (e.g., pollution) are low or absent like oceanic, depicting the global thunderstorm activity. Moreover, a single peak is exhibited at certain stations during winter time, particularly at high latitudes, showing high correlations with the Carnegie curve. The double peak is followed at continental stations and is generally synchronized with local time and the intensity of local effects, while the GEC signal is not always apparent and averaging over one or several weeks is needed to be shown. The morning effect was thoroughly detailed, with a special emphasis on the PG response to positive space charge transpositions. The dawn effect was highlighted in the results, which included a charge reversal from negative to positive at the time of sunrise, corresponding with an increase in PG. The reason of solar heating, according to the convection process, is the breakdown of a shallow positively charged layer electrode layer that was built up over the night and overlies the very first decimeters of the ground. The dilution of the electrode layer shortly

after dawn due to increased turbulence carries more and more positive charges over the EFM, eventually increasing PG values. Because of the downslope of a hilly terrain and the likelihood of valley or land wind closed circulation cells, the PG increase due to the sunrise effect may be amplified at Xanthi station. In such scenario, the electrode layer that developed on the mountain's surface throughout the night is likewise diluted after daylight, and the positive charges can be restored over the EFM via the returning cell circulation after being carried upslope. The importance of the dawn impact on the morning peak was also underlined in research for various stations, regardless of the site's type, such as normal continental, tropical continental, or island tropical. Aerosols have a direct influence on local conductivity because they function as recombination centres for the ions; at the same time, aerosols limit the mobility of the ions connected to them, lowering further conductivity. According to Ohm's law, a decrease in local conductivity, assuming a constant conduction current between the ionosphere and the earth, causes a rise in PG. Aerosols at the Xanthi site are predicted to have a higher arithmetic concentration at ground level throughout the morning to midday hours, resulting in higher PG values. The influence of aerosols on PG is exacerbated by the fact that the wind is generally blowing southeast to southwest at that time, transferring additional particles toward the EFM device. As a result, it is probable that at our station, the southern breezes and upwind road traffic, both of which are stronger around 9:00–10:00 LT, resulted in higher aerosol concentrations surrounding the station and followed the sunrise effect. This process may have resulted in a steadily growing influence on PG, which finally peaked at 11:00–12:00 LT. Thunderstorm activity in Asia, which was at its peak at the time, is another cause that might contribute to the morning growing trend of PG. Despite the fact that its contribution is deemed minor in comparison to the aforementioned elements, it is listed here as the only global component that

may have an effect on the local primary PG maximum. After the main high, PG began to fall and finally hit a low at 18:00 LT. This is due to the maximum of convective conditions in the late afternoon, which might induce dilution of aerosols near to the ground. Aerosols go upward, enabling ion concentrations to recover. Thus, according to Ohm's law under constant air–earth conduction current of $PG = JZ/T$, where JZ is the air–earth conduction current and T is total conductivity, local conductivity increases and PG decreases. Upward movement of aerosols progressively suppresses PG by lowering the conduction current. Because there is no mechanism for rapidly removing aerosols when they are high, columnar resistance rises, decreasing the air–earth conduction current (which generates PG force) and, as a result, PG. In comparison to the earlier data, when the comparable maximum occurred at 15:00 LT, a delay in columnar resistance maximising was seen at our location at 18:00 LT. We suspect that the delay is due to variations in advective circumstances at each location; greatest columnar resistance was found during low advection times. Both extremes, however, are subject to local influences that can either increase or suppress the global signal. The previously optimum convective circumstances that resulted in a minimal PG value were gradually weakened, resulting in increasing aerosol concentration near to the ground and, as a result, increased PG. The progressive change to nighttime stratification might result in radon and its offspring being trapped, resulting in strong ionisation conditions and the formation of negative space charge (reversed electrode effect), which would finally inhibit PG. Negative space charge can also invert PG polarity; however, negative values were not taken into account. On certain days, the influence of radon during nighttime inversion might also alter the PG minimum (05:00 LT). The amount and timing of the impacts of local parameters on the global signal of PG are difficult to quantify; hence, measurements of other variables such as aerosol soundings, ground aerosols, conductivity, and

radon are required. A comparison of the magnitude of the main peak with that of the Carnegie peak found a significant discrepancy, indicating that local effects dominate at Xanthi during the day considerably more than global influences. The diurnal fluctuation of AW–PG follows the same path as that of FW–PG, and it is held below the FW curve for the most of the day; this is consistent with PG behaviour at other locations. The predicted result was that DW circumstances were strongly recommended, and hourly variability was also obvious from the increased standard errors (SE), where $SE = STD/n$. Although it is not the same for all hours, it is sufficiently high to assure comparable PG values. The enhanced PG showed a pronounced intensity between 11:00 and 21:00 LT. During the same period, lightning activity is increased over Greece and Xanthi, the latter exhibiting the highest PG values. The perturbed condition coincides with the greatest divergence between the two curves, indicating the presence of non-PW. During some night hours, similar discrepancies between the two curves were also visible, however the non-PW circumstances here are more likely attributed to natural radioactivity. As a result, while the PW–PG typically followed a normal double-peak diurnal oscillation, the DW circumstances at our Xanthi site were sufficiently strong and frequent, leading the curve's minima and maxima to be much fuzzier than those of the FW–PG. Most of the days accompanied the general pattern described above, though in some cases, neither extreme was visible. During the warm months of June to October, the PG's primary maxima were at 10:00– 11:00 LT, but during the cold months of November to January, the maximum were transposed to 12:00–14:00 LT. The earlier onset of convective conditions during the warm months is ascribed to this transposition, as is the earlier activation of the dawn effect. The remaining months, such as February and May, exhibited intermediate behaviour, with maxima occurring between 11:00 and 12:00 LT. The secondary maximum does not appear in every month, indicating the effect of local variables on PG during

the global thunderstorm maximisation period. When a secondary maximum was seen in August, September, January, and May, it occurred within 1 hour of the Carnegie curve maximum at 19:00 UTC. The time variation might be related to seasonality of local variables like pollutants, regional changes in thunderstorm distribution that could disrupt the normal GEC cycle, or ionospheric disturbances. Finally, there was no seasonality in the two minima, which were located at 05:00 and 18:00 LT, respectively. Because the secondary peak occurs throughout the year, this effect is not purely seasonal. It is possible that it is the result of a combination of several contributing variables, including radon emanation, turbulence, and aerosol concentration and size distribution. Such assumptions, however, may only be hypothetical in the absence of pertinent evidence. Seasonal fluctuation in FW–PG observed from February 2011 to December 2014, with maxima (minima) during cold (warm) months. This fact, however, is inadequate to explain the higher aerosol concentrations close to the ground in winter because the primary heating sources in the area, notably the town of Xanthi and the village of Kimeria, are not upwind of the dominant wind directions found at the site. Furthermore, in Greece, columnar aerosol concentrations often peak in the spring/summer; however, other sources occur in the summer as well. In terms of air pollution, the boundary layer height (BLH) is the primary driver of aerosol concentrations near the ground. This arises on Mediterranean locations of the same latitude, the BLH during the summer may be up to ten times larger than that during the winter due to reduced convection during the winter. Large quantities of Aitkin nuclei efficiently lower the concentration of tiny ions that dominate the electrical conductivity of air, resulting in reduced local conductivity and, as a result, PG maximisation. During the summer months, the boundary layer is significantly deeper than in the winter, scavenging aerosols that are close to the ground. The proposed process is indeed consistent with previous atmospheric ion data obtained in

Athens. These observations revealed that small ion concentrations were highest (lowest) during the summer (winter). Large ions, on the other hand, which are positively associated with pollution and serve as a supplementary sink for small ions, followed the opposite trend: that of PG. As a result, the seasonality of ground aerosol concentration is linked to the long-term FW–PG fluctuation at our location, which is a typical continental site in the Northern Hemisphere. Variation in intense time and oscillations between the maximum and lowest may be attributed to variables influencing aerosol concentration, such as vertical mixing, and to possible worldwide climatic changes. Effects at the local against global levels Observing GEC from a single continental station is difficult because, as previously stated, local factors like as aerosols and space charge can totally obscure global changes. Local impacts, on the other hand, are either minimised at particular times or do not change much over time, allowing global signals to be observed. By comparing FW–PG with the Carnegie curve, an attempt is made to find similar periods for the Xanthi site. Because the GEC does not always follow a typical Carnegie curve due to factors such as local climate changes, rigid conclusions based on any sort of comparison with the Carnegie curve should be avoided. As long as the PG data are averaged over a sufficiently enough time, this curve is widely regarded as a fundamental tool for determining the periods in which PG represents GEC change. Furthermore, it has been observed that PG has a marginal latitudinal dependency, with the latitude impact influencing absolute PG levels. In the present study, the appropriate percentages of the means were used to compare local PG with the Carnegie curve. As a consequence, such impacts were no longer present. The FW–PG follows a similar path to global variation, with its minimum at 03:00 UTC and secondary maximum at 19:00 UTC coinciding with the Carnegie curve extremes; however, a disruption was seen during the development of the main maximum at 04:00–16:00 UTC. When the differences between the

two cycles are estimated ($DPG = FW - PG$, Xanthi as percentage of mean, the PG Carnegie curve as percentage of mean), the largest departure from the Carnegie curve occurs between 8:00 and 12:00 UTC, with a maximum divergence of 58 percent at 9:00 UTC. As previously mentioned, this is due to the dawn effect and aerosols. During the hours of 14:00–16:00 UTC, the PG at our location fell below the Carnegie curve, resulting in a negative DPG. According to Ohm's law, this sinking may be attributed to the maximum of convective circumstances, which resulted in a rise in the aerosol columnar load and a consequent drop in the conduction current and PG. DPG remained negative from 16:00–4:00 UTC, when the PG followed the same pattern as the Carnegie curve ($r = 0.98$, $p = 0.01$), but progressively decreased in amplitude during the night. Following the apex of convective conditions, the progressive suppression of the boundary layer and the consequent stratification of the atmosphere may have increased radon trapping. It might well result in an increase in negative space charge over the EFM, lowering the PG. With the completion of the shift to nocturnal stability, the variability of elements that might produce huge swings in PG, such as aerosols and radon, was decreased, allowing the PG to closely follow the Carnegie variation. DPG dropped below 25% between 21:00 and 04:00 UTC, and below 15% between 01:00–04:00 UTC, which were considered the best hours of the day for GEC observations at the Xanthi location. At the same times (01:00–04:00 UTC) have also been considered to be suitable for presenting GEC observations at Hungary's Nagyecenk Geophysical Observatory continental station. To identify which months deviated from the Carnegie curve most least and thus are better suitable for GEC observation. This pattern is linked to atmospheric convection, which is more strong during the warm months. The atmosphere is more stable during the winter months, resulting in fewer diurnal fluctuations in aerosol and radon concentrations. As a result, the fluctuation of columnar resistance and local conductivity is decreased. Changes in

the ionospheric composition induced by worldwide thunderstorm activity may also be to blame for the PG diurnal pattern. Cold months are similarly preferred in GEC data at other continental sites, where air convection seasonality is again thought to be the relevant process. The divergence from the typical trend of chilly months in November for the majority of the day might be due to increased atmospheric mixing or transient amplification of local variables such as aerosols and space charge. A PG values and local climatic conditions have been significant to global atmospheric electricity generation. Present studies have been performed on correlating local climatic elements with PG. By significance of the atmospheric electric field as a stratification indication in the evaluation of PG is demonstrated here. Although the atmospheric electric field and the PG are two entirely separate variables, they are both impacted by convective circumstances, therefore a common factor is used to understand the PG diurnal cycle. For the period June 2011 to May 2012, the mean diurnal variation of common PG and atmospheric electric field values is presented. The PG values used in this study were obtained from the AW dataset, excluding days with rain and days with $|PG|$ greater than 1 kV m⁻¹, the latter indicating the presence of heavily charged clouds. The previously mentioned values was excluded because they relate to disturbed situations that dominate PG variation with no influence. A comparison of the two cycles indicated an inverse connection between the PG and the atmospheric electric field ($r^2 = 0.36$, p value convection progressively increased, further decreasing the PG via an increase in columnar resistance and a consequent drop in the air–earth current). The latter mechanism, relating to PG, remained operational until 18:00 LT. The PW rose between 16:00 and 21:00 LT due to the progressive shift to nighttime stratification and the enforcement of atmospheric electric field sources. The PG approaches the secondary minimum around 18:00 LT and subsequently rises parallel to the CO₂ trend, displaying worldwide

thunderstorm activity. The late afternoon and early evening hours, 18:00–00:00 LT, were particularly interesting. The global signal was predicted to peak at that time, and the concomitant evolution of stratification might have changed or totally obscured the planetary effect via radon trapping. In a 1-min time series for May 1–3, 2012, PG, CO₂, DT (DT = T_{2.5m} - T_{1.5m}), and WS were studied as a case study. It should be emphasised that cloud cover was 0.5 m1 during those days, which disrupted the very high stratification (DT > 0.5 °C) while concurrently lowering CO₂. Following that brief period, calm wind conditions resumed, resulting in increased stability (DT rises), which led CO₂ to rise and PG to fall. The previous evening, May 2, the stability continued with no significant disturbances until the GEC peak time of 21:00 LT, with the exception of a brief period soon after sunset when the stratification decreased significantly. During that brief amount of time, the PG started increasing in response to the GEC oscillation, but the rate of CO₂ rise was momentarily decreased. During this period, CO₂ continued to rise quickly and reach a peak, but PG fell dramatically, reversing the polarity and failing to display the worldwide signal. On the night of May 3, diurnal stratification started and persisted uninterrupted, causing a linear increase in CO₂ and totally obscuring the GEC. The PG remained low as well as even negative. The fluctuation of PG and CO₂ over those nights, particularly when the GEC signal was expected, shows that when CO₂ levels are stable and high, PG is suppressed and GEC detection is impossible. As a result, CO₂ fluctuations during stable nights may be used to supplementarily classify days as appropriate or unsuitable for GEC monitoring, given the absence of variables that could only affect PG, such as charged clouds overhead and aerosols. Furthermore, single-point CO₂ data may be used as proxies for turbulence and can provide information on the development of atmospheric electrical characteristics. In this

technique, a positive correlation has been found between micrometeorology, atmospheric gases, and atmospheric electrical.

3.4 Conclusions

The first four years of PG observations from a newly built rural station in Xanthi, Greece, are given in this study, from February 2011 to December 2014. The seasonal FW–PG fluctuation is typical for a Northern Hemisphere continental station, with maxima (minima) during cold (warm) months. The mean diurnal variation of FW–PG follows a typical continental double peak, with the primary maximum between 11:00 and 12:00 LT and the secondary maximum around 21:00 LT. The prominent peak was entirely linked to local factors, especially the sunrise effect and a spike in aerosol arithmetic concentration, the latter caused by the start of anthropogenic activities. The dawn effect is likely to be enforced at the Xanthi site since the station is positioned at the base of a hill, and local circulation effects occur after sunrise. Because its occurrence corresponds with the Carnegie curve maximum, the secondary peak might be attributed to global causes. However, it is also vulnerable to local impacts since the change from maximum of convective circumstances to nighttime stratification may result in an increase in aerosol concentration (trapped radon) acting positively (negatively) on FW–PG. FW–PG had its main maximum at 10:00–11:00 LT during the warm months of June to October, while the equivalent maxima were transposed to 12:00–14:00 LT during the cold months of November to January. The next months, from February to May, showed moderate behaviour, with maxima at 11:00–12:00 LT. Only in August, September, January, and May was the secondary maximum visible, and it occurred within 1 hour of the Carnegie curve maximum at 19:00 UTC. Although the AW–PG levels were typically lower, the diurnal fluctuation of AW–PG largely mirrored that of FW–PG. The significant thunderstorm activity at the location caused the AW–PG curve to

deviate from the FW–PG curve, as well as high AW–PG hourly variability. The nighttime FW–PG curve of Xanthi was highly linked with the conventional Carnegie curve. At the Xanthi location, the best hours for GEC observation were between 01:00 and 04:00 UTC, and cold months favoured global signatures more than warm months. Finally, it was demonstrated that collocated atmospheric CO₂ data may be utilised as stratification proxies to detect circumstances that promote radon trapping and, as a result, change PG. PG was inhibited and GEC monitoring was impossible during steady nighttime conditions, when CO₂ rose steadily and at high quantities. A reverse connection between PG and CO₂ during the occurrence of a global signal might supplement the categorization of days as suitable or unsuitable in GEC monitoring.

CHAPTER 4

Analysis of Atmosphere Electric Field Characteristics during Lightening

4.1 Introduction

Lightning is a high-energy luminous electrical discharge that occurs from inside, or even between dark clouds and also it's accompanied with sudden pressure fluctuations rippling in the earth environment. Finally, it seems to have a tremendous impact on human life and their facilities, and is a major concern specifically in the regions where precipitation and thunderstorms occur frequently. Lightning is caused by the Cumulonimbus (Cb) cloud, which is the largest of all cloud groups. The creation of such clouds is primarily caused by two kinds of processes. They are known as Frontal or Convective thunderclouds depending on the type of formation. Frontal thunderclouds form as cold and warm air masses interact, and they can happen at any time of day or night. The convective Cb cloud formation starts in the afternoon with the initiation of the convective cycle, which is caused by solar radiation. Usually they mature by the afternoon and majority of the lightning strikes from this type occur in the afternoon hours. Thundercloud formation in a local region is determined by the cloud's charging mechanism where the number of charged cells produced and local meteorology are responsible. As a result, the activity of Cb clouds varies across the globe. The typical cumulonimbus cloud developed upto tropopause nearly 15–18 km from the surface. There are three types of lightning discharges: (i) within a thundercloud (intra-cloud), (ii) from one cloud to another (inter-cloud) and (iii) from cloud to ground (CG). Cloud top produces a positive electrical charge, the lower stage a negative electrical charge. Although air is a poor conductor of electricity, there is no current flow between them. Positive charge accumulates on all objects below a thundercloud as it

passes overhead. When these positive charges are striving to meet the cloud's negative charge, they tend to accumulate at the top of the highest object in the vicinity. Lightning happens when the electrical potential difference between the +ve and -ve charges is high enough to transcend the resistance of air and force a conductive path between the cloud and the earth. It's probable that such a potential is as large around 100 million volts. In a few tens of milliseconds, a strong electrical discharge in the atmosphere heats the air to nearly 30,000°C. This mechanism generates shock waves, whose propagation we hear as thunder. Thunder improves in approximately estimating range. Thunder (sound) travels one kilometer in three seconds, so the time (seconds) between seeing a lightning flash and hearing sound, separated by three, gives the slant range in kilometers. Further, the higher the pitch of sound of thunder, the closer is the lightning.

4.2 Atmospheric Electric Field during Lightening

According to concept, an atmospheric electric field is a measurable key factor observing the intensity of the lightening at any given point in space and time. In fair weather, the atmospheric electric field near the earth's surface ranges from 100 to 300 V/m. It is a positive field that travels from the atmosphere to the earth. Poor weather occurs simultaneously in all places around the world in which there is no thunderstorm activity. According to the conductivity theory of the global electric field, at thunderstorm locations, this field reverses direction and rises thousands of volts per meter. It has been observed that the electric field exhibits a sudden bipolar peak at the time of a flash at very specific times to a lightning strike. The range of electric field values in fair weather conditions varies significantly from one region to another and it is based on several of certain dependent variable. There are significant variations in the intensity of the atmospheric electric field from the fair weather value during a thunderstorm, and thus this might be used as a

parameter for the analysis of lightning during thunderstorms. Atmospheric electric field data can be accessed using a number of widely available instruments such as EFMs, dipole antennas, flat plate antennas, and so on. Electric field fluctuations are known as sluggish (or static) or rapid (dynamic) in statistical experiments, and changes in both are associated with the lightning mechanism. Sluggish electric field antennas effectively reverse field changes over duration of a lightning discharge, including data on the discharge edge leader process, and continued flow. Strong electric field antennas analyze discharge portions on a quicker timeframe and return shifts on a microsecond time scale. An Electric Field Mill (EFM) is an electronic circuit which measures the intensity of the static atmospheric electric field at the instrument's location. It functions by revealing a transmitter component as well as an unidentified response to the electric field simultaneously. When heated to an unidentified analog, the sensor element becomes activated by the external electric field and then discharged. Charge amplifiers convert the sensor element's induced charge to a voltage that is proportional to the external electric field. Variations in the electric field are shown in both clear and cloudy weather. A comprehensive review will show distinct changes in the electric field before and after a strike. Since modifications prior to a strike help in prediction, a study in Brazil explores a technique of lightning warning systems based on electric field variations. Electric field data obtained from an EFM has been used in a simulation experiment, and the results compared with lightning data collected from the BrasilDAT data repository. The characteristics of an electric field that can predict a lightning strike also include reversal of electrostatic field polarity and an increase in field magnitude. While lightning location systems are considered to be more accurate, EFMs have the potential to enable to detect the development of a thunderstorm directly over the area of concern, enabling them to predict. even first strikes. According to the Brazilian simulation outcome, the field

threshold for precise warning signals becomes 0.9kV/m for a range of 10km, with the fair weather value of field being 300V/m. Preliminary Breakdown (PB) is a dynamic electrical process that happens within the cloud prior to lightning and occurs even before the cloud initiates. Meteorological conditions have been discovered to have an effect on these electrical pulses. A bipolar pulse train with a normal duration of a few milliseconds is used to identify the PB process in electric field records. The time interval between the preliminary breakdown and the first return stroke is referred to as the actually stepped leader duration. An assessment of lightning strikes in Florida reveals that approximately 29 percent of the strikes had a detectable PB pulse train. When the signal-to-noise ratio was increased through filtering, the percentage rose to 47 percent. Detectability was also affected by location. They discovered that at higher latitudes, a greater proportion of flashes had visible PB pulse trains than at lower latitudes. Other factors influencing PB pulse detectability include storm type, distance, and first return stroke peak current. The observations here validate the arithmetic and geometric means of PB pulse duration as 3.6ms and 2.1ms, respectively, which are close to Nag and Rakov's findings. The ratio of the strongest PB pulse peak to the first return stroke pulse peak ranges from 0.05 to 0.9 for 93 of 104 flashes (excluding 11 saturated records), with an arithmetic mean of 0.26 and a geometric mean of 0.20. Another Malaysian study discovered a preliminary break-down signature in more than 95 percent of the flashes observed. The polarity of the characteristic pulses was found to be the same as that of the first return stroke.

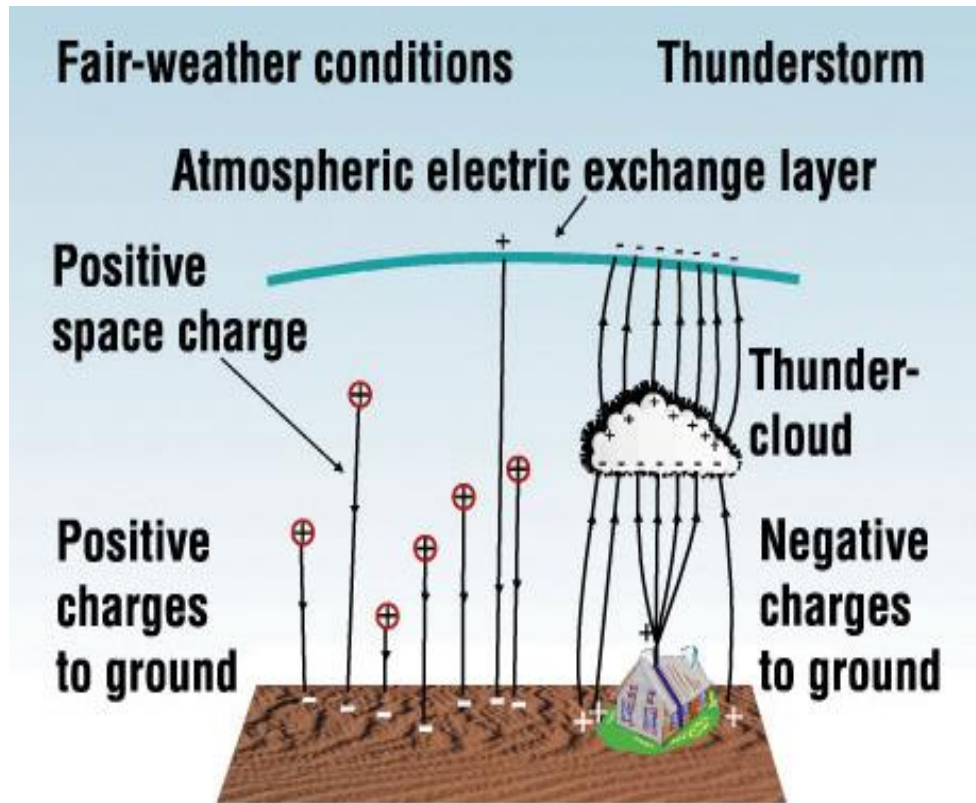


Fig 4.1 Earth Atmospheric Exchange Process

4.3 Methodology

Around 80% of the recorded flashes were discovered to be consistent with the BIL model. A proposed model of Clarence and Malan explain the phenomenology of lightning. A BIL model can be studied from an experiment of parallel plate antenna which captures the vertical component of the atmospheric electric field by using the buffer circuit, GPS, DSO, data logging system. The waveform describes the initial breakdown (B) stage, which lasts milliseconds, and the intermediate stage (I), which lasts several hundred milliseconds. The final stage is the stepped leader (L), which lasts a few milliseconds. The stepped leader stage concludes with a very intense return stroke, which is the perceived lightning flash as charges flow from the ground to the clouds through the lightning channel. The most prevalent method for analyzing electric

field variations is to investigate them in either the static or dynamic domains, but not both at the same time. However, a different technique was used in a Polish experiment: frequency domain analysis. This spectral analysis is intended to aid in the correct identification of lightning-related electrical processes such as preliminary breakdown, stepped leader, ongoing current, and other separate electrical processes. A rapid change in the electric field caused by lightning strikes result in a high level of power spectral activity. When slow field changes are represented by low frequency components, preliminary breakdown and return stroke are represented by faster components. The particulars of their experiment demonstrate the importance of determining the components of preliminary breakdown in order to improve existing detection systems. In this experiment, they suggested using a narrow STFT window for preliminary breakdown or return stroke analysis. We used the Short-Time Fourier Transform to identify the different lightning stroke components such as preliminary breakdown (PB), return stroke (RS), and continuing current (CC) in the power spectrum density analysis of lightning electric fields (STFT). The parameters for lightning detection can be divided into two groups: those concerned with determining the precise time and location of a strike, and those concerned with physical parameters such as lightning current, electric field, amplitude, polarity, and strike type.

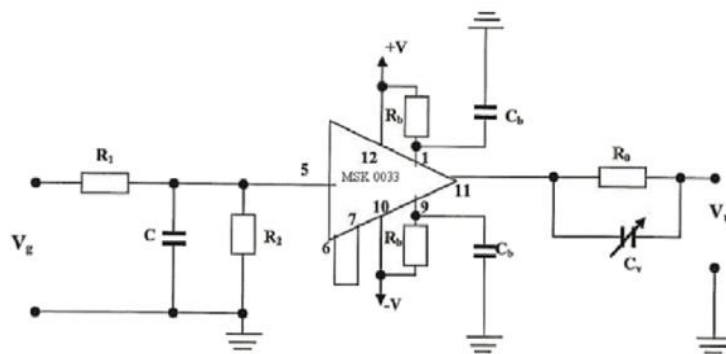
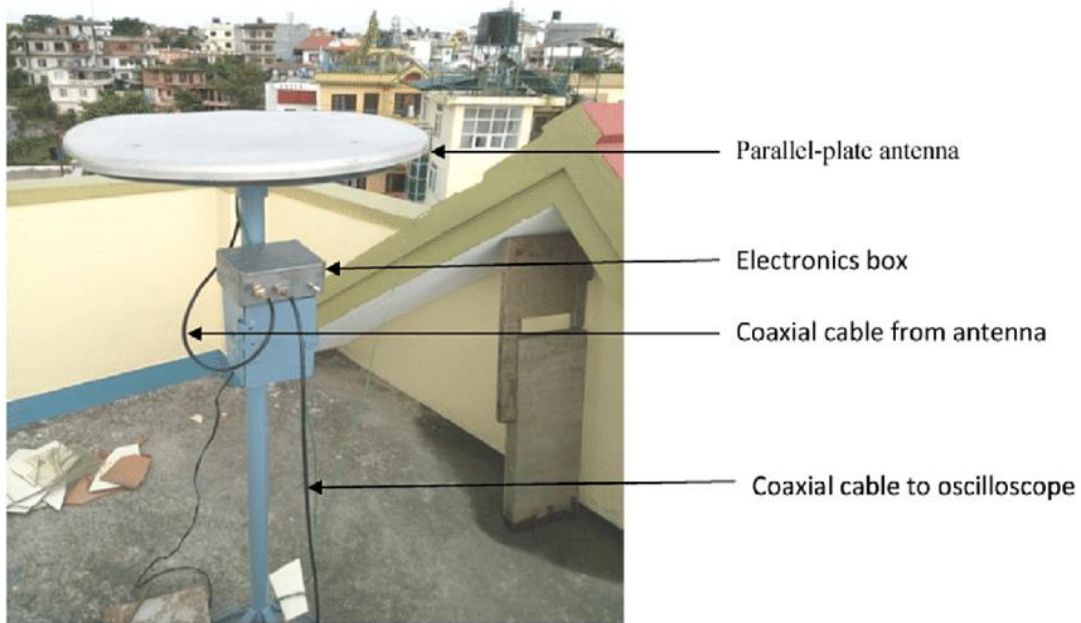


Fig 4.2 Atmospheric Electric Field Measurement Equipment

Atmospheric Electric Field

A quantitative term denoting the electric field strength of the atmosphere at any specified point in space and time. The transfer of charge from the thundercloud to the ionosphere above and the earth below is what creates the earth's electric field. On the earth's surface, the electric field can be as strong as 100 to 300 V/m. **Atmospheric electricity** is the study of electrical charges in the Earth's atmosphere (or that of another planet). The movement of charge between the Earth's surface, the atmosphere, and the ionosphere is known as the global atmospheric electrical circuit.

Atmospheric electricity is an interdisciplinary topic with a long history, involving concepts from electrostatics, atmospheric physics, meteorology and Earth science

Atmospheric Electric Potential

The total potential difference from the surface of the earth to the top of the atmosphere is about 400,000 volts. Atmospheric electricity is the study of electrical charges in the Earth's atmosphere (or that of another planet). The movement of charge between the Earth's surface, the atmosphere, and the ionosphere is known as the global atmospheric electrical circuit.

Lightning Intensity

A typical lightning flash is about 300 million Volts and about 30,000 Amps. In comparison, household current is 120 Volts and 15 Amps. If you count the number of seconds between the flash of lightning and the sound of thunder, and then divide by 5, you'll get the distance in miles to the lightning: 5 seconds = 1 mile, 15 seconds = 3 miles, 0 seconds = very close.

4.4 Lightning Datasets

Sonnblick Observatory, Austria, provided the electric field measurement values. Sonnblick Observatory is situated in the Austrian Central Alps at an elevation of 3106 m a.s.l. at the top of the mountain "Hoher Sonnblick." It is centered at the alpine main divide, and is a distinct climatological boundary. It is also found in the "Nationalpark Hohe Tauern," which comprises 1856 km² of the Austrian Alps on the frontier of the provinces of Salzburg, Carinthia, and Tyrol. The nearest villages are Heiligenblut (10 km away) to the south and Rauris (10 km away) to the north (20 km away). The accessible infrastructure from gold mining operations was a significant factor for the creation of the Sonnblick Observatory in 1886. Sonnblick analysis is currently

being conducted in the research program ENVISON. It has a large surveillance network and several scientific programs that address three major topics (the environment, the cryosphere, and the biosphere). Sonnblick is renowned for its long-term temperature monitoring and research on glacier transitions. Sonnblick Observatory, one of Austria's largest meteorological observatories, is exclusively devoted to the collection of data of global scientific significance after a thunderstorm and prior to a lightning strike. The initial weather station has become an interdisciplinary research center thanks to its location at the main peak of the Alps at over 3,100 meters above sea level in a nearly free atmosphere, as well as the ZAMG technicians' year-round support. Electric Field measurements were taken at two Electric Field Mills in Sonnblick and Kolm from March 29 to April 2, 2016 Local Time. Lightning is accompanied by localized changes in the electric fields of the atmosphere. Changes in ambient electric fields can also be detected at the ground a few minutes before a strike in cloud-to-ground strike areas. A great deal of study has also been conducted on the electrostatic shifts that occur in the area above ground prior to lightning. With the aid of COMSOL Multiphysics simulations, we analyze the effects of lightning electric fields on/underground in this work. Horizontal and vertical voltage gradient, electric field, polarisation, and other profiles are studied. Experiments were carried out using a general model of lightning electric fields generated from data obtained by Electric Field Mills (EFMs) from three different locations around the world: Kennedy Space Centre (KSC), Florida (using GHRC datasets), and Sonnblick Observatory, Austria. Sandstone was used as the base model for land in COMSOL simulations of the global electric circuit. Previously, similar works of literature only dealt with lightning electric fields above level. This study is the first step toward creating a high-level simulation of the effects of atmospheric electric fields on/below ground. The outcomes of this simulation work will assist with lightning forecasting and

preparedness by opening up new avenues for voltage-based prediction methods at field. It is also a medium for comprehending phenomena such as fulgurites, the corona effect, and so on. It also assists in the construction of buried cables and more efficient grounding schemes. This research may also be a first step toward identifying localised possible changes at the ground during lightning strikes.



Fig 4.3 Sonnblick Observatory, Austria for Atmospheric electric field measurement

4.5 Results

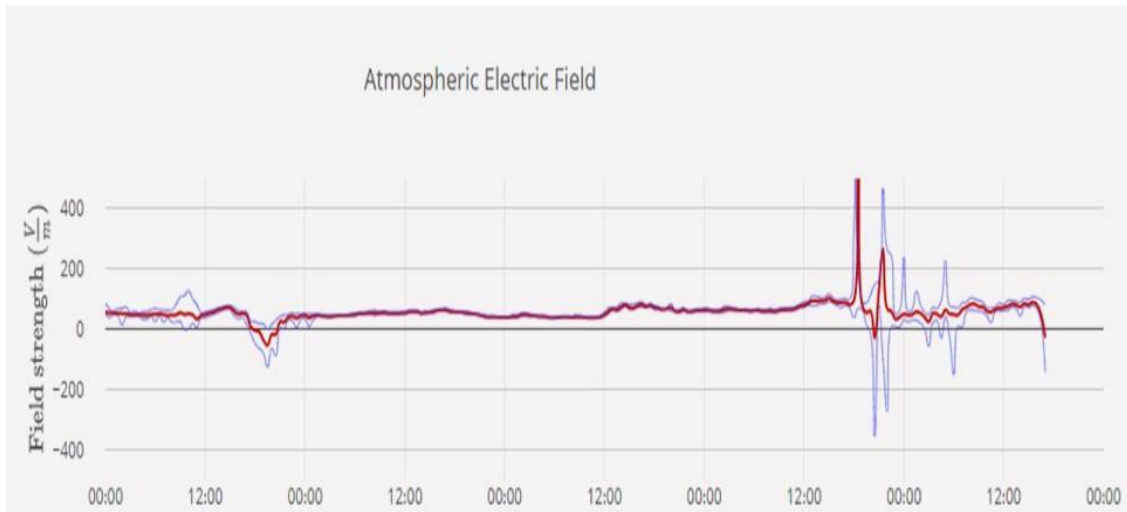


Fig 4.4 Atmospheric Electric Field during perturbed day

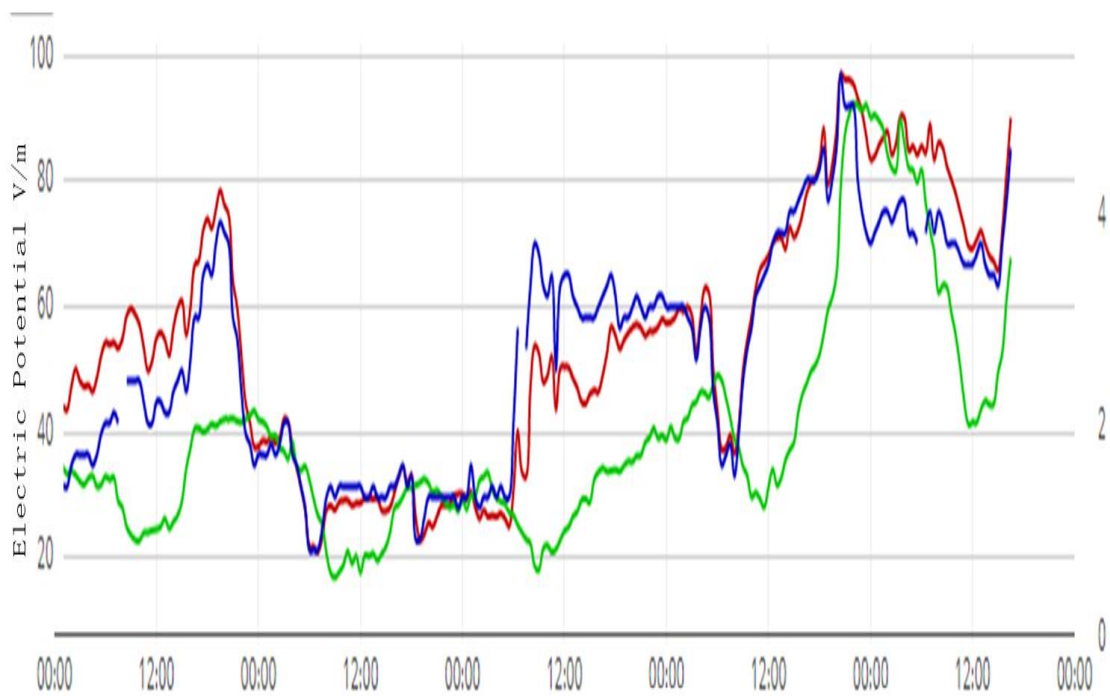


Fig 4.5 Atmospheric Electric Potential during perturbed day

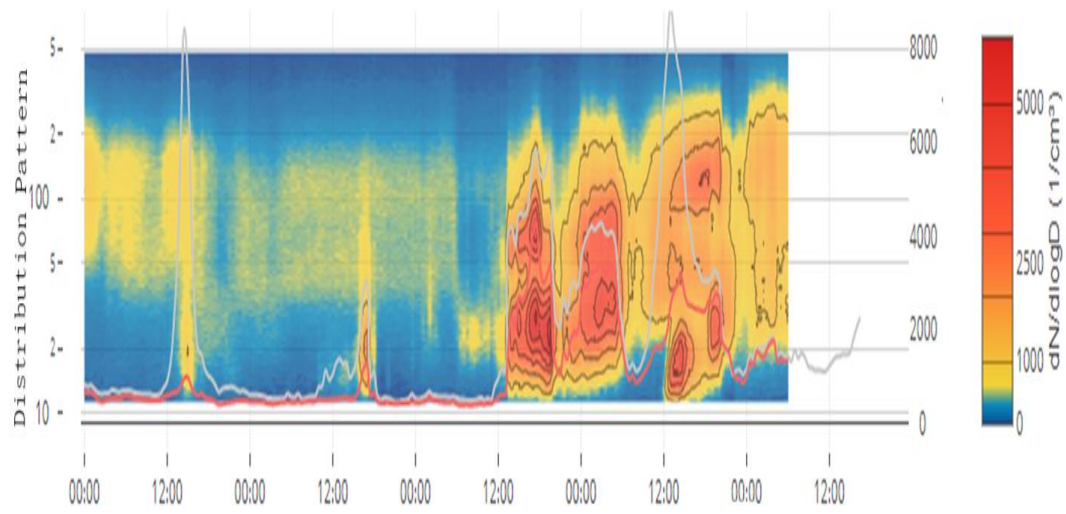


Fig 4.6 Electric Distribution Pattern during perturbed days

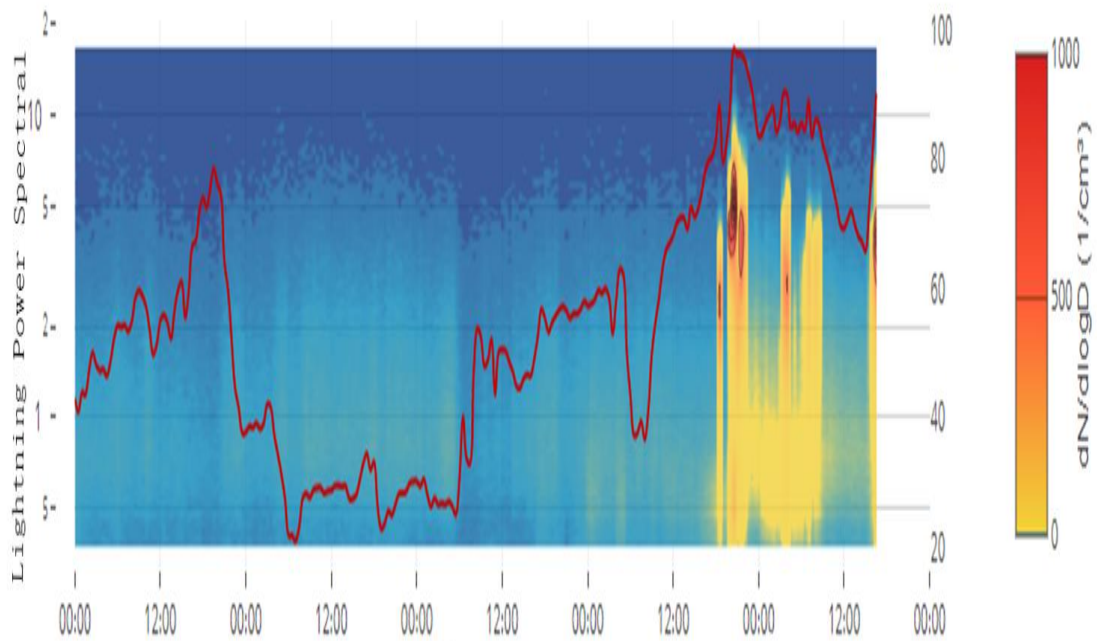


Fig 4.7 Lightning Intensity during observation period

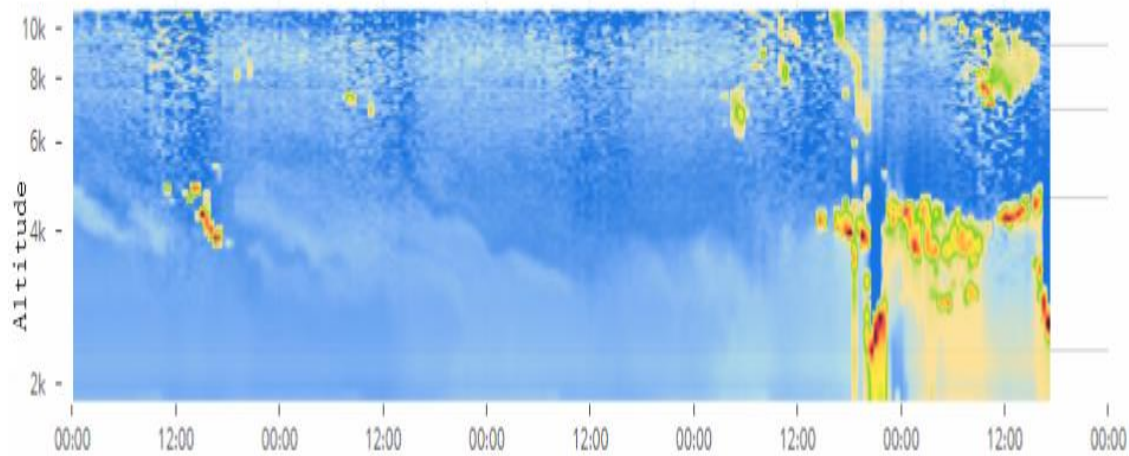


Fig 4.8 Altitude-wise perturbations during perturb time

4.6 Conclusion

This particular dataset was used because of the presence of lightning strikes during the considered interval. The parallel plate antenna for atmospheric electric field at Sonnblick Observatory makes measurement, when the field is below 500 V/m and 2 measurements / second when the field is above. Lightning characteristics and their statistical information supported by accurate analysis pave way for a good lightning detection system. The study of electric field data from geographically diverse countries Austria and gives an insight into how this analysis can be used on a global basis. The EFM of Sonnblick Observatory readings in the Sonnblick data, shows a peak buildup of about 6000V/m preceded by a drop in value due to a reversal of electric field that is characteristic of a lightning electric field prior to the strike. In the Fig.s 7 to 9 represent the data from the National Centre for Earth Science Studies, Trivandrum on dates 8/10/2011, 25/10/2011 and 30/10/2011. 8th October is a representative day of fair weather, and it can be seen that the electric field values are confined to less than 500V/m. On 25th of October, a

thunderstorm occurred in the early morning hours close to Fig. 6. Data from Sonnblick Observatory Fig. 7. NCESS data for 08/10/2011 – fair weather day Fig. 8. NCESS data for 25/10/2011- thunderstorm day Fig. 9. NCESS data for 30/10/2011- thunderstorm with lightning flash midnight and the fields can be clearly seen to have risen till 2500 V/m. NCESS equipment only measures the magnitude blinding us on the polarity. And on 30th October 2011, electric field buildup to about 5000V/m was observed and a lightning had occurred in agreement with their lightning incident Electric field measurements and their analysis assist the meteorologists in predicting the very difficult first stroke. The paper focuses on the review study of electric field data from National Centre for Earth Science Studies, Trivandrum and Sonnblick observatory, Austria. The experimental datasets from both the regions were found to be consistent with the literature study. Such a comparison of data from two very diverse places points out the observed similarities in the behavior of electric field prior to lightning and it helps to formulate a general mechanism to effectively predict lightning. Also, this research work will be a first step towards formulating a standard model of atmospheric electric field characteristics prior to lightning strike for other research and early warning systems. recordings. Due to lack of polarity measuring devices in the Trivandrum Centre, the dip before the peak could not be identified as the reversal of polarity which is a characteristic of electric field variations. However, the magnitude variations are clearly visible. The build up and flip in polarity of electric field prior to strike is a key parameter that can be used effectively in lightning detection. whenever a charge separation occurs over or nearby an EFM, or whenever a mature thunderstorm approaches the area of concern, there is a reversal of electric field polarity which is accompanied by an increase in magnitude. This means that the electric field becomes a large negative value before a lightning strike.

CHAPTER 5

Measurement of Atmosphere Electric Field during Disturbed Interplanetary Magnetic Field

5.1 Introduction

The worldwide atmospheric electric field is behave like a current, like an electric circuit atmospheric electric currents flow upward during disturbed geomagnetic conditions. The atmospheric electric current penetrates into the ionosphere, and down to the surface of the Earth. In any measurement of atmospheric electric field, earth electrical environment plays a vital role. The continuous measurements of atmospheric electrical parameters, like atmospheric electrical field, atmospheric conductivity is characterize the atmospheric global electrical circuit (GEC). Consequently, when the lower troposphere, the ionosphere and the magnetosphere are connected by this global electric circuit, which assess by atmospheric parameters. A long-term observation from multiple locations is to be found helpful to resolve the climate change-related issues. Sensitivity of the interactions between atmospheric electrical energy, solar cycles, and atmospheric air quality are inadequate for broad experiments, taking into the consideration of strong record of atmospheric electric data and its observations might be carried out for further investigations. Therefore, throughout the atmospheric electrical systems, the non-linear effect can be important, because the thunderstorms are non-steady, but electric charges may play an important role in the electrification of the thunderstorm. Several studies have shown that the effects of solar activity due to ionospheric electric field fluctuations can significantly control by the global electrical circuit. In explaining Global Electric Circuit (GEC), observations of Polar Regions are of great importance because of these regions are virtually free from anthropogenic emissions. An ice covering of polar region and maximum part of the continent convection are

generated by the element of radioactivity at the surface of the earth. The electrical conductivity of the ice surface is greater than that of air among many magnitudes. In the Antarctica the atmospheric electrical experiments are beneficial for studying the large-scale electrical phenomenon that is specific at high latitudes. In the lower atmosphere generators (mostly powered by thunderstorms) and upper atmosphere generators (ionosphere/magnetosphere) are used in the global electric circuit. The effect of this external generator on the surface electric field depends on the measurement site's magnetic co-ordinates. Atmospheric electrical parameters were calculated and recorded by several physicists at high latitude polar region.

The measurement of the surface electric field at Maitri station, Antarctica during local summer observed the effect of coronal mass ejection and function of electrodynamic coupling. It's like a 'Carnegie curve,' the so-called electric field pattern produced by thunderstorms. It is also noted that on particular days the classic diurnal variation is not seen daily, but only when several days are averaged. An additional issue is that horizontal ionospheric electric fields map down to the surface of the Earth while attempting to analyse the global electric circuit in the high latitude-polar-cap area. The two-cell convection pattern in the polar area is caused by this dawn-to-dusk horizontal potential gap due to the solar wind's contact with the Earth's magnetosphere ($V \times B$). In this section, the main component analysis was carried out by taking the Maitri station, Antarctica surface electric field data and reported that the first own value provides information on the contribution of the thunderstorm to the global electric circuit. Information on the E-region ionosphere dynamo and the solar wind-magnetosphere dynamo, respectively, will be given by the second and third elements. In contrast to those of the solar wind magnetosphere dynamo at high latitude during solar active period, the currents and electric fields produced by the ionospheric wind dynamo are comparatively small, because cross-polar cap potential has a major

effect in the high-latitude area and has spread up to 40 magnetic co-latitudes. The expanded horizontal electric field to the lower atmosphere is progressively downward (dawn-dusk potential). In order to raise the upward vertical electric field and current on the ground, the clockwise cell can map. The anti-clockwise convection will be mapped down to the measured electric field and current in the atmosphere. In terms of magnetic dawn at dusk, the nature of the convective cell depends on the relative location of the station. More direct effects of the deep penetration of the interplanetary electric field into the mid- and low-latitude ionosphere can include changes caused by solar wind. At the auroral and polar latitudes, the greatest signs of solar wind encounters with the systems of the magnetosphere and ionosphere are highly noticeable. Many surface electric field experiments have been carried out in high and polar Arctic and Antarctic regions, but the magnetospheric/ionospheric contribution to atmospheric electricity at sub-auroral stations has been correlated with these effects. It noted that the association between the difference at high latitude of the surface electric field and the measured horizontal electric potential (model Weimer 05) is negligible and that the correlation is comparatively related to the frequency of auroral electrojets. There were no consistent findings from previous experiments, however, and a comparable technique is not used at the equatorial auroral boundary station. The temporal difference of the electric surface field measured at Maitri ($70^{\circ} 45'52''S$, $11^{\circ} 44'03''E$, 117 m msl) and its departure during the disrupted geomagnetic times. A strong ground-based metric for research is the fair-weather current, which flows down from the ionosphere through the atmosphere in fair-weather regions to the Earth's surface. In fair-weather areas, this wave of conduction current produces a vertical electric field (EZ), also known as potential gradient (PG) (potential difference). The PG usually has a magnitude of ~ 120 V/m at 1 m above the surface in good weather conditions, with the potential increasing favorably with

increasing height. Thunderstorms and electrified clouds, which send charges from the cloud tops to the ionosphere, are the main generators that lead to the global electric circuit. Ionospheric tides and the solar wind/magnetospheric dynamo are two secondary generators that are more active at middle and high latitudes. The latter generator is active in polar cap regions where the incoming solar plasma, through open geomagnetic field lines, disturbs the magnetosphere-ionosphere structure. At the time of the geomagnetic storm and sub-storm where the immense volume of energy is fed into the magnetosphere, this impact is tremendously enhanced. In general, the sub-storm phases (expansion and recovery phases) are thought to be the product of a series of events starting with an increased energy coupling into the magnetosphere of the Planet. The current systems in the magnetosphere are caused by the collision of the incoming solar wind plasma with the magnetic field of the Earth. Due to the high electrical conductivity present along and across the magnetic field lines, due to this interaction map to the polar cap ionospheric altitude, all electrical fields, generally magnetospheric ($V_{SW} \times B$), created due to the interaction map of the polar cap ionospheric altitude where two cell electrical field convection patterns between dawn and dusk are formed. This large-scale ionospheric potential differential (> 300 km) maps downward effectively in the direction of reducing electrical conductivity in the lower atmosphere. During calm geomagnetic cycles and greater fluctuations during geomagnetically disrupted periods, the magnetospheric generator will create disturbances of ± 20 percent in the current and PG at high latitudes. The creation of magnetospheric storms results in an increase in precipitation of energetic particles to the lower ionosphere in the strengthening of the ionospheric electric field. It is also meant to modify the conductivity of the lower ionosphere and effect the variation of the surface electrical field. Short-term space weather phenomena, including energetic particle precipitation and large-scale ionospheric electric field effect on

current density and fair-weather electric field observations, have been formed coronal mass ejection (CME) and solar energetic particle events. During large magnetic sub-storm cases, a significantly investigated ground level atmospheric current intensity, increase density of the ambient current as well as the electric atmospheric field at ground level indicating the change towards downward mapping of the horizontal electric ionospheric field.

A synchronous measurements of the atmospheric electric field, geomagnetic fields and other geophysical parameters from a network of polar stations across the Arctic regions are restricted, but the impact of solar wind-induced geomagnetic storms on atmospheric electrical parameters at middle and high latitudes has been widely observed. This inconsistency may be attributed to the variety of physical processes which involved in geo-effective storms in the near-surface atmosphere, It is a daunting job to observe the effects of geomagnetic sub-storms on the atmospheric electric field or current from the network of stations (latitudinal/longitudinal), Since the electrical fluctuations are largely controlled by the conditions of local weather. In the category of addressing the sub-storm behavior of the Northern Hemisphere, geomagnetic disturbances from nearly conjugate stations, there are few findings. Especially, Due to sub-storm disruptions, the departure of the atmospheric electric field at middle latitudes was studied and a related analysis for large geo-effective storms was conducted. The effect of the solar flare/ground level occurrence on the atmospheric electric field measured from the mid- to high-latitude stations was analysed in recent studies and confirmed that the changes. It is subject to a variety of variables, such as the relative location of the Sun-Earth, interplanetary space conditions, and the status of the ionosphere and atmosphere at mid- and high latitudes. In addition, when studying several stations becomes very tedious, the magnitude of geomagnetic substorms affecting the atmospheric electrical parameters will vary at various periods of time. There is less

mention of the parallel measurements of the atmospheric electric field from high latitudes and the influence of magnetospheric/ionospheric generators on the electric field of the atmosphere. Thus, it is fair to assume that multistation experiments and widely spaced atmospheric electric field measurements would produce substantial and compelling findings, That should be able to illustrate the association of variations in the surface electric field with variations in solar wind. A large geo-effective storm ($K_p = 8$) on 5 April 2010 and its impacts on atmospheric electrical parameters measured at three high-latitude stations on the Antarctic plateau have been recorded in this review. The findings concentrate on the latitudinal shifts in the geomagnetic disruption of the ground level electric field influenced by the solar wind-magnetospheric generator and its imprint over three closely spaced stations in the Antarctic during the substorm periods. Some typical morphological characteristics of electric field disturbances correlated with various geophysical conditions have been discovered in this chapter. However, the spectrum of knowledge on these observations of atmospheric electric field and effect of geomagnetic field intensity remains high and shown clear characteristics have been revealed in this study.

5.2 Methodology & Data Analysis

In this segment, the atmospheric electric field activity during fair weather condition is studied when no or minimum climatic disturbance has been detected. Atmospheric electric field measurements were performed at ground-based station at Maitri station is shown in the figure

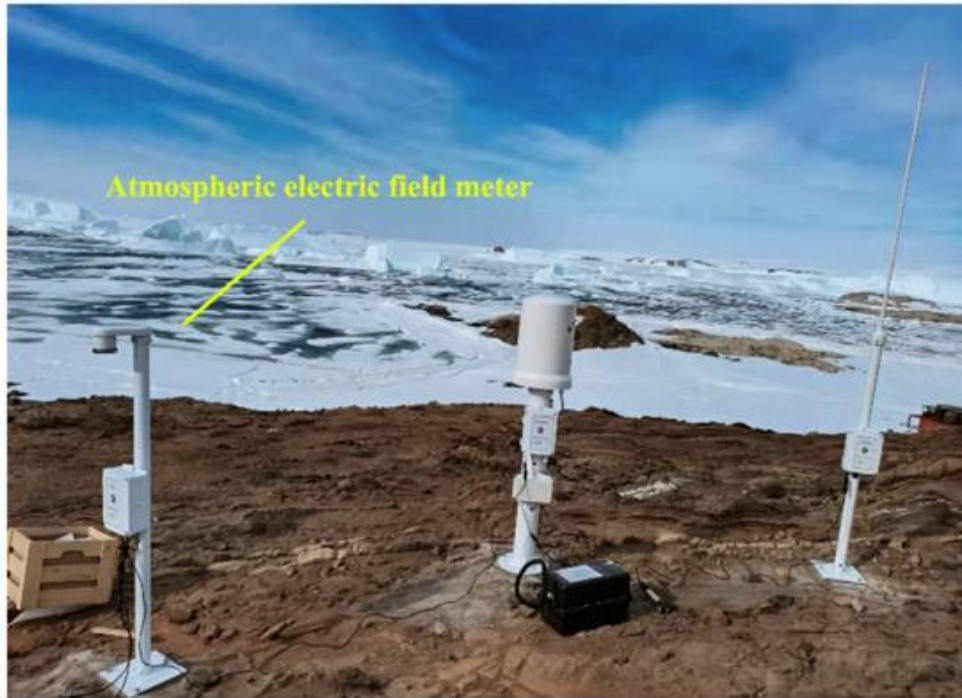


Fig 5.1 Atmospheric Electric Field Mill at Maitri Station, Antarctica

Antarctica and atmospheric electric field data is obtained from [www. glocaem.wordpress.com](http://www.glocaem.wordpress.com). As far as the atmospheric electric field activity is concerned, only 06 days which is in the month of January 2019 as fair weather conditions. An electric field intensity pattern of selected days are display more or less similar characteristics representing local climatic conditions. The minimum and maximum fluctuations of the atmospheric electric field have been standardized in order to provide an understanding of the behavior of the atmospheric electric field in typical weather conditions in contrast to the study of disturbed interplanetary magnetic field conditions.

Magnetic Field Intensity

It is represented as vector H and is defined as the ratio of the MMF needed to create a certain Flux Density (B) within a particular material per unit length of that material. Magnetic field intensity is measured in units of amperes/metre.

Atmospheric Electric Field

The total potential difference from the surface of the earth to the top of the atmosphere is about 400,000 volts. Atmospheric electricity is the study of electrical charges in the Earth's atmosphere (or that of another planet). The movement of charge between the Earth's surface, the atmosphere, and the ionosphere is known as the global atmospheric electrical circuit.

For this atmospheric research, the electric field mill available at ground-based stations is used, atmospheric electric field of 06 days in the month of January have been during the 24 hours of Gwalior's chosen good weather days from January to December 2013. In this chapter, the problem statement deals with the study of the electric atmospheric field under fair weather conditions. A temporal period is characterised by the state of fair weather conditions in the atmosphere, where different parameters such as maximum and minimum temperature, wind speed, hurry, fog, humidity and precipitation the atmospheric fair weather condition. 26 days over a span of one year (January 2013 to December 2013) were chosen on the basis of fair weather conditions to examine and research the effects. This chapter describes the ambient electric field diagrams of the chosen days of the lower Earth (Fig. No. 3 to Fig. No. 3) and presents the different atmospheric parameters on page No. 41. Fig. Fig. Fig. To fig. The modification of the electric field with various climatic variables such as wind speed, precipitation and falling rain is seen on page 42 to page 46. The 5-min average PG and magnetic field variance data measured at Maitri on 5 April 2010 as shown in Figure 2. It is also possible to break the influence of a geomagnetic substorm on PG into three periods. A reduction in the horizontal portion of the Earth's magnetic field is defined by the first interval between 04:20 and 8:20 UT. As high as ~ 150 nT, the horizontal portion ($|H|$) varied considerably, and its related PG changes are meagre or absent. However, as seen in Figure 2, the occurrence of magnetic

perturbation is more distinct from the magnetometer readings. A slight departure of PG accompanied by a sharp increase in amplitude is observed during the second period from the time of substorm beginning to 11:30 UT. It coincides with sharp geomagnetic field oscillations (H) in time. Substorm inception was reported at approximately 08:24 UT in the DFM data, and a simultaneous response was observed on the PG as a minor departure about 08:25 UT as seen in the second interval (Figure 2). The effect of the substorm on PG is high in the subsequent stages since the intensification of the PG correlates to the period of expansion of the substorm. The PG change started at around 09:00 UT, followed by an extreme high at around ~09:40 UT, where the magnetic disruptions increased from 09:15 to 09:20 UT, as seen in Figure 2. In addition, about 11:00 UT, the PG rebounded, followed by a positive increase. The resulting difference in PG can be correlated with a shift in the portion of the vertical magnetic field ($Z = 76$ nT) about 10: 15 UT. An rise in the electric field can be seen in the third interval from 11:30 to 13:45 UT; this can be followed by an increase in wind speed/local influence. The time series of AWS channels was analysed in order to process the local weather effect on the measured atmospheric electric field at Maitri. Figure 3 displays the normal variation on an hourly rate of wind velocity, wind speed, pressure at ground level, temperature, and humidity. In general, fair weather is classified as cloud cover of less than 4 octa and wind speed of less than 10 m/s in the absence of snowfall or fog. Meteorological criteria have been tracked for the whole duration of observation to assess the weather conditions. Wind speeds, for example, ranged below 6 m/s, and later rose from 13:00 UT to 10 m/s. If the wind speed rises, the spike in the electrical field could be attributed to blowing snow/space charges. The powerful variations on the PG are established by wind direction, and it is found at the end of the second interval.

5.3 Results

Ace RTSW (Estimated) MAG

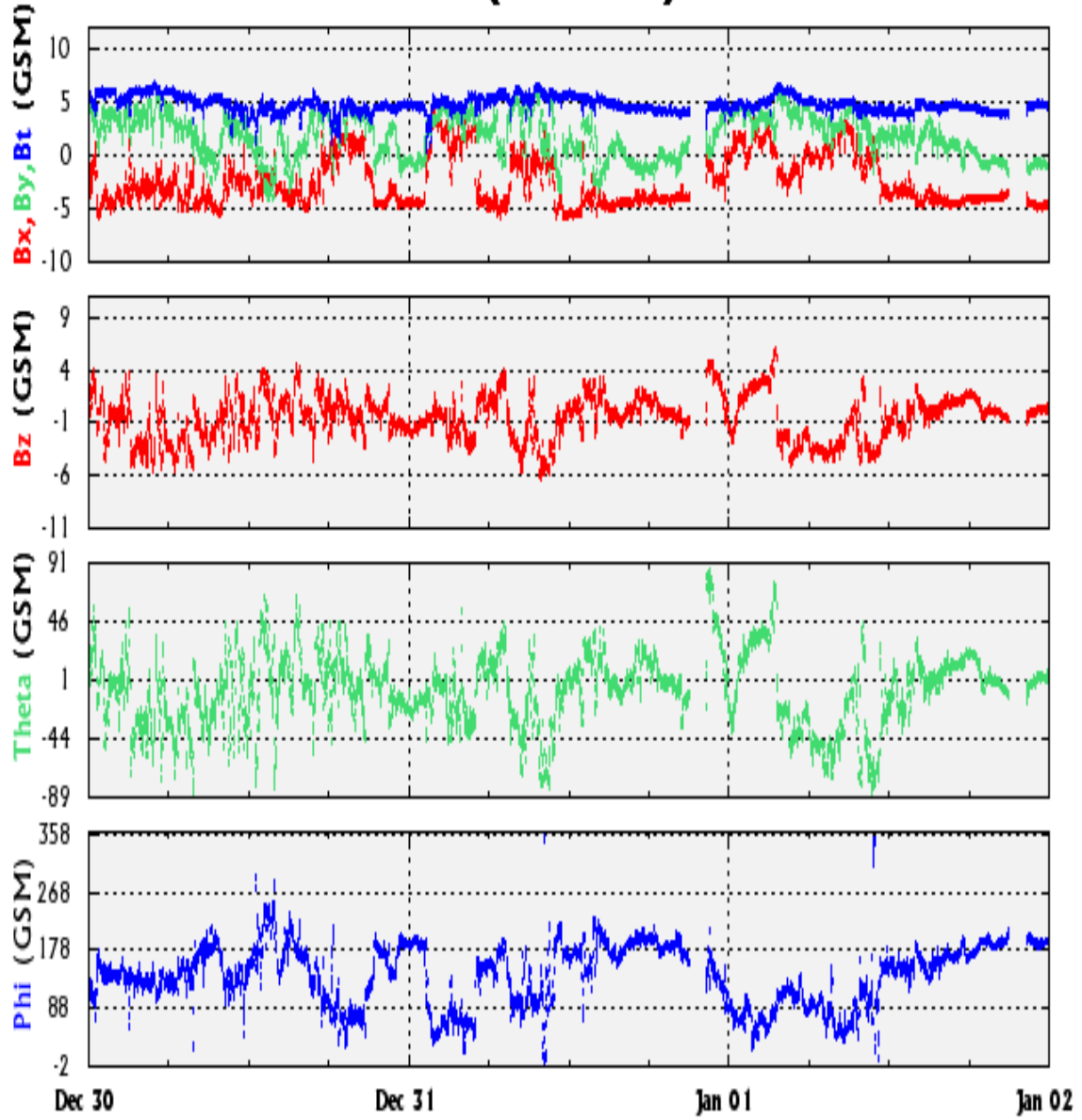


Fig 5.2 Magnetic Field Intensity on 01/01/2019 - 02/01/2019

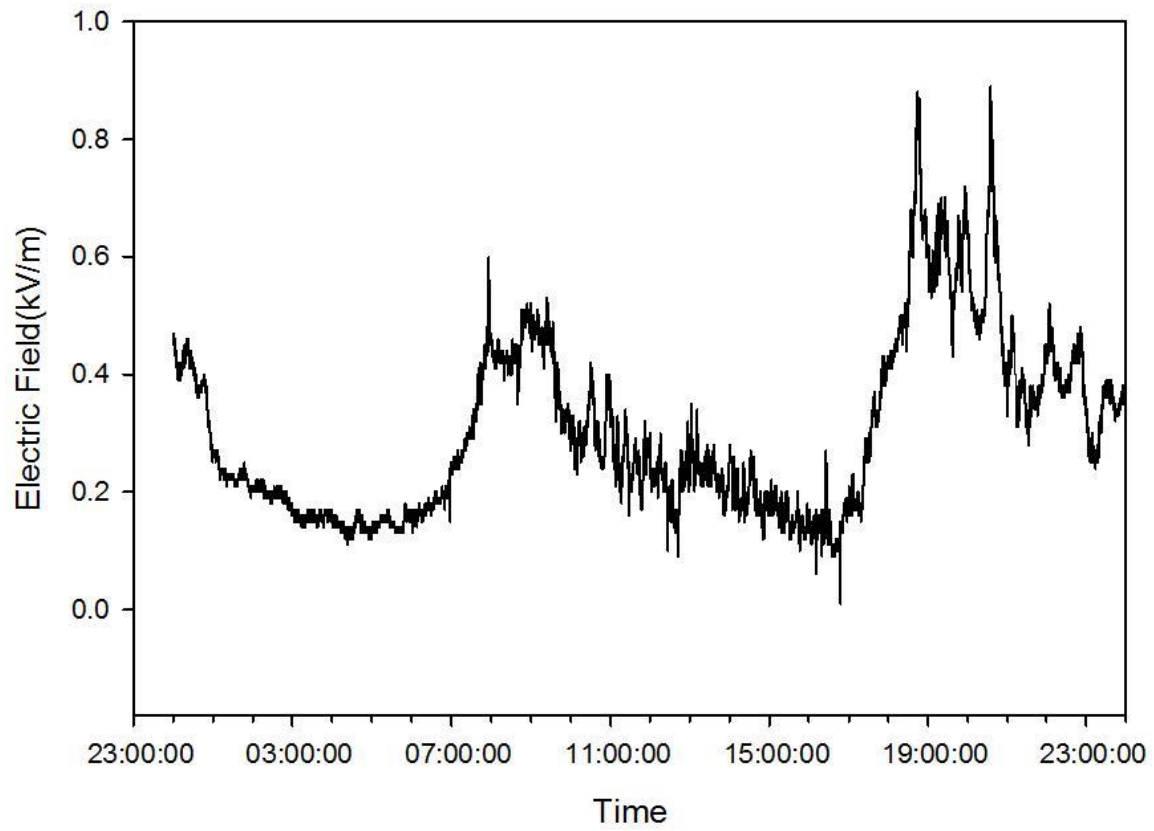


Fig.5.3 Variation of Atmospheric Electric Field (AEF) on January 1, 2019

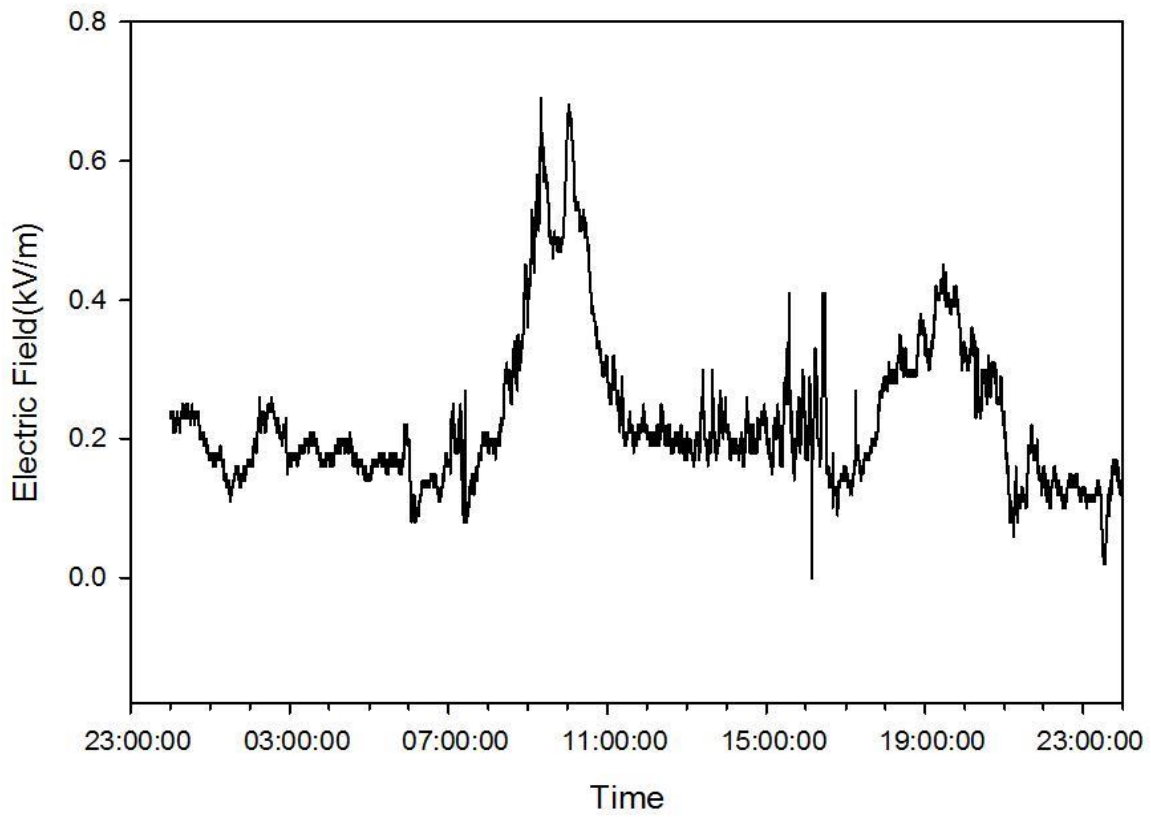


Fig.5.4 Variation of Atmospheric Electric Field (AEF) on January 2, 2019

Ace RTSW (Estimated) MAG

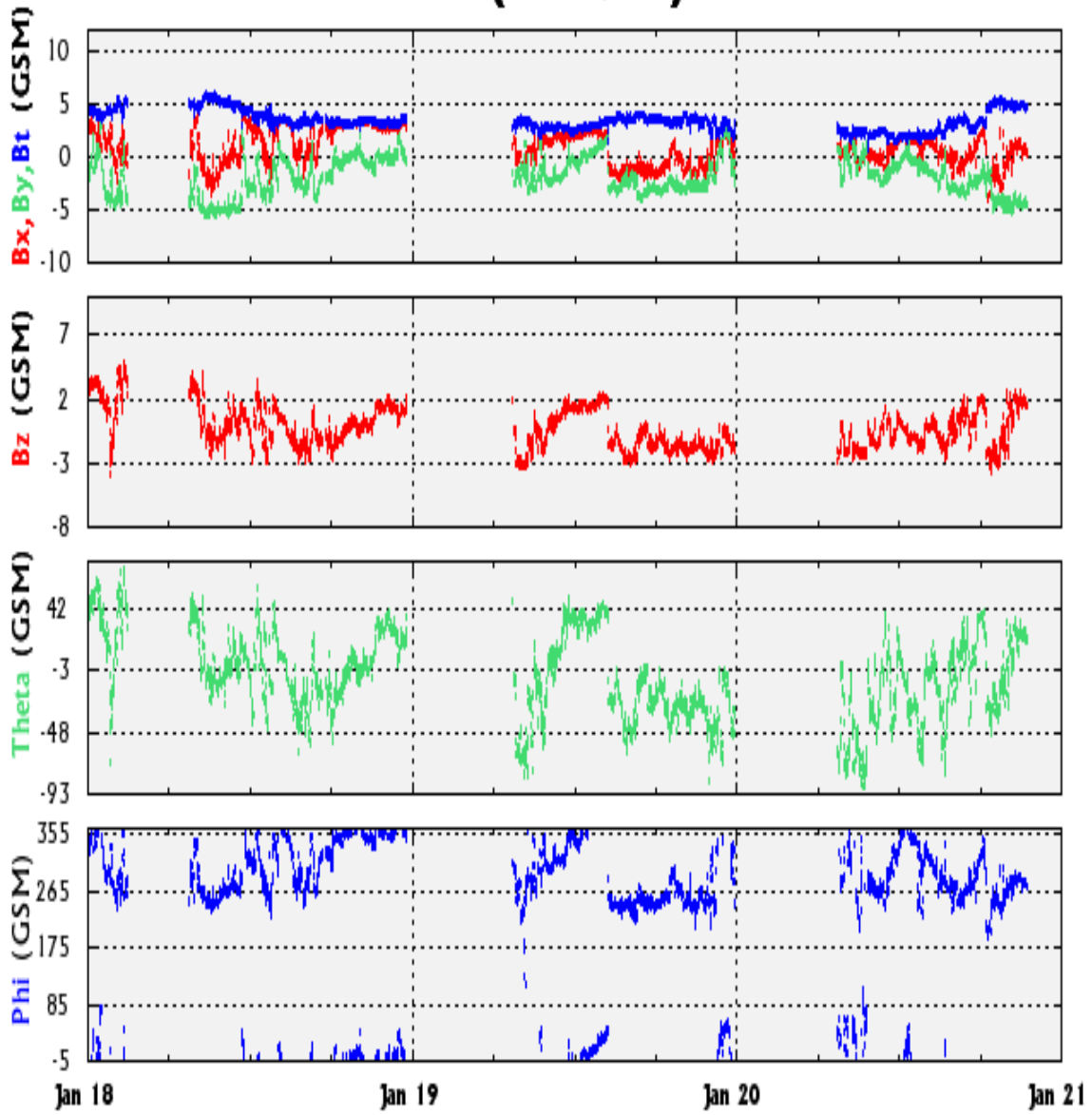


Fig 5.5 Magnetic Field Intensity on 19/01/2019 - 21/01/2019

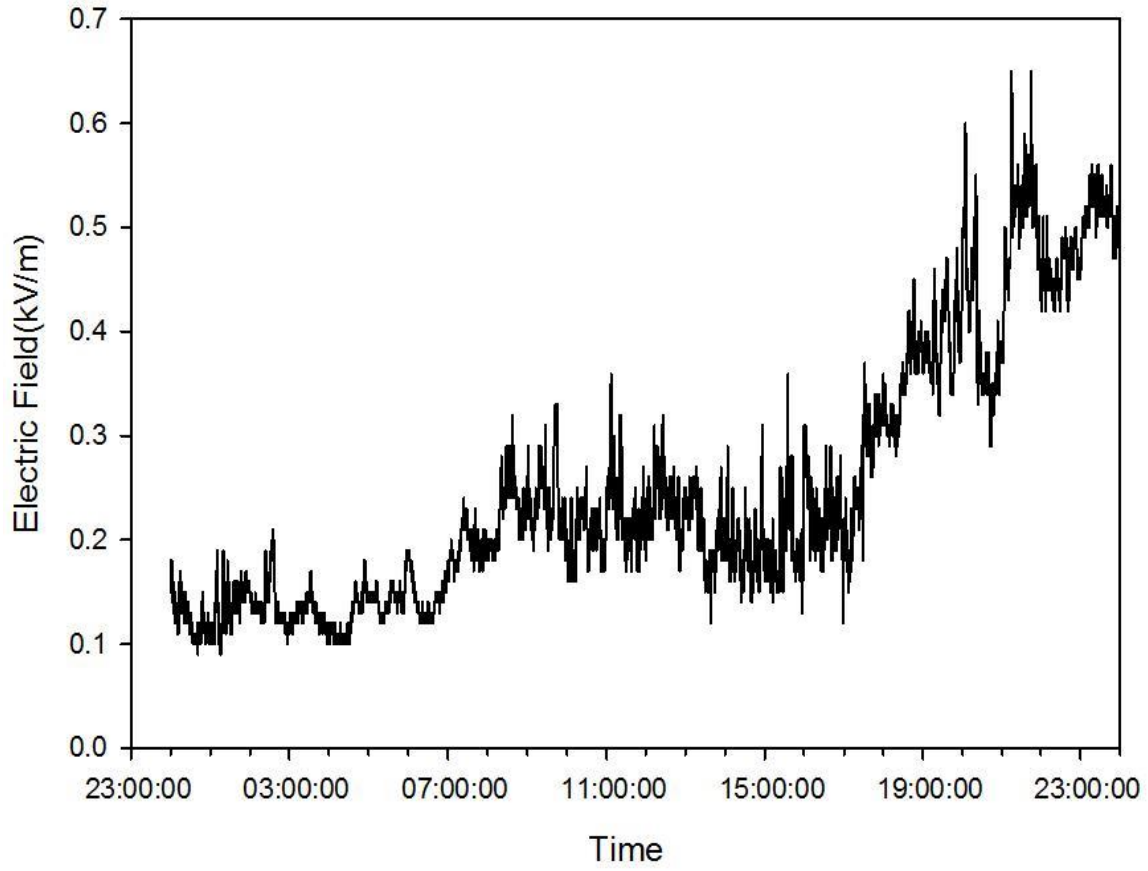


Fig 5.6. Variation of Atmospheric Electric Field (AEF) on January 19, 2019

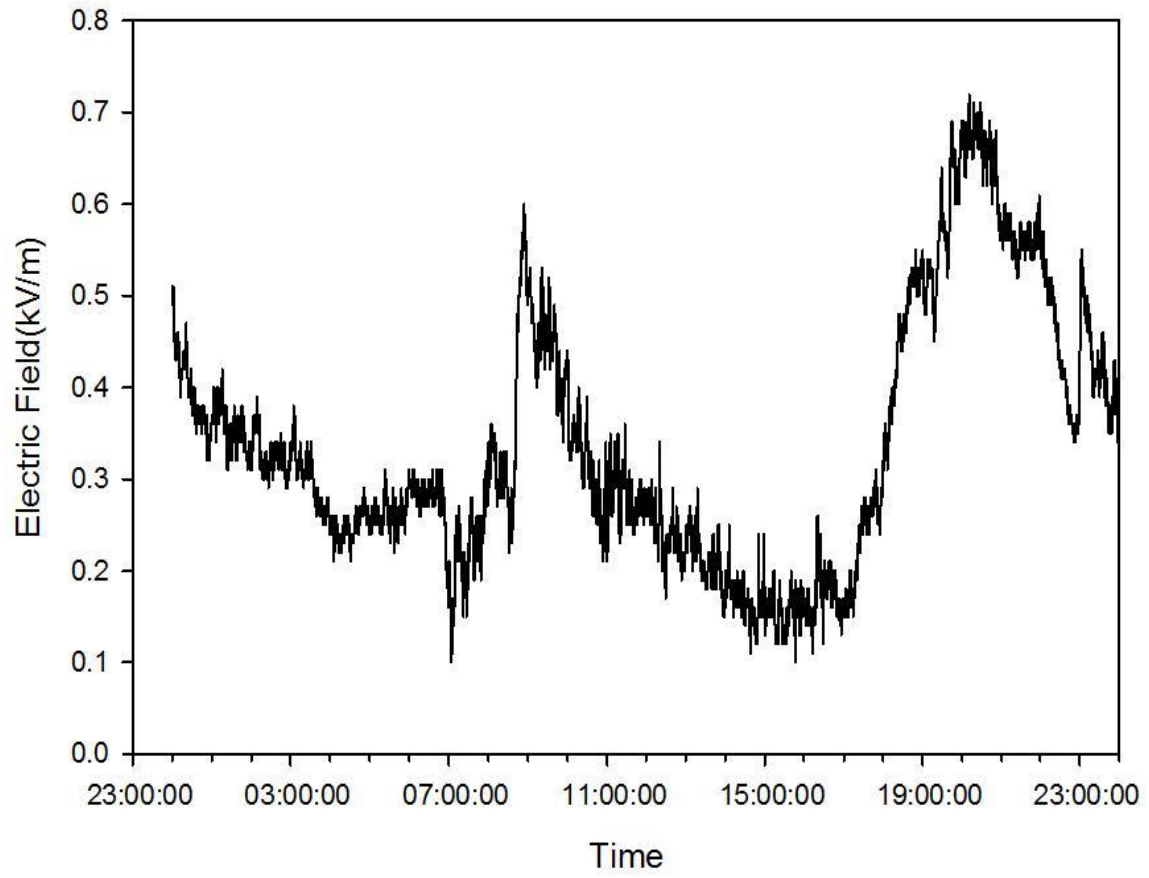


Fig 5.7 Variation of Atmospheric Electric Field (AEF) on January 20, 2019

Ace RTSW (Estimated) MAG

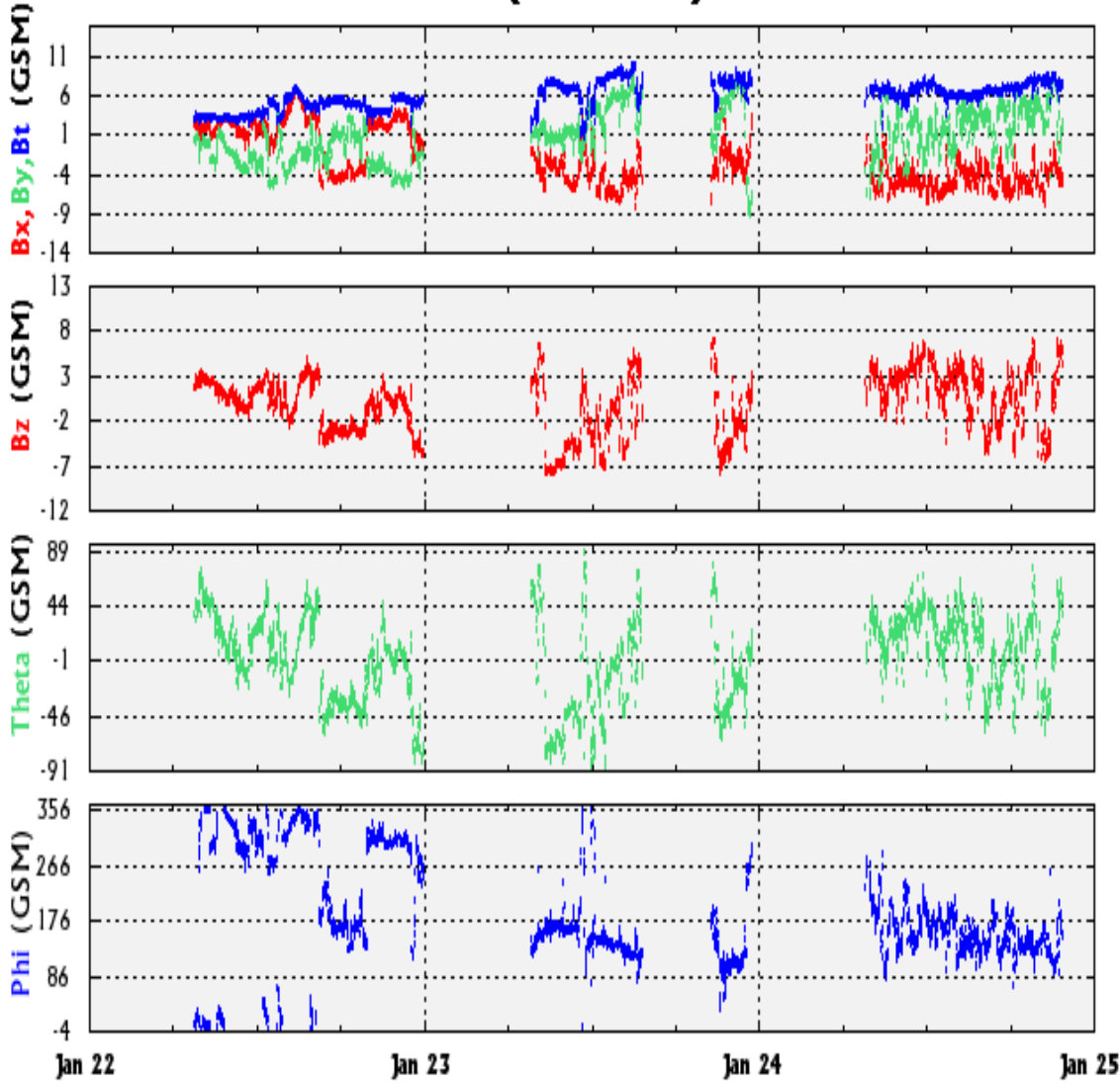


Fig 5.8 Magnetic Field Intensity on 22/01/2019 - 25/01/2019

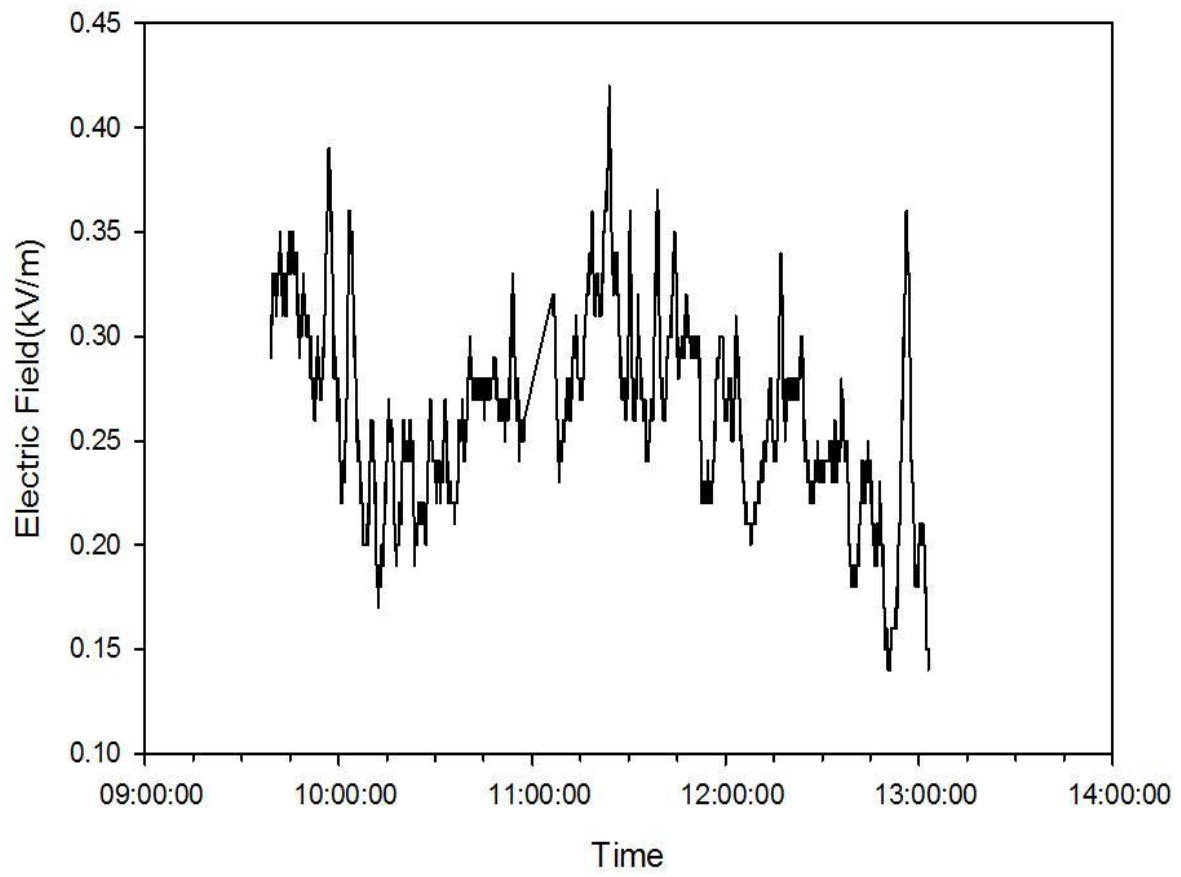


Fig 5.9 Variation of Atmospheric Electric Field (AEF) on January 24, 2019

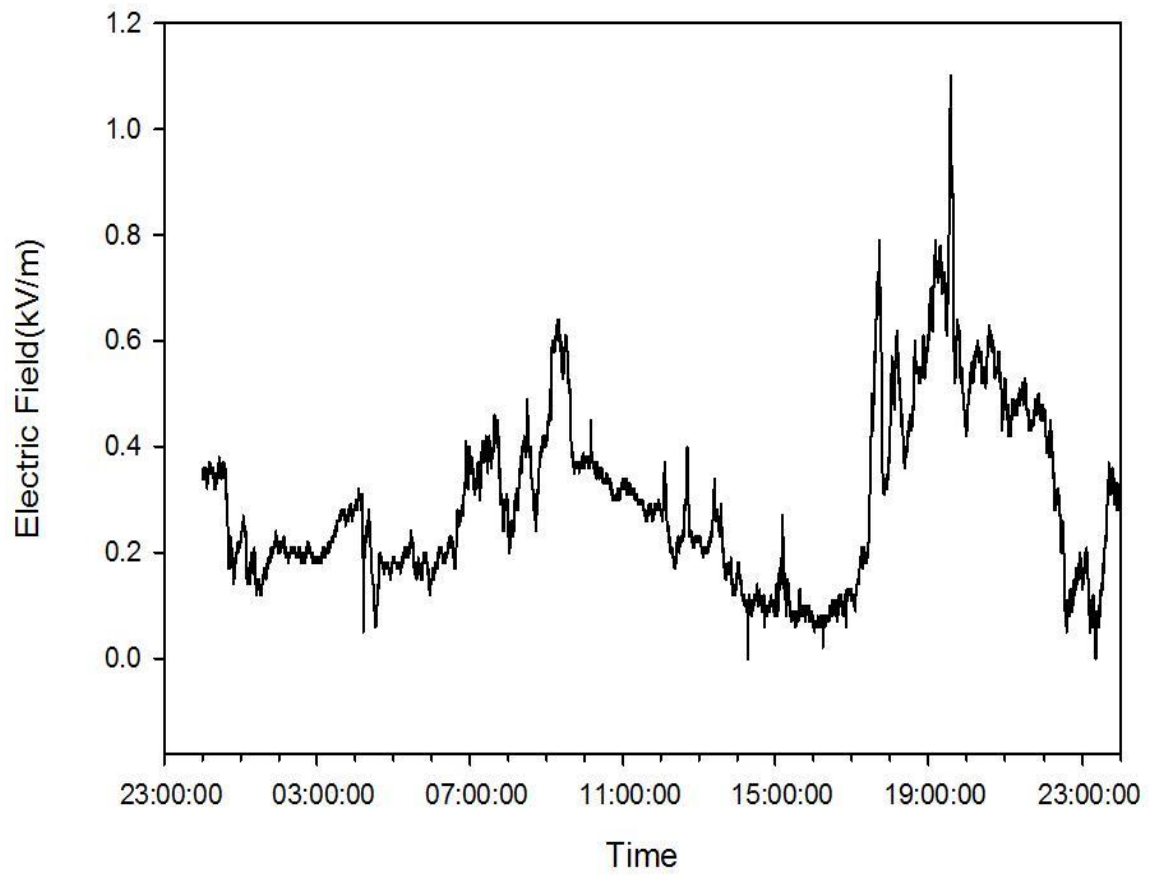


Fig.5.10 Variation of Atmospheric Electric Field (AEF) on January 25, 2019

5.4 Summary & Conclusions

Results analyzed the variation of atmospheric electric field measurements from high-latitude station during a disturbed geomagnetic perturbation. But the results are inconsistent; it may due to the complexities of the physical process involved in the mechanisms and the choice of the location of measurements. Ultimately, the overall understanding of the physical mechanism is thought to come only if a network of many station observations is possible. The location of the observatories selected for this analysis is Maitri (magnetic latitude: 67°S ; $12 \text{ MLT} = 11 \text{ UT}$), situated at the equatorward boundary of the auroral zone. It is inferred from the present analysis that the magnetic field variation and the associated changes observed on atmospheric electric field in each interval is unique. It is understood from the variation in meteorological parameters that local effects are almost negligible during the entire period of observation. The local dominant factors such as orography, prevailing weather conditions, and elevation of the stations from the sea level may perturb the atmospheric electric field measurement [Sheftel et al., 1994]. In addition to the geomagnetic disturbances on PG, there also exists a day-to-day variability of the thunderstorm electric field [Tinsley, 2000]. Figure 7 compares the normalized PG values with respect to its average value (daily mean) from the three high-latitude stations on 5 April 2010. To estimate the deviation of PG from its background field, the so-called thunderstorm-generated electric field, the diurnal average curve of PG at Vostok (April) and the Carnegie curve (average of March-April-May (MAM)) [Harrison, 2013] are displayed in Figure 7. During the first interval, the substorm activity is quite unclear, and it seems to be only observed at Maitri, since the other two observatories show insignificant changes in their magnetic field measurements. In addition, the PG observed at the three stations also varied as reference curves (Vostok (April) and Carnegie (MAM)). So the influence of this short-term/ small-scale magnetic

variation on PG is small compared to other periods and may be indistinguishable from other local effects. It is therefore difficult to determine whether the first interval of the response has any noticeable effect on the PG. We have noticed, during the second interval, the substorm signature is recorded on magnetic measurements (DFM) at 08: 25 UT (Maitri), and its associated changes on PG were observed as a peak from 08:30 to 08:40 UT at Maitri. In general, the onset of a substorm is frequently associated with a southward turn of the IMF-BZ and it is directly related to the enhancement of the ionospheric convective electric field, which is generally controlled by the solar wind parameters. This ionospheric horizontal electric field is thought to significantly alter the PG measurement at the ground level. It is interesting to note that the PG at Vostok and Dome C is influenced by the substorm onset occurring around ~08:30 UT, where the amplitude varied as high as 185–195 V/m with a background field of 125 V/m (daily mean) as shown in Figure 7. The variation of PG observed at Dome C is rather high compared to that observed at Vostok during the second interval. The departed UT variation of PG with respect to its reference curves is thought to be due to the downward mapping of the solar wind-magnetospheric electric field [Park, 1976; Roble, 1985]. The southward turning of IMF and enhanced solar plasma density with high speed during this interval are plausible for strong solar wind interaction with the Earth's magnetic field. Since the magnetospheric convection cell is more active over near-polar-cap regions, a slight change in ionospheric potential difference is sufficient to influence atmospheric electric field measurements. The difference between the normalized PG and reference curves, $\frac{\Delta PG}{PG_{ref}}$ at Dome C is $\sim 54\%$; Vostok; and Maitri UT $\frac{\Delta PG}{PG_{ref}}$ at Dome C and Vostok is $\sim 54\%$ and $\sim 28\%$, respectively. In the case of Maitri, the variation of PG is fairly less, which is apparent from Figure 7. The subsiding effect of mapping of a large-scale horizontal ionospheric electric field to lower

atmosphere may vary from high latitude to subauroral latitude. The effect of coupling of the ionospheric electric field with PG depends on the position of the station with respect to the foci of the convection cells. In the course of a substorm, the ionospheric electric potential (horizontal electric field) and current patterns over the high latitude consist of two basic components. The first one is related with magnetospheric convection patterns, and the second is the westward electrojet in the dark sector associated with the three-dimensional substorm current circuit. These two components were identified as a signature of the solar wind-magnetosphere-ionosphere interaction [Kamide et al., 1994]. The most significant control of instantaneous changes in IMF components on the convection pattern and its associated ionospheric potential difference is expected to occur in the closest region where a direct interaction ($V_{SW} \times B$) is possible (magnetic daytime) [Frank-Kamenetsky et al., 1999]. Similarly, during the next course (~09:40–11:30 UT), the gradual changes in the IMF-BZ maximum of 15 nT significantly enhance the ionospheric potential difference. In addition, a sudden peak signature in the AE and AL indices around ~09:45 UT suggests that the auroral geomagnetic field responded to the shock front [Möstl et al., 2010]. This effect is significantly recorded on ΔH as a strong negative phase, and it depicts the westward motion of the electrojet overhead of measuring site; in other words, the westward electrojet indicates the position of the convection pattern over the station [Feldstein, 1991]. In this scenario, it is expected that an intense horizontal electric field exists at the ionospheric altitude, which may produce electrical perturbations through downward mapping. On account of this downward mapping, PG values for Vostok and Dome C are substantially increased 2.2 times than that of the average values (reference curves) at 10:30 UT, whereas Maitri PG increased up to 1.8 times to that of the average. This source of the ionospheric electric field is manifested in the atmospheric electric field (PG) with different weights depending on

measurement locations with respect to the magnetospheric convection cell [Tinsley and Heelis, 1993; Michnowski, 1998]. It is noted that the three observatories were significantly influenced by solar wind-magnetospheric interaction. The recovery phase of the PG values at 10:45 UT infers that the ionospheric potential is being weakened, and this effect is also consistent with the DFM records by recovery of the ΔH and ΔZ components. A long recovery phase of PG reached well below the ambient values (reference curve). This negative phase, a lesser amplitude than the reference curve at a given UT hour, infers the phase reversal of the superposing downward ionospheric electric field, which may be caused by the polarity changes in the magnetospheric electric field. This strong penetration of the electric field from the interaction of the solar wind and Earth's magnetic field is observed from the polar cap to subauroral latitude. In addition, the weather is also favorable during the course of measurements at all the three stations. Hence, the attenuation ratio for downward mapping due to local weather factors is almost negligible. In the third interval, PG enhancement is observed at about 11:30 UT at Vostok and Dome C, which is associated with the third magnetic perturbation observed over two stations. A small-scale variation of this magnetic perturbation is inferred from the magnetic field records from Vostok and Dome C as depicted in Figure 6 (top and middle panels). Because the northward ($IMF-BZ > 0$) and sunward ($IMF-BY < 0$) phases of the IMF may confine the plasma motion only over the polar cap regions, this substorm generation is closely associated with the variation of space-time distribution of charged particle precipitations on the upper atmosphere [Akasofu and Chapman, 1972; Kamide, 1988]. In this context, the IMF-BY plays an important role in solar wind-ionosphere coupling, and particularly during large changes of the BY component, the ionospheric current and potential distribution patterns undergo drastic changes near the polar cap region owing to polar cap FACs [Stauning et al., 1995; Michnowski, 1998]. The resultant effect

of these current systems was recorded on the magnetometers as two small peaks at 12:00 and 13:00 UT. A similar pattern has also been observed on solar wind density and particularly on the IMF-BZ parameter as shown in Figure 1a. Interestingly, the PG values obtained from ground measurement have a clear footprint of a similar pattern, which is more apparent from Figures 4 and 6. This observation might strongly pronounce the direct link between PG ground measurement and solar wind-magnetosphere interaction, which has also good agreement with the earlier observations at Vostok [Frank-Kamenetsky et al., 1999, 2001]. The magnetic latitudes (~4 latitude degree) of Vostok and Dome C are almost close to the south magnetic pole, where the magnetospheric convection cell is strong and active. Since this third-interval magnetic perturbation seems to occur over polar cap regions, no significant change is observed at the subauroral latitude (Maitri). A particular peak observed on Maitri PG may be attributed to blowing snow/space charges as the wind speed increases. It is of interest to note that Smirnov [2014] reported the variation of the atmospheric electric field measured at Kamchatka (52.9°N, 158.25°E; mag: 46°N) on 5 April 2010. He reported that a sharp PG enhancement was observed during our second interval (08:24–11:30 UT) and no further variations were addressed on account of this geomagnetic perturbation (Figure 2 in the reference), because the magnetic perturbation during the second interval is considerably strong so that its magnetospheric field influence may penetrate up to the middle latitude, which in turn alters the PG. Moreover, the first- and third-interval magnetic perturbations are relatively weak and they have been observed only over high latitudes. Evaluation of these two observations witnesses that the influence of the dawn-dusk potential and its spatial expansion from the magnetic pole (~Dome C-Vostok-Maitri) reached up to 46° (Kamchatka) magnetic latitude. This extension may be even possible at further low latitudes, depending on the level of geomagnetic activity [Hairston and Heelis, 1990; Huang

et al., 2005]. The difficulty in associating auroral and substorm activities with the atmospheric electric field is that the phase and magnitude of the electric field response likely depend on the magnetic local time and location of the site with respect to the auroral substorm [Kleimenova et al., 2011]. We summarize that the first interval exhibits a substorm activity only at Maitri unlike in Vostok and Dome C. The observed variation on the PG at Maitri is negligible. During the second interval, due to strong substorm activity, significant variations are observed on PG from the three observatories. In the case of the third interval, Vostok and Dome C are under the polar current system and the identified variations on magnetic field and PG measurements are significantly influenced, but Maitri and middle-latitude stations are potentially weak in this regard. It is inferred that variation in the amplitude of PG depends on the magnetic latitude during substorm onset. During the substorm expansion phase, when the convection cell is at overhead, PG is significantly enhanced due to the downward mapping of the ionospheric horizontal electric field. The deviation of PG with respect to the typical diurnal reference curves clearly indicates that spatial and amplitude variations of the ionospheric convective electric field significantly alter the atmospheric electric field measured over the three highlatitude stations. A network of observatories helps us find the nature of the dawn-dusk convection cell over the observation point. It is still difficult to establish a complete understanding of the observed effects in atmospheric electricity with the help of a single observation. However, these observations are strong enough to state for the variation of the PG during geomagnetic disturbances. Eventually, for the first time, this analysis demonstrates the influence of the dawn-dusk convection cell from the near-magnetic pole to middle latitude, and it also exhibits the successful downward mapping of the ionospheric horizontal electric field on PG at ground level. Measurements from three high-latitude stations formed a more reliable data set. It is reasonable to expect that the good amount

of significant results emerge from multistation observations and widely separated atmospheric electric field measurements which should be able to demonstrate the correlation of surface electric field variations against solar wind variations. Figure no. 3.3.1 to figure no. 3.3.24 shows the graphs of the atmospheric electric field obtained from the Electric Field Mill. These plots show certain similar characteristics of the electric field during non perturbed atmospheric condition.

- The plots show a similar direction of electric field which is towards the Earth without any negative inversion which is very much in line with the set standards of the normalized weather conditions.
- Every plot shows at least two peaks during the day which is specifically once in the morning hours and again during the evening hours. It can be speculated this excess electric charge may be result of the increased aerosols present in the atmosphere which has earlier been established through several researches [92]
- Except for a few cases all fair-weather days graph shows a relatively lower wind speed. Some exceptional days demonstrate the wind speed above 8mph which is possible due to other meteorological variations.

Through this work the data sets for the non turbulent atmospheric conditions have been plotted. The aim of this analysis which has been carried out is to deduce the nature of localized electric field in the vicinity of Gwalior region ($26^{\circ}14'N$, $78^{\circ}10'E$). This would establish a reference range for the localized electric field and will help to understand the comparative investigations in the subsequent chapters. It has been observed that the localized electric field under fair weather conditions vary tentatively between 1.11 – 0.0932 kV/m. The approximated value has been determined through the calculation of average maxima and minima ranges. It is in agreement

with the experimental results performed through similar techniques [references], thereby establishing a platform for any further investigation.

It is even observed under steady atmospheric conditions there is a variation during the morning and evening hours (day and night transition). Such variations are found in agreement with the earlier work performed [69].

In order to analyse the fair weather data the following parameters have been discussed.

1. Maximum and minimum temperature
2. Wind Speed
3. Gust
4. Humidity
5. Cloud density
6. Precipitation
7. Rain Fall

The work carried out in this chapter is expected to benefit in the following ways

1. It would help to set bench mark in the variation of the Earth's atmospheric electric field in the relatively fine weather days.
2. Long term study of diurnal variation would become possible by observing and investigating the data sets recorded, with similar characteristics.
3. It may be considered as the reference standard to study the weather conditions other than fair weather days.

CHAPTER 6

Summary & Conclusion

6.1 Introduction

This thesis is an outcome of an investigation of the correlation between the behaviour of atmospheric electric field and various meteorological factors. This study has been carried out in Gwalior which a district located in the northern zone of the state of Madhya Pradesh in India. Therefore the investigation results are specific to this climatic zone. The Gwalior region is semi arid characterised by a rain fall of 200 to 300mm per year with the summer temperature ranging between 26 to 46°C and winter temperatures that sometimes drops even below 5° C. The wind speed in this region varies between 1kph to 61 kph and the precipitation falls in the range of 0mm to 100mm. The investigation for this research has been delimited to the range of 12 months in the year 2013. Depending on these climatic conditions, the different parameters which were considered for this study were Maximum temperature, minimum temperature, wind velocity, gust, cloud density, precipitation, rainfall and geomagnetic indices (Kp index and Ap index). While the behaviour of atmospheric electric field under the influence of the above factors was measured using Electric Field Mill (EFM-100), The meteorological data were obtained from [www.worldweatheronline .com](http://www.worldweatheronline.com) and the geomagnetic data from Kyoto, Japan. To measure the localized electric field or vertical potential gradient an electric field mill was employed to observe and record the variation of the localized earth electric field regularly in Gwalior region. To avoid the interferences EFM is mounted on the roof top of the Madhav Institute of Technology and Science, Gwalior, Madhya Pradesh with isolation. Using EFM-100 the behaviour of atmospheric electric field during selected specific weather days in a radius of 27

miles around MITS, Gwalior has been examined. For this investigation correlation graphs of the behaviour of AEF with respect to different atmospheric parameters and geomagnetic factors were developed.

6.2 Excepted Outcomes

The investigation and discussion of this thesis have been elucidated under chapters II – IV. Chapter II, Atmospheric Electric Field during Fair weather examines the characteristics of the atmospheric electric field under fair weather which means no perturbations in any of the factors taken under study (Maximum temperature, minimum temperature, wind velocity, gust, cloud density, precipitation and rainfall). The correlation graphs between these factors and the values of atmospheric electric field demonstrate a perfect interdependence of the two.

The direction of the electric field is demonstrated to be towards the Earth during a fair weather day. Moreover there is no negative inversion which further confirms to the set standards of the normalized weather conditions. Slight variations in the electric field are observed only during the morning and evening hours which might be influenced by the increased aerosols and suspended particulates in the atmosphere. This chapter establishes that there is a perfect harmony visible in the correlation graphs between AEF and different atmospheric parameters which confirm that the intensity of the AEF is essentially governed by these meteorological factors.

Chapter III, Effect of Geomagnetic Indices on Atmospheric Electric Field, evaluates the effect of geomagnetic indices (Kp index & Ap index) on the behaviour of atmospheric electric field. This chapter substantiates the established theories of the correlation between in these indices and the local atmospheric electric field. The analysis of the atmospheric electric field during the selected geomagnetic wave struck days presented in different graphs indicates that there is a high degree

of perturbations in the atmospheric electric field pertaining to its maxima as well as minima. These values exceed the general fair weather parameters of the waves which were discussed in the previous chapter. These waves are fluctuating strongly in the negative direction too. These negative inversions are never observed on fair weather days. These wave structure also show a high density of crest and troughs which confirms to high propensity of geomagnetic threats.

Chapter IV, Study of Atmospheric Electric Field under Perturbed Weather Conditions, examines the behaviour of atmospheric electric field under the influence of various indicators of perturbed weather like rainfall, precipitation, humidity, gust and wind velocity. There has been an attempt to establish a correlation between the intensity of these factors and that of the atmospheric electric field. The comparative graphs illustrating the correlation between these factors and the changing patterns of the atmospheric electric field demonstrate a high interdependence between these phenomena and the intensity of atmospheric electric field. This chapter also aims at exploring the propensity of developing the behavioural patterns of the atmospheric electric field when it is affected by climatic turbulences, which can be further taken as a contrasting reference to the behavioural graphs of atmospheric electric field during a clear weather so that any forthcoming natural disasters may be forecast well in advance and precautionary decisions may be taken.

6.3 Highlights of Results:

- i. When the weather conditions of a place are normalised, i.e. there is no turbulence of any kind like rain fall, thunderstorms, high wind velocity, gust and precipitation, the behaviour of the atmospheric electric field confirms to these peaceful weather conditions.

- ii.** Most specifically, under such a weather, the direction of the electric field remains incessantly continuously towards the earth; there are no negative inversions observed in the atmospheric electric field.
- iii.** The range of the atmospheric electric field under a fair weather atmosphere is calculated under the categories of maxima, minima and average atmospheric electric field. The maxima of the field were found to be within the range of 0.1604 – 1.117 kV/m while the minima were within the range of 0.0932 – 0.3867 kV/m. The average atmospheric electric field on a fair weather day fell within the range of 0.00014 – 0.3106kV/m.
- iv.** The analysis of the above data proves that the atmospheric electric field has a peaceful behaviour during unperturbed weather conditions as all the values of the electric field in maxima, minima and average are found to be between 0.09 – 1.11 kV/m which is more or less insignificant electric field value.
- v.** The graph patterns of such days illustrate turbulence in the atmospheric electric field only during the morning and evening hours when slightly higher peaks are observed. This is speculated that these peaks are indicative of local disturbances only. Excluding these small bands of disturbance the remaining duration of the days record a comparatively peaceful behaviour of the atmospheric electric field.
- vi.** There are no sudden and sharp peaks and dips in the atmospheric electric field graphs even during the morning and evening hours when slight disturbances are usually observed which means these disturbances are gradual and mild.
- vii.** The patterns of atmospheric electric field examined during high geomagnetic wave-struck days display very high fluctuations pertaining to the peaks, dips as well as the density of these disturbances.

- viii.** The direction of the atmospheric electric field on such days oscillates between extreme negative values and intense high values. Furthermore these oscillations are very sudden and have high density.
- ix.** The maxima of the atmospheric electric field on these days fall within the range of 0.25 – 20.897 kV/m, which in comparison to fair weather day is in extreme contrast as these values under stable weather conditions were found to be significantly low and closer to the lowest value (1.117 kV/m).
- x.** The minima of the atmospheric electric field during the days having geomagnetic disturbances fall within -20.708 – +0.025 kV/m. This shows the extreme negative troughs formed in the direction away from the Earth, which is a very contrasting phenomenon in comparison to the wave behaviour in a graph of a fair weather day when there is no instance of such negative inversions anywhere in the range of selected days. The minimum value of the atmospheric electric field seen in these days is 0.0932 kV/m, which is much higher to the highest positive value of the current during geomagnetically affected days which is +0.025 kV/m.
- xi.** The average atmospheric electric field value on geomagnetic wave-struck days has been evaluated in the range of -0.148 – +0.5011 kV/m which is a very broad range including a range value of +0.6491 kV/m which shows the extremely turbulent wave behaviour: the troughs falling in extreme negative depths and the crest rising extremely high. In contrast to the average values on fair weather days with a very narrow range of +0.3105 kV/m, the values of such disturbed days have approximately double range value. This scrutiny of the wave behaviour substantiates the hypothesis that geomagnetic waves have extreme influence on the behaviour of the atmospheric electric field.

- xii.** The comparative graphs of the Kp index and Ap index with the atmospheric electric field show a perfect synchronisation between the behaviour of the geomagnetic indices and the electric waves. The crest and troughs registered in these indices are always followed by the corresponding peaks and dips in the atmospheric electric field waves. This again is very in line with the hypothesis stated above.
- xiii.** A perfect synchronisation of the atmospheric electric field wave behaviour with the local weather conditions is perfectly demonstrated through the graphs that examine a perturbed weather day. High turbulence in the weather conditions under the effect of different weather factors like wind velocity, gust, rainfall, precipitation, cloud density and temperature influences intense and drastic wave turbulences in the atmospheric electric field.
- xiv.** The maximum atmospheric electric field intensity evaluated during a perturbed weather ranges between $+0.0607 - +20.89$ kV/m. When these values are compared to those examined during fair weather days, the difference in the highest field intensity is $+19.77$ kV/m (highest maxima of perturbed weather being $+20.89$ kV/m and that of fair weather days being $+1.12$ kV/m). This difference shows very high peaks of atmospheric electric field under extreme weather conditions.
- xv.** Negative inversion in the atmospheric electric field pattern is a recurrent phenomenon when the weather is turbulent. The minimum value of the field extends to the extreme negative side till -20.71 kV/m in the direction opposite to the Earth. The range of such inversions fall between $-20.71 - +0.06$ kV/m. This again is very much in contrast to the field patterns investigated during fair weather days when the least value of the

atmospheric electric field was +0.932 kV/m, which is much higher than the highest value of the minima under perturbed weather conditions.

- xvi.** The average atmospheric electric field intensity analysed under perturbed weather falls in the range of -0.31 – +0.50 kV/m. The range of average electric field under such conditions was observed to be very broad with a range value of 0.81 kV/m in contrast to the narrow range value of the average atmospheric electric field examined during fair weather days which is +0.31 kV/m. This difference in the range value confirms that on perturbed weather days the wave patterns have recurring high crest and deep troughs.
- xvii.** The graphical representation of the atmospheric electric field wave patterns demonstrates the effectiveness of the instrumentation used for this study. The slightest turbulence in the weather conditions influence the intensity of the wave patterns both in positive and negative directions.
- xviii.** All the parameters of a perturbed weather have equivocal influence on the atmospheric electric field patterns. The rainy days cause the wave intensity to fluctuate between -20.708 – +20.72 kV/m causing turbulence of high intensity in the wave structure. Wind speed and precipitation also influence the atmospheric electric field in similar fashion causing the wave to oscillate between extreme crests and troughs in the range of -20.709 – +20.726 kV/m.
- xix.** The tabular interpretation of the atmospheric electric field value in correlation with different perturbed weather parameters insinuates a perfect coordination in the contours of electric field waves as well as the waves drawn for these parameters. The highest values of each parameter coincide at the same point when the atmospheric electric field has approximately the broadest range with very slight variations. This range, more or

less, falls within the minimum value of -20.709 kV/m and the maximum value of +20.89 kV/m.

6.4 Recommendations and Scope for Further Investigations:

The experimental observations and critical analysis of the data collected during the current investigation strongly establishes a perfect coupling between the perturbations in the different geomagnetic indices as well as natural weather phenomenon. It also substantiate the use of EFM-100 as a state-of-the-art machinery to detect and examined such correlation. These correlations insinuate towards a plethora of possibilities of using atmospheric electric field or vertical potential gradient as indicative factor for monitoring, investigating as well as controlling various weather related human problems.

This study can be taken as model for further examining similar atmospheric electric field behaviour in other zones. Furthermore a comparative analysis between two zones can also be a potential field of study.

Through the conclusion drawn under this study it is evident that atmospheric electric field is highly sensitive to the weather as well as geomagnetic activities. The findings of this investigation can be applied either directly or indirectly in i) weather forecasting ii) developing agriculture support system iii) standard air quality measurement.

As a result of the study suggests the atmospheric electric field during a fair weather is generally governed by the vertical wave behaviour under which the field intensity is usually positive. Except for slight variations of turbulent behaviour due to local effect arising from aerosol concentration the remaining wave structure stays undisturbed. The atmospheric electric field is highly sensitive to even a minuscule amount of agitations in lower atmospheric stratum. This

interdependence can be further exploited to develop a powerful monitoring and warning system for upcoming climatic threats. If used successfully the system can be instrumental in shaping the administrative decisions related to precautionary activities.

Climatic conditions have very strong influence on the behaviour of atmospheric electric field. Slightest change in relative humidity, cloud density and precipitation affects the wave behaviour very strongly. This correlation can be powerfully harnessed to monitor the favourable conditions for agriculture and plant growth. This monitoring system if employed successfully can help the farmers in planning their crop choice and farming itinerary.

Moreover studies have established atmospheric electric field as well as geo magnetic activities has substantial influence over plant growth development and evolution (Massimo E. Maffei, 2014 and Fredrick Warner Wheaton, 1968). Taking this into consideration the results of this study can help in augmenting crop yield by increasing or decreasing the vertical potential gradient in the fields by developing different methods. Apart from electric field the magnetic field also consider to be a significant atmospheric factor which substantially affects the growth and quality of the plants as the use of instrumentation suggested in this study is very effective in tracking the magnetic fields in a particular zone. The results can be used in agriculture by measuring and magnetically pre treating the farms before planning.

An urban environment is predominantly affected by a combination of local pollution factors like suspended air particles, aerosols concentration, dust etc. This study prevents the behaviour of the atmospheric electric field under the influence of these factors. Using these results a model wave behaviour can be mapped which will help in monitoring the standard air quality by comparative analysis of two different air quality zones. Furthermore the same can also be employed in developing the industrial emission monitoring & pollution control systems.

6.5 Scope for Further Study

Similar studies can be carried out in different climatic and geographical zones for comparative analysis. A study of similar kind can be done for the impact of different polluting agents like smok, carbon mono oxide (CO), sulphur and other metallic ions suspended in the air which will have a high propensity for developing a strong industrial emission monitoring and pollution control system. An exclusive study of the atmosphere electric field behaviour and cosmic activities can be carried out for future applications in the area of geomagnetic studies. Further researches can be carried out in similar model for the correlation between seismic activities and atmospheric electric field which will be very useful in deciding an earthquake prone area. This can also be useful in fields like oil and natural gas outsource locations.

Chapter	Topic	PageNo
Chapter1	Real-time Analysis of Atmosphere Electric Field	01-25
Chapter2	Review of Literature	26-35
Chapter3	Measurement of Atmosphere Potential Growth (PG) Variations at Local Climate Specification	36-61
Chapter4	Analysis of Atmosphere Electric Field Characteristics during Lightning	62-76
Chapter5	Measurement of Atmosphere Electric Field during Disturbed Interplanetary Magnetic Field	77-104
Chapter6	Summary & Conclusions	105-115
	Bibliography	116-130
	Publications	

COPYRIGHT TRANSFER CERTIFICATE

Title of the Thesis: "***Real-time analysis of atmospheric parameters during the processing of variations in the electric and magnetic field of space plasma***"

Candidate's Name: ***Bharat Singh Jayant***

COPYRIGHT TRANSFER

The undersigned hereby assigns to the P.K. University, Shivpuri all copyrights that exist in and for the above thesis submitted for the award of the Ph.D. degree.

Date:

Research Scholar

Bharat Singh Jayant

Enrollment No.

161595006205

Note: However, the author may reproduce/publish or authorize others to reproduce, material extracted verbatim from the thesis or derivative of the thesis for authors personal use provided that the source and the University copyright notice are indicated.

DECLARATION BY THE CANDIDATE (PARA 26-B)

I declare that the thesis entitled “*Real-time analysis of atmospheric parameters during the processing of variations in the electric and magnetic field of space plasma*” is my own work conducted under the supervision of **Dr. S. Choudhary (Supervisor) at P.K. University, Shivpuri (M.P.)** approved by Research Degree Committee. I have put more than 240 days of attendance with Supervisor at the center. I further declare that to the best of my knowledge the thesis does not contain any part of any work which has been submitted for the award of any degree either in this University or in any other University without proper citation.

Besides this –

1. I have successfully completed the Course Work of one semester as per UGC Regulation 2009 norms.
2. I have also given a pre – Ph.D. presentation and successfully incorporated the changes suggested on the basis of feedback and comments received.
3. I have also published two research papers in an ISSN/ referred journal from the research work of the thesis and have produced an evidence of the same in the form of acceptance letter/ or the reprint.

Research Scholar

Bharat Singh Jayant
Enrollment No. 161595006205

